Broadband supercontinuum generation in specialty fibers

Yemineni, Sivasankara Rao

2019

Yemineni, S. R. (2019). Broadband supercontinuum generation in specialty fibers. Doctoral thesis, Nanyang Technological University, Singapore.

https://hdl.handle.net/10356/89263

https://doi.org/10.32657/10220/48038

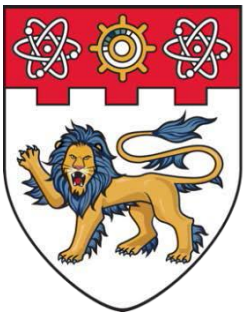

NANYANG TECHNOLOGICAL UNIVERSITY
SINGAPORE

BROADBAND SUPERCONTINUUM GENERATION IN SPECIALITY FIBERS

YEMINENI SIVASANKARA RAO

SCHOOL OF ELECTRICAL & ELECTRONIC ENGINEERING

2019

Broadband Supercontinuum Generation in Specialty Fibers

YEMINENI SIVASANKARA RAO

School of Electrical & Electronic Engineering

A thesis submitted to the Nanyang Technological University
in partial fulfillment of the requirement for the degree of
Doctor of Philosophy

2019

Statement of Originality

I hereby certify that the work embodied in this thesis is the result of original research, is free of plagiarized materials, and has not been submitted for a higher degree to any other University or Institution.

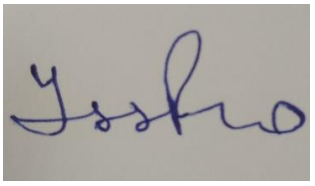

11/02/2019

. . . . . .

Date

. . . . . .

Yemineni Sivasankara Rao

Supervisor Declaration Statement

I have reviewed the content and presentation style of this thesis and declare it is free of plagiarism and of sufficient grammatical clarity to be examined. To the best of my knowledge, the research and writing are those of the candidate except as acknowledged in the Author Attribution Statement. I confirm that the investigations were conducted in accord with the ethics policies and integrity standards of Nanyang Technological University and that the research data are presented honestly and without prejudice.

11/02/2019

. . . .

Date Arokiaswami Alphones

Authorship Attribution Statement

This thesis contains material from 1 published paper and 2 under review papers in the following peer-reviewed journal(s), and from 9 published international conference papers where I was the first and/or corresponding author.

Chapter 5 is published as: Sivasankara Rao Yemineni, Wenn Jing Lai, Arokiaswami Alphones, Ping (Perry) Shum, "Mid-IR supercontinuum generation in a single-mode ZBLAN fiber by erbium-doped fiber laser," Opt. Eng. 57(11), 111804 (2018), doi: 10.1117/1.OE.57.11.111804.

The contributions of the co-authors are as follows:

- Assoc. Prof Arokiaswami Alphones provided the initial project direction, helped in editing the manuscript and in submitting the manuscripts to the journals.
- I conducted the experiments, collected the data and prepared the manuscripts. Dr. Wennjing Lai helped me in conducting the experiments and analyzing the experimental results. She also helped me in answering the reviewers' questions.
- I have prepared the manuscript drafts. The manuscript was revised by Prof. Shum Ping Perry. He also helped in pointing out the probable questions from the reviewers and also suggested the experts in the field to give prepared reviewers list during manuscript submission.

Chapter 3, 4 & 5 content is under review in the Optics Communication Journal as follows:

1. Sivasankara Rao Yemineni, W. J. Lai, A. Alphones and P. Shum, "Broadband supercontinuum generation in sub-meter length of HNLF with a carbon-nanotube based passively mode-locked femtosecond fiber laser," [Under review, Optics Communication].
2. Sivasankara Rao Yemineni, W. J. Lai, A. Alphones, and P. Shum *"*Broadband supercontinuum generation in PCF, HNLF and ZBLAN fibre with a carbon-nanotube-based passively mode-locked erbium-

doped fibre laser," [Under review, Optics Communication].

The contributions of the co-authors are as follows:

- Assoc. Prof Arokiaswami Alphones provided the initial project direction, helped in editing the manuscript and in submitting the manuscripts to the journals.
- I conducted the experiments, collected the data and prepared the manuscripts. Dr. Wennjing Lai helped me in conducting the experiments and analyzing the experimental results. She also helped me in answering the reviewers' questions.
- I have prepared the manuscript drafts. The manuscript was revised by Prof. Shum Ping Perry. He also helped in pointing out the probable questions from the reviewers and also suggested the experts in the field to give prepared reviewers list during manuscript submission.

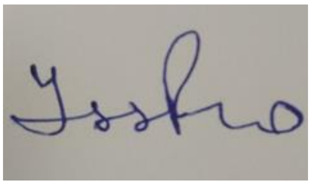

11/02/2019

. . . .

Date   Yemineni Sivasankara Rao

Acknowledgments

Approaching the final phase of pursuing doctoral degree in NTU, I would like to take this opportunity to acknowledge the depth of my gratitude to the wonderful people who have encouraged me and helped me throughout my journey in NTU for the past four years.

First of all, I would like to offer my sincere and warmest thanks to my supervisor Prof. Arokiaswami Alphones for his continuous encouragement, concrete guidance and support throughout the project. The most important thing he taught me is that a good researcher should equip with independent, critical and logical thinking as well as good writing and presenting skills along with the organizing capabilities of technical seminars and conferences. He supports me by resourcing all the necessarily experimental facilities and seeking for collaboration to ensure the smoothness of my research projects. In addition, he encourages and supports me to attend international conferences where I can communicate with experts, enrich my knowledge and generate new ideas. In the past few years, whenever I encountered setbacks and failures, his kindness and guidance encouraged me to buck up and challenge difficulties.

I would like to express my gratitude to Prof. Shum Ping for his help during the critical phase of my project as a co-supervisor. He encouraged me to attend many conferences and helped me to get conference funding with his strong recommendations. He also helped me to meet many industrial people and many researchers in the field of optics to understand the current scenario of research progress in the field optics. His constant support and encouragement helped me a lot to back up my strength during the difficulties. I also take this opportunity to thank IEEE Photonics Society for awarding IEEE Photonics Conference Travel Grant (2017 &2018) twice to attend IPC-2017 and IPC-2018. I also thank IEEE Photonics Society Singapore Chapter for their encouragement by through awarding travel grant to attend IPC-2017.

I take this opportunity to express my sincere thanks to TAC members: Dr. Lai Wennjing and Prof. Yoo Seong Woo for being there all the time whenever I needed their opinion and suggestions on my work. Dr. Lai Wennjing helped me a lot to resolve the experimental related issues and supported me to conduct my experiments by providing proper guidance on the each and every equipment usage and also helped me to barrow the equipment's that I needed for my experiments from others. She helped me a lot in writing conference and journal papers

by giving concrete feedback. She encouraged me to keep calm and focus on work when something is not working in my way, those words help me a lot to focus and relieve the stress.

I would like to thank Dr. K. K. Chow for bringing me to NTU and into the field of optics, he helped me and encouraged me to learn the basics of nonlinear optics and the project related literature at the initial phase of the project. I also take this opportunity to thank Prof. Sheela Adithya and Prof. Lee Yee Hui for their encouragement and suggestions.

I would like to thank staffs and students who have fruitful discussion and give me valuable suggestions on my research projects. They are DR. Liu Huanhuan, Dr. Venkatesh Mamidala, Dr. Yang Ye, Dr. Yung Chuen, Huang Jieyuan, Dr. Betty, Dr. Zhilin, Dr. Yunxia, Dr. Qize Dr. Luo, Dr. Yu Xuechao, Siddhartha, Dr. Luo, Dr. Wu Zhifang, Zhang Zhing, LuLu, Grorge, Hailang, Nan Zhang, Shao yang, Mengying, Damien, Linda, Debby, Manoj Kumar and Shilpa Manandhar. Their selfless help and valuable suggestions motive me to go further in the particular field of study. In addition, I sincerely appreciate my technicians of Fibre Technology Lab Mr. Chong Lui Tat Anthony and Ms. Yang Xin for their generous help in the past few years. I would like to thank all my friends who were there in my high and low moments, starting from my childhood.

Last but not least: I give my deepest appreciation to my parents (Annapurna & Sambasiva Rao), Brothers, Sisters, Uncles, Aunties and especially to my eldest brothers Siddhu, Ramu and to my elder brother Dr. Y S L V Narayana, for their unconditional love which makes me feel confident of the pursuit of excellence all along the way.

Abstract

Broadband supercontinuum (SC) generation is of great scientific and technical interest, and emerged as one of the best broadband light sources in a range of applications including optical communication, precision spectroscopy, optical coherence tomography (OCT), optical frequency metrology, hyperspectral imaging, light detection and ranging (LIDAR) and, chemical and remote sensing. Hence the broadband SC generation is of strong motivation.

Supercontinuum (SC), is a process of generating broadband optical spectrum by launching optical pulses into a nonlinear medium, continuous interaction of laser pulses with nonlinear optical medium leads to the emission of a wider optical spectrum with a bandwidth many times greater than the bandwidth of the launched pulses. The key nonlinear physical phenomena involved in this processes are stimulated Raman scattering (SRS), modulation instability (MI), cross-phase modulation (XPM), self-phase modulation (SPM), four-wave mixing (FWM) and soliton related dynamics. The SC generation compromises of two parts: a seed laser and a nonlinear medium. The seed laser can generate femtosecond (short) pulses, picosecond or nanosecond (long) pulses or even continuous-wave (CW) laser. The nonlinear media such as normal single-mode-fibre (SMF) or specialty fibres such as highly nonlinear fibre (HNLF), highly nonlinear photonic crystal fibre (PCF), tapered fibres and soft-glass fibres like ZBLAN (ZrF4-BaF2-LaF3-AlF3-NaF). In this project, the carbon-nanotube (CNT) based saturable absorber (SA) is used for the realization of passively mode-locked femtosecond erbium-doped fibre laser (EDFL) as a seed to the specialty fibres, to generate the broadband SC generation and also to study the different aspects of spectral broadening phenomena inside each specialty fibre. Therefore, this thesis focuses on the generation of CNT-SA-based passively mode-locked femtosecond EDFL and generation of broadband SC spectrum from specialty fibre.

The CNT-SA based passively mode-locked EDFL has achieved a pulse width of 620 fs with a pulse repetition rate of 18 MHz at a center wavelength of 1565 nm with a 3-dB bandwidth of 5 nm. The output of the mode-locked laser pulse has pulse peak power of 18.5 W and average power of 0.21 mW respectively at the stable mode-locked condition. Throughout this project, the CNT-SA based passively mode-locked femtosecond EDFL is used as seed laser to broadband SC spectrum from all the specialty fibres. For efficient activation of nonlinear phenomena inside each specialty fibre and, also to study the variation of spectral broadening with respect to the variation in input pulse power, the pulse power is further boosted through the amplification using a pulsed erbium-doped fibre amplifier (EDFA).

The spectral broadening inside a 60-meter-long PCF with respect to the variation in input pulse power is observed. The input power to the PCF is varied from 0 dBm to 20 dBm and achieved a maximum SC spectrum bandwidth of 1080 nm from the output of PCF spanning from 1090 nm to 2170 nm. In the next step, the spectral broadening inside the HNLF is studied with respect to the variation in input pulse power from 0 dBm to 20 dBm and obtained a maximum SC spectrum bandwidth of 1400 nm covering from 1060 nm to 2460 nm. In addition to input pulse power variation, here the length of HNLF is also varied and studied the effect of the length variation on spectral broadening and SC spectrum bandwidth. The effect of tapering also observed by applying tapering ratio of two on a short length of HNLF.

In order to overcome the limitations of silica-based fibres and to extend the SC spectrum further towards mid-infrared (mid-IR) side, soft-glass ZBLAN fibre is considered. The input pulse power to a 25-meter-long ZBLAN fibre is varied from 0 dBm to 25 dBm. A maximum SC bandwidth of 2100 nm spectrum extending from 1100 nm to 3200 nm is observed from the output of ZBLAN fibre.

Table of Contents

List of Figures

List of Acronyms

Abbreviation	Full Expression
CNT	Carbon-Nanotubes
CW	Continuous Wave
DS-HNLF	Dispersion Shifted Highly Nonlinear Fibre
EDF	Erbium-Doped Fibre
EDFA	Erbium-Doped Fibre Amplifier
EDFL	Erbium-Doped Fibre Laser
FWM	Four-Wave Mixing
GVD	Group Velocity Dispersion
MI	Modulation Instability
NLSE	Nonlinear Schrödinger Equation
OSA	Optical Spectrum Analyser
PC	Polarization Controller
PCF	Photonics Crystal Fibre
SA	Saturable Absorber
SC	Supercontinuum
SMF	Single-Mode Fibre
SPM	Self-Phase Modulation
SRS	Stimulated Raman Scattering
SSFS	Soliton Self Frequency Shift
WDM	Wavelength-Division-Multiplexing
XPM	Cross-Phase Modulation

Chapter 1 Introduction

This introductory chapter outlines the basic overview of the supercontinuum generation background along the broadband laser sources, the motivation, and objective of this thesis and lists the major contribution of work accomplished. This chapter also outline the organization of thesis. Section 1.1 introduces the background and motivation of the research, 1.2 states the research objectives and sections 1.3 and 1.4 present the major contribution achieved in this thesis and the provides the outline of whole thesis respectively.

1.1 Background and Motivation

Broadband laser sources: the sources that covers the laser emission over a broad wavelength region have attracted many researcher's attention due to their potential applications in many fields such as in spectroscopy and biomedical field. There is no such a broadband laser source which is available readily, possible way to achieve such broadband laser sources is to use the frequency conversion techniques using the available laser sources and the nonlinear media. One of the best possible and reliable techniques to achieve such broadband laser sources is "supercontinuum (SC)" generation. SC is a process of generating broadband optical spectrum by launching optical pulses into a nonlinear medium, continuous interaction of laser pulses with the nonlinear optical medium leads to the emission of a wider optical spectrum with a bandwidth many times greater than the bandwidth of the launched pulses. The key nonlinear physical phenomena involved in this process are stimulated Raman scattering (SRS), modulation instability (MI), cross-phase modulation (XPM), self-phase modulation (SPM), four-wave mixing (FWM) and soliton related dynamics. The first demonstration of SC generation in bulk media was reported by Alfano and Shapiro in 1970 [1-2]. Since then, this research field remains interesting for many researchers and it has

enormous attractive application potential in the field of optical coherence tomography [3], micromachining [4], nonlinear frequency conversion [5], LIDAR [6] and many more.

The SC generation strength depends on the interaction length of the seed laser with the nonlinear medium and nonlinearity of the medium. Therefore, optical fibres are preferred for flat and broadband SC generation providing very efficient seed laser beam confinement in a small fibre core over a long distance. Moreover, fibre-based SC sources are attractive, offering great reliability, stable and compact design. Realization of SC sources from all-fibre-based design consists of at least two parts: a nonlinear medium and a seed laser. In addition, to achieve high SC output power a cascaded amplifying system is added followed by the seed laser. There are a variety of fibres that can be used as a nonlinear medium such as single mode fibre (SMF), highly nonlinear fibre (HNLF), photonic crystal fibre (PCF), and many more special, and soft glass fibres. Each fibre has its own merits and demerits when it comes to SC generation, which will be discussed further in the literature review. The seed laser can generate femtosecond (short pulses), picosecond or nanosecond (longer pulses) or even continuous-wave (CW) light, which then needs to be amplified to achieve the required power level. It is worth stating here that the SC generation using CW laser as the seed has the advantages of lower cost, higher stability and simpler design when compared to pulsed seed lasers. However, the spectrum broadening efficiency of a CW laser is on the much lower side than in the case of pulsed lasers, which forces to use the longer nonlinear fibres. Moreover, achieving the high output power with the CW laser is a quite challenging task. Therefore, pulsed lasers are preferred as pump sources to achieve high SC output power and to cut down the fibre length [7].

The flatness and bandwidth of the SC spectrum depend on the relationship between the pump wavelength and zero-dispersion wavelength (ZDW) of the nonlinear medium, and the duration of pump pulse [8]. Depending upon the region i.e. normal dispersion region or anomalous dispersion, in which the fibre is pumped and the pump duration decides the dominant nonlinear phenomena that are responsible for the spectral broadening inside the fibre and it also decides the SC spectrum dynamics. Suppose the fibre is pumped with longer pulses in normal dispersion region, the spectral broadening and SC dynamics is dominantly decided by SRS and FWM, when it comes to short pulses, SPM is the dominant processes [9]. Whereas in anomalous dispersion region, MI is the main nonlinear phenomena for longer pulses [9] and, soliton fission [10] and soliton self-frequency shift [11] is responsible for spectrum broadening in case of short pulses.

To offer the possibility of broad and flat SC spectrum generation from a nonlinear fibre, efficient activation of nonlinear properties is much needed. Such nonlinear properties activation is possible with the high input power. However, achieving high power with CW lasers is quite a challenging task as compared to pulsed lasers. Pulsed lasers can be obtained by applying a mode-locking technique to the CW laser. Mode locking is a technique in which the phase relationship among many neighboring longitudinal modes is matched by imposing periodic loss over the CW laser signal in the cavity of each roundtrip. This kind of phase locking can be obtained by active or passive methods. Each of these mode-locking techniques has its unique way of producing the optical pulse with different attractive properties. Through active mode-locking technique, optical pulses with high pulse quality and high repetition rates can be generated. However, pulse duration and pulse peak power are limited. On the other hand, higher peak power and shorter pulse width can often be achieved through passive mode-locking technique, and after amplification, it can be boosted to over 1 MW of peak power [12-

13]. Such high peak power and short pulse width systems are attractive in nonlinear optics to generate SC [14]. There are various passive mode-locking techniques available to date such as nonlinear polarization rotation (NPR) [16], nonlinear amplifying loop mirrors (NALM) [15], and saturable absorbers (SA) [17-18]. Among these, SA-based mode-locking is preferred to be more environmentally stable and efficient over NPR and NALM [19]. There is a different kind of SAs available such as carbon nanotubes (CNTs) [18], semiconductor saturable absorber mirrors (SESAMs) [17], and graphene recently [20-21]. Throughout this project, CNT based SAs has been chosen for experiments to achieve passive mode-locking due to its attractive properties such as ease of fibre integration, ultrafast recovery time and cost-effective production [18, 22-24].

1.2 Objective

The objective of this project is to generate the broadband SC using femtosecond CNT-based passively mode-locked EDFL as the seed pulse and specialty fibres such as PCF, HNLF and ZBLAN fibre as the nonlinear media. It covers: 1. the generation of passively mode-locked femtosecond pulse from EDFL using CNT as SA; 2. study of spectral broadening phenomena inside PCF, HNLF and ZBLAN fibre with respect to the variation in input pulse power; 3. Study of spectral broadening with respect to the variation in nonlinear media length; 4. observing the effect of tapering on spectral broadening.

1.3 Major Contributions

The original contribution of this thesis as follows:

- Demonstrate the generation of passively mode-locked femtosecond EDFL using CNTs as the SA. In the mode-locked condition, CNT-SA-based EDFL produced a femtosecond

pulse train with a repetition rate of 18 MHz having optical pulse spectrum center wavelength at ~1565 nm with a 3 dB bandwidth of ~5 nm. The mode-locked laser pulse has a pulse width of 620 fs. The average power achieved through the passive mode-locking is 0.21 mW. The pulse has the peak power of 18.5 W with pulse energy of 11.76 pJ.

- Demonstrate the broadband SC spectrum generation from highly nonlinear PCF and spectral broadening variation inside PCF with respect to the variation in the input pulse power. The input pulse power is varied from 0 dBm to 20 dBm and observed a 20 dB bandwidth of 1050 nm SC spectrum spanning from 1080 nm to 2130 nm.
- Demonstrate the broadband SC spectrum generation using HNLF and spectral broadening variation inside the HNLF with respect to the variation in the input pulse power. The input pulse power to the HNLF is varied from 0 dBm to 20 dBm and observed a 20 dB bandwidth of 1400 nm SC spectrum extending from 1050 nm to 2450 nm. The variation of spectral broadening with respect to the HNLF length is demonstrated. The length of the fibre is varied from 30 cm to 1 m and the variation of SC spectral broadening is observed by applying a tapering ratio of 2 with different tapering lengths.
- Demonstrate the broadband SC spectrum generation from ZBLAN fibre and spectral broadening variation inside the ZBLAN fibre with respect to the variation in input pulse power. The input pulse power to the ZBLAN fibre is varied from 0 dBm to 25 dBm and observed a 20 dB bandwidth of 2000 nm SC spectrum covering from 1100 nm to 3100 nm.
- The novelty of this thesis work is that, for the first time CNT-based femtosecond pulse is used as seed to generate broadband SC spectrum from the three different nonlinear

fibres PCF, HNLF and ZBLAN fibre. Able to generate broadest spectrum from 100-cm-long HNLF at the minimal input pulse power of 20 dBm. Tapering is applied on HNLF to further reduce the length of the fibre at the achieved SC spectrum bandwidth of 1400 nm spanning from 1050 nm to 2450 nm. The complexity of the experimental setup is reduced by simply using the single stage amplification input pulse power. For the first time to my best knowledge, a CNT based passively mode-locked femtosecond EDFL based SC generation in ZBLAN fibre is demonstrated.

1.4 Thesis Organization

The thesis is organized as follows:

Chapter 1 gives a brief introduction to the research project including motivation, objective and major contribution.

Chapter 2 introduces the fundamental principles of laser, laser mode-locking, passive mode-locking and SA-based passive mode-locking. Different ways of SC generation were given. The SC generation fundamentals i.e. the basic nonlinear phenomena responsible for spectral broadening inside the fibre media and also the different regimes of pulse propagation inside the nonlinear fibre under the influence of fibre nonlinearity and fibre dispersion. The nonlinear phenomena such as SPM, FWM, SSFS, and SRS were explained in detail to understand the phenomena of SC spectral dynamics. The background of available SC laser sources is reviewed.

Chapter 3 presents the experimental generation of passively mode-locked femtosecond erbium-doped fibre laser (EDFL) incorporating carbon-nanotubes as a saturable absorber in the ring cavity.

Chapter 4 presents the generation of a broadband SC in specialty fibres such as in Highly nonlinear PCF and HNLF using femtosecond CNT-SA-based passively mode-locked EDFL. Spectral broadening phenomena inside PCF and HNLF with respect to the input pulse power variation have been demonstrated. The HNLF length also have been varied to study the effect of fibre length variation on SC spectral dynamics such as bandwidth and flatness. Tapering has been applied on the short-piece of HNLF and studied the tapering ratio and tapering length effect on SC spectral dynamics.

Chapter 5 demonstrates the generation of broadband mid-infrared (mid-IR) SC generation inside the soft-glass ZBLAN (ZrF4-BaF2-LaF3-AlF3-NaF) fibre. The spectral broadening phenomena inside ZBLAN fibre have been demonstrated with respect to the variation in input pulse power.

Chapter 6 gives the conclusions to the research accomplished and recommends the possible future works.

Chapter 2 Literature Review

This chapter introduces the fundamental principles of laser and CNT-SA-based passive mode-locking. The SC spectrum generation fundamentals i.e. the basic nonlinear phenomena (SPM, SRS, FWM, and SSFS) responsible for spectral broadening inside the fibre media and also the different regimes of pulse propagation inside the nonlinear fibre media is explained. The background of available SC laser sources is reviewed.

2.1 LASER Principle

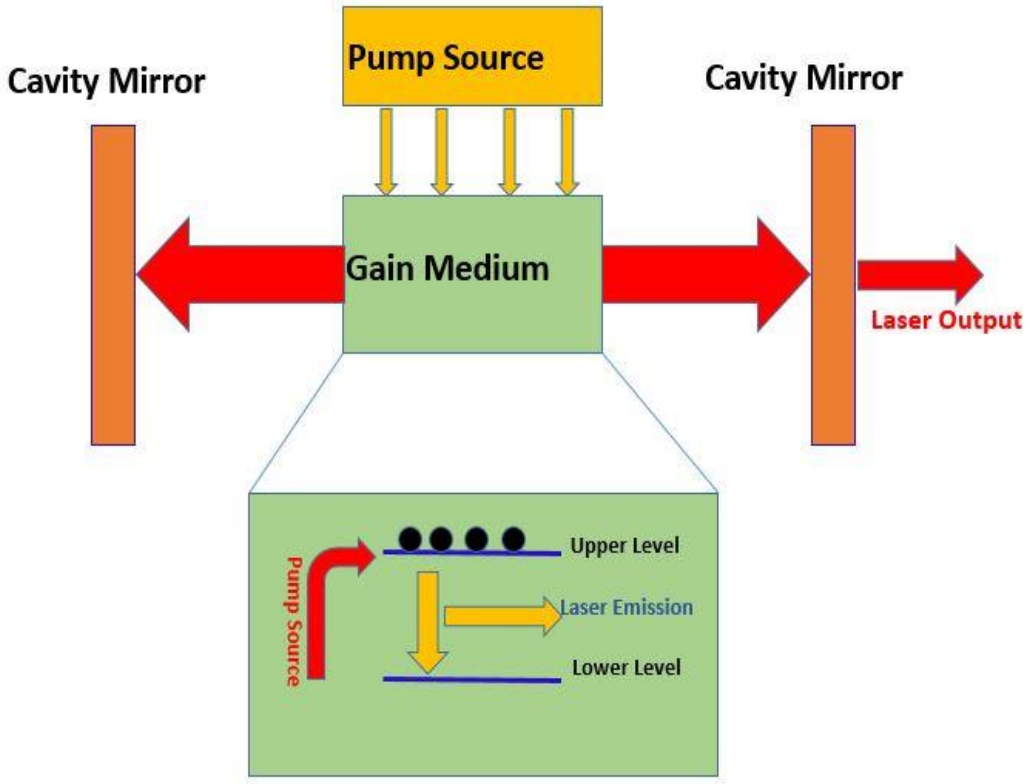

Figure 2. 1 Basic schematic of laser setup

The LASER is an acronym for Light Amplification by Stimulated Emission of Radiation. In early 1917's Albert Einstein predicted the possibility of constructing a laser by using the concept of "stimulated emission". Four decades later, the theory was proposed, Theodore Maiman was the first person who demonstrated the first laser as Ruby laser and Ali Javen

demonstrated first He-Ne laser [25]. When compared with other conventional light sources, the laser has unique characteristics such as highly directionality, high intensity and long coherence length.

A typical laser looks like as shown in Figure 2.1, it includes three essential parts: active laser medium or gain medium to give amplification through stimulated emission, a cavity for laser oscillations and pump source to supply energy to the gain medium to achieve population inversion which is responsible for amplification through stimulated emission.

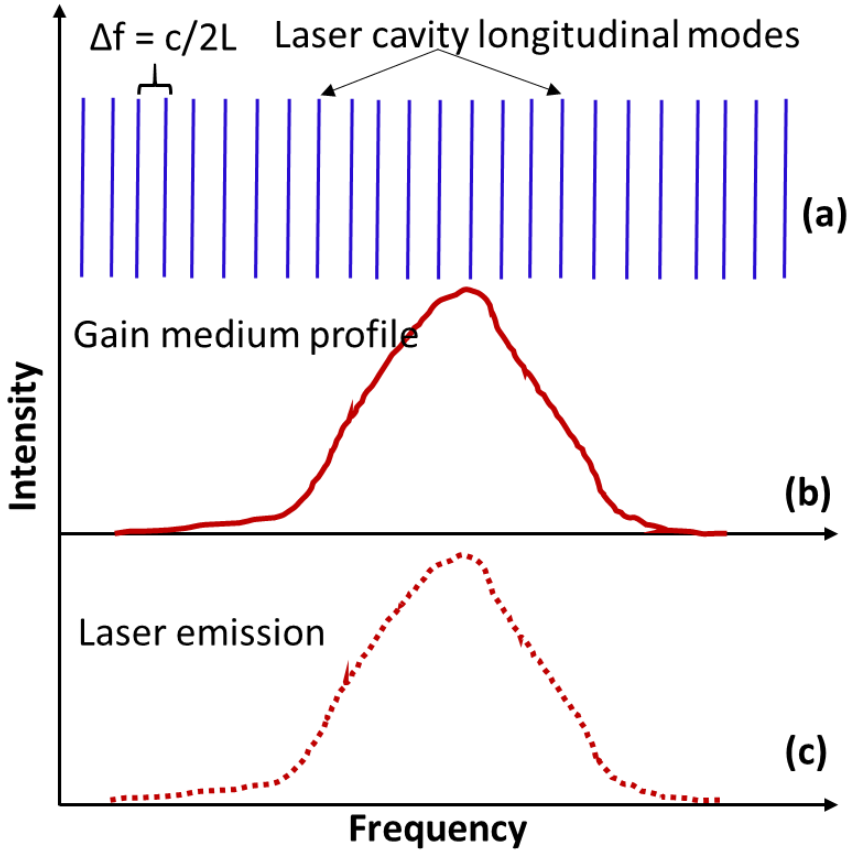

Figure 2. 2 The laser emission process: (a) Laser cavity longitudinal modes, (b) Laser Gain medium profiles, (c) laser emission frequency range

Figure 2.2. (a) shows the longitudinal modes of the laser cavity which arises from the formation of the standing waves between the laser cavity mirrors. The two mirrors in the laser cavity act as a resonator and the light interfere constructively and destructively when it

bounces between the mirrors and leads to the formation of standing waves. The longitudinal modes oscillate constructively at certain frequencies and all other frequencies are suppressed by the destructive interference. The frequency separation (Δf) between any two adjacent longitudinal modes is decided by the length (L) of the cavity or the distance between the two mirrors as follows:

$$\Delta f = c/2L \tag{2.1}$$

Where c is the speed of light (≈ 3×10^8 m/s).

Even though the cavity emits many longitudinal modes at different frequencies, only a few frequency components experience amplification in each round-trip due to the finite bandwidth of the gain medium. Therefore, the laser cavity emission frequency range is decided by the bandwidth of the gain medium and the resonator. Figure 2.2 (b) shows the gain medium profile and Figure 2.2 (c) shows the laser emission frequency range.

2.2 Fibre Laser Classification

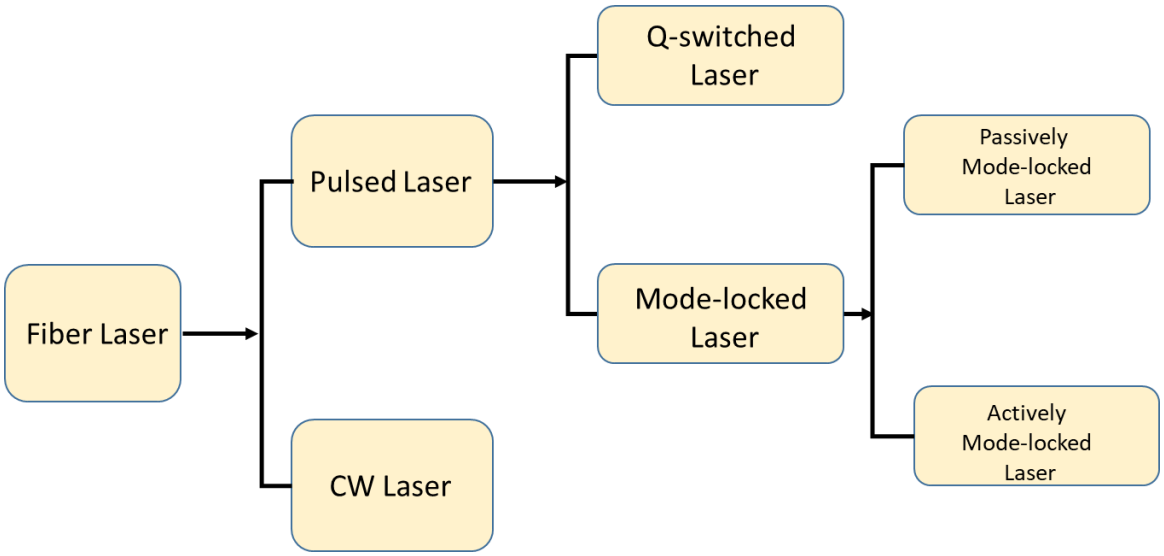

Figure 2. 3 Fibre laser classifications: CW: continuous wave.

Koester and Snitzer demonstrated the first fibre laser in 1963 [26], using Nd-doped glass fibre as the gain medium and achieved the laser output at 1061 nm. Various fibre lasers at different emission wavelengths with different output powers are developed to meet the requirement of various applications. Based on the nature of the fibre laser output, the fibre lasers are classified into two types: continuous wave (CW) lasers and pulsed lasers as shown in Figure. 2.3. The output of the CW laser is a continuous wave in the time domain with a constant output power and emit a narrow line-width light almost at a mono-frequency. Whereas, the pulsed lasers show the discrete nature in the time domain which emits optical pulses at a certain time period with a wide spectral bandwidth. Pulsed lasers are very useful and widely used in laser surgery, manufactory and nonlinear optics due to its high peak power. Pulsed lasers can be generated by applying two mechanisms on CW laser: Q-switching and mode-locking. Out of two, a mode-locking mechanism based pulsed fibre lasers show excellent performance in terms of pulse repetition rate, pulse width, peak power and spectral bandwidth. The following section explains the fundamentals of mode-locking.

2.3 Mode-Locking Fundamentals

The mode-locked lasers can be drawn from the Lamb's work where he investigated the mode-locking of three modes in frequency domain [27]. DiDomenico predicted the mode-locking theoretically in 1964 [28]. The first mode-locked laser was demonstrated in the same year by Hargrove *et al* [29]. By means of internal modulation using an acoustic-optical modulator, stabilization of frequency and amplitude of the modes in He-Ne laser was achieved. An optical pulse train of 2.5 ns pulse width with a repetition rate of 56 MHz was observed.

Mode-locking is the technique, in which locking-in the phase of many logitudinal modes of the laser cavity. As shown in Figure. 2.1, as the laser light is confined within the two cavity

mirrors, it emits laser light at discrete resonance frequencies which are referring to them as cavity longitudinal modes as shown in Figure.2.2 (a). These discrete longitudinal modes can emit from the cavity if the cavity gain is greater than the cavity loss. Each longitudinal mode doesn't operate at a single frequency rather it has a narrow range frequency or bandwidth over which it operates, decided by the finesse of the laser cavity. The bandwidth of each longitudinal mode is much smaller than the inter-mode frequency spacing or the frequency separation between the two adjacent longitudinal modes ' Δf ', therefore assumed them as idle plane wave and then the multi-mode lasing can be described as shown in the equation 2.2.

$$E_i(t) = \sum_{i=0}^{N-1} E_i exp[j(2\pi f_i t + \emptyset_i)] \tag{2.2}$$

Where E_i is the electrical field amplitude , $f_i = f_0 + i\Delta f$ (f_0 is the carrier frequency, *i* is an integer), $\emptyset_i$ is the phase of i^{th} longitudinal mode, respectively. The frequency of each longitudinal mode is fixed by the laser cavity and the phase of each mode is arranged randomly and, the amplitude of each mode is different. To make it simple, let's consider all the longitudinal modes have a same and equal amplitude E_0, and the phase of all modes is locked :

$$\emptyset_i = \emptyset_{i+1} = 0 \tag{2.3}$$

$$E_i = E_0 \tag{2.4}$$

By applying the above two conditions then the output power $(I(t))$ of the mode-locked laser is:

$$I(t) = |E(t)|^2 = \left| \sum_{i=0}^{N-1} E_0 exp[j(2\pi f_i t + 0)] \right|^2$$

$$= E_0{}^2 \left| \sum_{i=0}^{N-1} exp\, j(2\pi f_i) \right|^2$$

$$= E_0{}^2 \frac{sin^2(N\Delta\omega t)}{sin^2(\frac{\Delta\omega t}{2})} \quad (2.5)$$

Where $\Delta\omega = 2\pi\Delta f$ is the frequency separation between two adjacent longitudinal modes and *N* is the total number of longitudinal modes. After mode-locking, the laser cavity emits a periodic pulse train which looks like as follows in Figure 2.4.

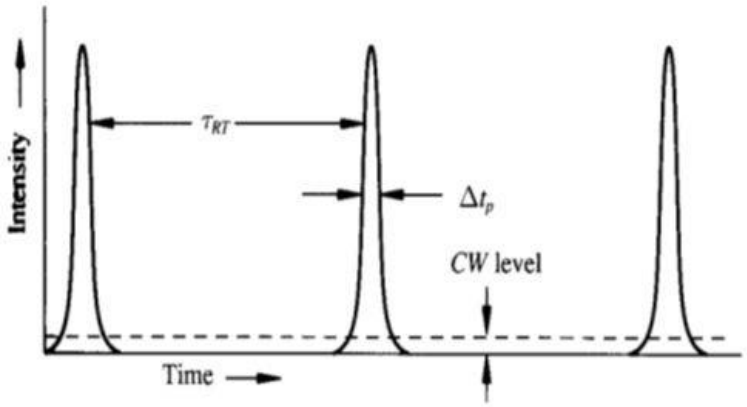

Figure 2. 4 Schematic of mode-locked laser emission.

The peak power of each mode-locked laser pulse is equaled to 'NE_0^2', repetition rate $\tau_{RT} = 1/\Delta f$ and pulse width $\Delta t_p = 1/N\Delta f$. The peak power and the pulse width depend on the number of modes that are phase-locked. Therefore, the more the longitudinal modes phase-locked, the narrower the pulse width and then higher pulse peak power. The different mode-locking techniques is given in the following section

2.4 Different Mode-Locking Techniques

The laser cavity as shown in Figure 2.1, emits only CW laser, in order to achieve laser pulses from CW laser, an additional component such as loss modulator (LM) is required as shown in

Figure 2.5. To achieve mode-locking, periodic modulation of a laser signal inside the laser-cavity is an effective method [6]. The LM induces periodic loss over the CW signal in each roundtrip of the cavity, leads to the breakup of CW signal into a sequence of the optical pulse train. Depending upon the LM type, there are two types of mode-locking techniques: active mode-locking and passive mode-locking as shown in Figure 2.6.

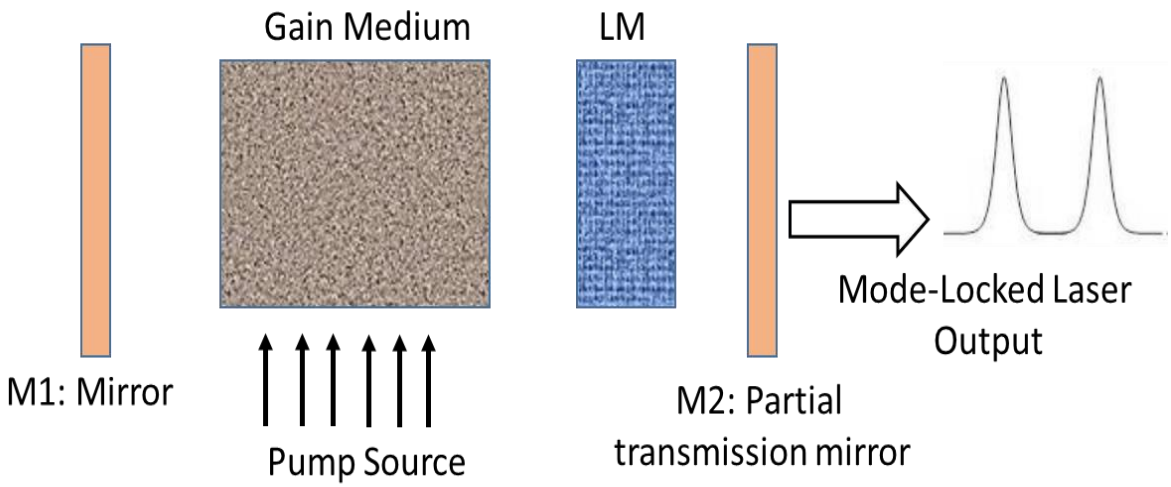

Figure 2. 5 Schematic of mode-locked laser: LM: Loss modulator.

If the LM is of active device type, then the mode-locking technique is labeled as active mode-locking technique and the laser is called as an actively mode-locked laser. In case of active mode-locking, an LM (electro-optic modulator (EOM)) modulated by an external signal should be applied. The modulator can be a phase modulator (FM) or an amplitude modulator (AM) [31,32]. On the other hand, the LM can be of passive device types such as nonlinear polarization rotation (NPR), nonlinear amplifier loop mirror (NALM) and saturable absorber (SA), therefore the mode-locking technique is called as passive mode-locking technique and the laser is labeled as a passively mode-locked laser. A detailed description of passively mode-locked fibre lasers is given in the next section. In this project, the passive mode-locking

technique is used to generate laser pulse and then observe the SC spectral variation inside different fibres by using passively mode-locked laser pulse as seed laser.

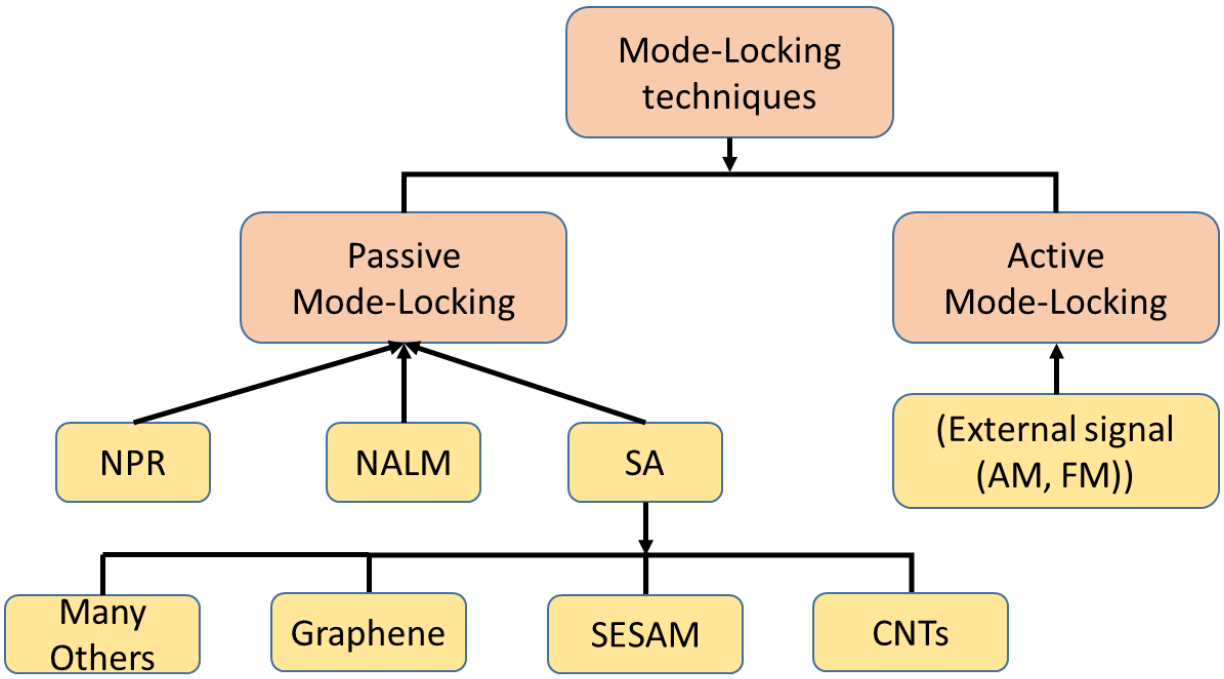

Figure 2. 6 Classification of mode-locking techniques: NPR: nonlinear polarization rotation, NALM: nonlinear amplifying loop mirror, SA: saturable absorber, SESAM: semiconductor saturable absorber mirror, CNTs: carbon-nanotubes, AM: amplitude modulator, FM: frequency modulator

2.5 Passively mode-locked Fibre Lasers

In 1965, Mocker and Collins were observed the passive mode-locking for the first time in Q-switched laser, however, the mode-locking was unstable [33]. In 1972, Ippen, Shank, and Dienes for the first time demonstrated the stable passively mode-locked laser and achieved a 1.5 ps pulse train in a dye laser [34]. After 20 years of the first fibre laser demonstration, the mode-locked fibre laser was reported for the first time in 1984 by Mollenauer and Stolen [35]. Thereafter the passively mode-locked fibre lasers have attracted many researchers to investigate thoroughly and have been developed different passively mode-locked fibre lasers for different applications. The stable passively mode-locked fibre laser pulses with ultra-short

pulse width, ultra-low jitter and high pulse energy has been achieved with different cavity designs [36-38].

2.5.1 Passive mode-locking

As mentioned in the previous section there are two types of mode-locking mechanisms that involved in achieving pulsed lasers: passive mode-locking and active mode-locking. In active mode-locking technique, to achieve mode-locking an external signal source needs to applied whereas in passive mode-lock technique it doesn't need any external signal source [34]. A passive component called the saturable absorber (SA) must be incorporated in the laser cavity to achieve mode-locking in passive mode-locking technique as shown in Figure 2.7.

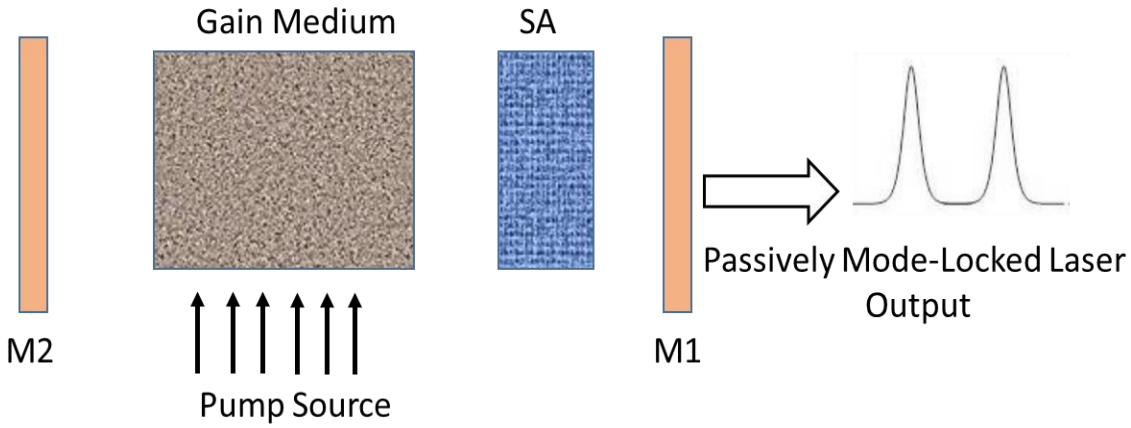

Figure 2. 7 Schematic of the passively mode-locked laser; M1: partial transmission mirror, M2: Mirror, SA: saturable absorber.

The SA is an intensity dependent passive optical device [39]. The mirrors M1 and M2 form a cavity structure to provide oscillation and SA component provide "positive feedback" to the laser cavity which provides higher transmission to the higher intensity optical components. The SA behaves differently to different intensity components i.e. it imposes a high loss on low-intensity optical signal and low loss on the high-intensity optical signal. This process

repeats in each roundtrip as the signal oscillates between the mirrors and leads to the absorption of low-intensity signal and amplification of the high-intensity signal. This process builds up a train of optical pulses after many oscillations and leads to the emission of a mode-locked laser pulse train. The mirror-based passively mode-locked laser structure can be replaced using the laser ring cavity structure as shown in Figure 2.8.

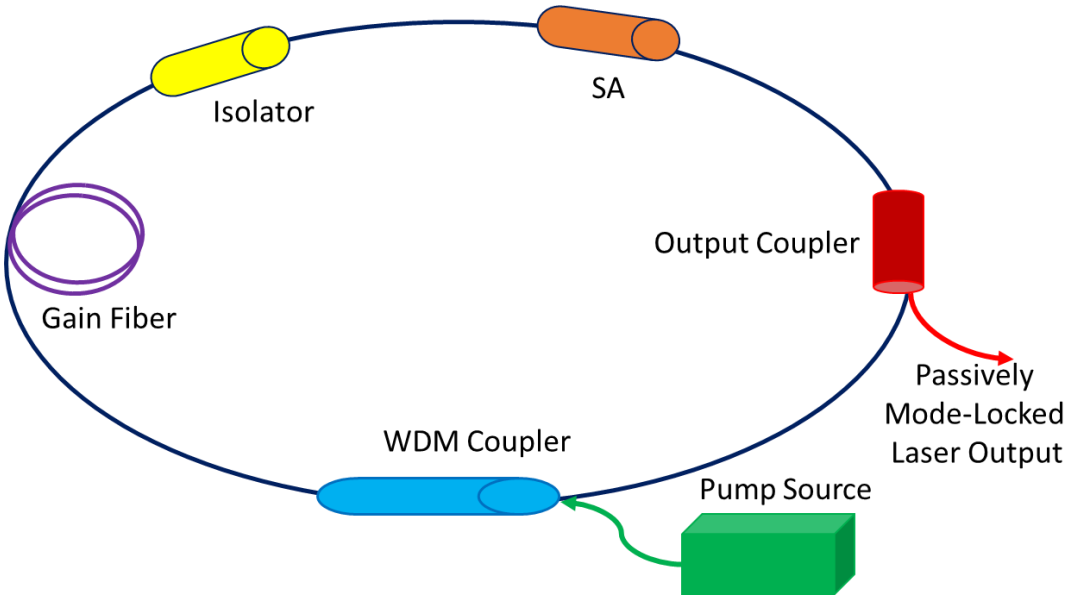

Figure 2. 8 Schematic of passively mode-locked fibre laser ring cavity; SA: saturable absorber, WDM: wavelength-division-multiplexing.

Figure 2.8 shows the schematic of passively mode-locked fibre laser using a fibre ring cavity structure. Depending upon the output wavelength requirement, different gain fibres and different pump wavelengths can be used. Here ring structure serves the purpose of mirrors and provides the oscillations for efficient mode-locking.

The concept of passive mode-locking can also be understood from the view of frequency domain. The SA acts as a modulator and modulates the light in the laser cavity periodically with a time period of a roundtrip. In most of the passively mode-locked fibre lasers, the laser emits a mode-locked pulse train at a fundamental repetition rate as the SA modulation

frequency is equal to the fundamental frequency of the laser ring cavity. SA based mode-locking can be termed as self-sustaining and self-starting mode-locking as it doesn't need any external signal reference to achieve mode-locking.

As the modulation frequency equals to the fundamental frequency of the laser cavity which is low and due to long laser cavity length, the repetition rate of the passively mode-locked fibre laser is on the much lower side compared to the actively mode-locked fibre laser. However, the repetition rate of the passively mode-locked fibre lasers can be increased by employing the harmonic mode-locking but it experiences high noise and poor stability [40]. When compared to actively mode-locked laser pulses, passively mode-locked laser pulses on much shorter pulse width side i.e. in the range of femtosecond (fs) and provides much higher pulse peak power which can be easily boosted to over 1 MW [12-13]. Such ultra-short high peak power pulses are very attractive in nonlinear optics, micromachining and laser drilling.

2.5.1.2 Saturable Absorbers

The SA is an intensity-dependent passive optical device. There are many mechanisms that can serve the function of SA. Semiconductor materials can provide saturable absorption at specific wavelength in the form of quantum dots or quantum wells [41-43]. As shown in the Figure 2.6, there are other methods based on fast artificial saturable absorption including NPR, NALM, SPM in nonlinear loop mirrors (NOLMs) and Kerr-lens mode-locking [44-50]. The most widely used SAs for passively mode-locked fibre lasers are SESAM, CNT, and graphene.

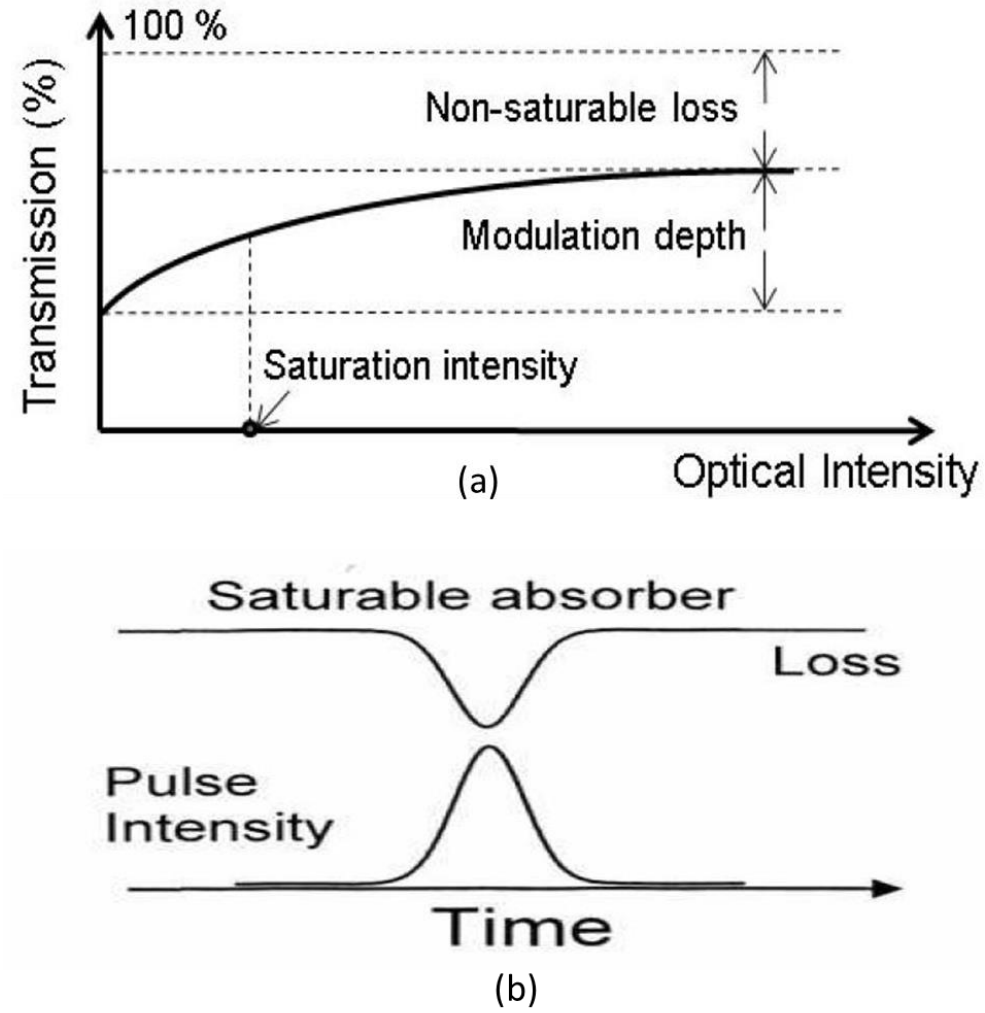

Figure 2. 9 Schematic representation of (a) SA nonlinear transmission (b) the SA-based pulse reshaping [51, 52].

The SA acts as LM in the cavity and plays a significant role in the formation optical pulse train in passively mode-locked fibre lasers. Figures 2.9 (a) and (b) show the interaction of a SA with an incident optical pulse. Due to the intensity-dependent absorption of SA, the optical pulse under different absorption at different intensity levels while it passes through the SA. The trailing and leading edges of the optical pulse are cleared up by the strong absorption due to low intensity. Whereas the center part of it passes through the SA with low attenuation as it has high intensity, which leads to the enhancement of optical pulse signal-to-noise ratio (SNR). This kind of pulse-reshaping is very crucial in the initial phase of pulse formation. At

certain input pump power, the pulse gradually built-up after several oscillations and emits a soliton-like pulse.

In general, there are four parameters that are used to evaluate the performance of SA: saturation intensity, modulation depth, recovery time, and non-saturation loss as shown in the Figure 2.9 (b). The recovery time of the SA corresponds to the decay time of excitation after exciting a pulse. If the recovery time is smaller than the duration of pulse then the SA is labeled as a fast SA. On the other hand, it is a slow SA. The saturation intensity denotes the optical intensity where saturable absorption is reduced to the half of its unbleached value. This one determines the threshold power to achieve mode-locking in a laser. The non-saturation loss refers to the intrinsic absorption of a SA at the unbleached value. The difference between the maxim and minimum absorption gives the modulation depth of a SA. The modulation depth determines the pulse reshaping capability of a SA.

2.7 Supercontinuum Generation Fundamental

Supercontinuum (SC) generation is the process of generating broadband optical spectrum by launching high intense optical pulse inside the highly nonlinear fibre medium. The reason for spectral broadening through the new frequency generation inside the fibre medium is due to the nonlinear interaction of the pulse with the fibre medium. Broadband SC can be generated in different ways such as by launching long or short optical pulses into different kind of optical fibres such as normal single-mode fibre or specialty fibres. Depending upon the input pulse characteristics and the fibre medium, different nonlinear properties will act on the propagating pulse and generates broad optical spectrum with a bandwidth many times greater than the input optical pulse.

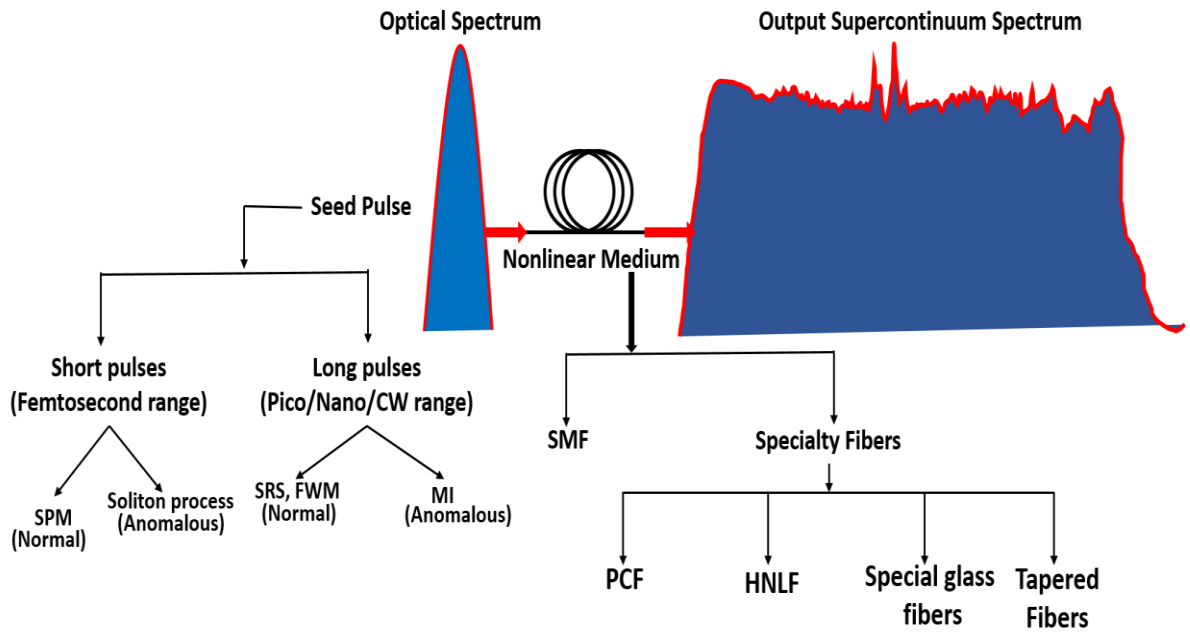

Figure 2. 10 Schematic illustration of SC generation process.

Figure 2.10 shows the possible ways of SC generation and different nonlinear properties responsible for spectral broadening inside various fibres. Suppose the input seed pulse is launched in femtosecond regime, then SPM is the dominant nonlinear phenomena responsible for spectral broadening in the normal dispersion region and, in anomalous dispersion region soliton process is dominant nonlinear phenomena. In case of long pulses such as picosecond/nanosecond/CW laser, stimulated Raman scattering (SRS) and FWM are key nonlinear phenomena responsible for spectral broadening in normal dispersion region and MI is responsible for spectral broadening in anomalous dispersion region. Coming to the nonlinear medium, there are variety of fibres such as single-mode-fibre (SMF) and specialty fibres. SMF as a nonlinear medium can generate reasonable SC but the problem is very high input power needs to be applied to the fibre to activate nonlinear properties, where these are very week in normal glass fibres. By using specialty fibres like PCF, HNLF, ZBLAN, and

tapered fibres, very broad and flat SC spectrum cab be generated at low input powers when compared to normal fibres.

Specialty fibres are the optical fibres that are having at least one specialty when compared to standard optical fibres. One of the many applications of the specialty fibres is the new frequency generation through nonlinear conversion. The nonlinear properties that are possessed by the specialty fibre can cause new frequency generation. They occur either due to intensity dependence of the refractive index of the fibre or due to the inelastic scattering phenomenon. The intensity dependence is due to the Kerr effect, which manifests itself to several nonlinear effects such as SPM, XPM, MI, soliton-self frequency shifts and FWM. At high power levels, Raman scattering is responsible for the nonlinear effects [53]. If the specialty fibre is not properly designed with phase-matching condition, which is a condition necessary to produce an efficient nonlinear interaction in a medium, as well as the incident beam being a single pulse, the generated SC generated can be considered as a result of SPM. While SPM occurs due to phase modulation of the pulse itself, XPM occurs due to co-propagating pulses, where the optical phase of a light experiences a change due to interaction with the co-propagating beam [54]. Coming to FWM, which is a phase-sensitive process, its effect can efficiently accumulate over longer distances only if the phase matching condition is satisfied. Otherwise, when there is a strong phase mismatch, FWM is effectively suppressed.

It is important to note that the nonlinear effects depend on group velocity dispersion (GVD) of the fibre, which is the group velocity in a medium that is dependent on the optical frequency. GVD is responsible for compression of ultrashort pulses or dispersive temporal broadening. Depending on dispersion properties and regimes at which the optical beam is

pumped, the SC spectral profile may differ, therefore dispersive effects have to be taken into account for SC generation [55]. One of the methods to achieve a flat SC spectrum is to use a fibre of high nonlinearity and pumping the source in normal dispersion regime [56]. Whilst it is usually more common to achieve substantial broadening through pumping into the anomalous regime whereby soliton effects are predominantly responsible for broadening, with the use of ultra-short pulses, SPM can cause significant spectral broadening. Therefore, knowing the nonlinear dispersive effects that happen inside the optical fibre, the Nonlinear Schrödinger's Equation is the most suitable form of equation that can help explain the effects that occur at different instances along the fibre. The parameters that are comprised in the equation clearly represent the effects that take place. Since supercontinuum generation is very multi-dimensional, where there are several parameters that influence the resulting output spectrum, it can make solving it to be quite confusing. However, the solution to NLSE possesses clear parameters that represent the effects that take place. Whether it is dominantly dispersive, nonlinear or the interplay of these effects. Understanding of NLSE helps us to interpret the experimental results in the best possible way. Therefore, in the following sections, the key parameters such as fibre dispersion and fibre nonlinearity are given, the optical pulse propagation inside single mode fibre is explained, the Nonlinear Schrödinger equation is derived and the different regimes of pulse propagation in the optical fibre in the presence of different nonlinear phenomes is explained.

2.8 Analysis of Pulse Propagation inside the Optical Fibre

In order to better understand the pulse propagation in optical fibres, the effect of fibre parameters on the pulse propagation such as dispersion and nonlinearity is discussed here. The main role of the passive fibre is to support pulse propagation whereas active fibre is to give amplification to the pulse. While pulse propagates through passive fibre, it experiences

two effects one is chromatic dispersion and other one is self-phase modulation. With the help of NLSE, two effects experienced by the pulse when it propagates through the passive fibre such as the chromatic dispersion *i.e.* the dependency of phase velocity on the optical frequency when optical pulse interacts with the dielectric medium which is responsible for pulse broadening and self-phase modulation *i.e.* self-induced shift experienced by a high intense optical pulse can be easily explained.

2.8.1 Optical Fibre Dispersion

The major dispersion in the optical fibre is chromatic dispersion which refers to the optical pulse with different frequencies experiences different group velocities when it interacts with the dielectric medium. The origin of dielectric medium chromatic dispersion is related to the resonance frequencies where the dielectric medium absorbs the electromagnetic radiation through oscillations of bound electrons [57]. So the different frequencies experience different refractive indexes of the dielectric medium:

$$n^2(\omega) = 1 + \sum_{i=1}^{q} \frac{B_i \omega_i^2}{\omega_i^2 - \omega^2} \qquad (2\text{-}6)$$

Where ω_i is the resonance frequency, B_i is the strength of ith – order resonance. For a given medium ω_i and B_i can be determined. The speed of the light in medium is related to the refractive index of the medium *i.e.*$c\ /\ n(\omega)$ different frequency components of the pulse travel with different speed which is known as chromatic dispersion.

Chromatic dispersion is responsible for the broadening of optical pulse when it travels through optical fibre as the pulse contains different frequency components. This can be explained by expanding the mode-propagation constant β in Taylor-series at the center frequency of pulse spectrum (ω_0).

$$\beta(\omega) = \beta_0 + (\omega - \omega_0)\,\beta_1 + \frac{1}{2}(\omega - \omega_0)^2\,\beta_2 + \frac{1}{6}(\omega - \omega_0)^3\,\beta_3 + \cdots \qquad (2\text{-}7)$$

Where

$$\beta_q = \left(\frac{d^q\beta}{d\omega^q}\right)\omega = \omega_0 \qquad (q= 1, 2, 3 \ldots) \qquad (2\text{-}8)$$

$$\beta_1 = \frac{1}{v_g} = \frac{1}{c}\left(n + \omega\,\frac{dn}{d\omega}\right) \qquad (2\text{-}9)$$

Where v_g is group velocity and given as$v_g = c/n_g$, here $n_g = \left(n + \omega\,\frac{dn}{d\omega}\right)$ is the group refractive index and *c* is the speed of light in vacuum.

$$\beta_2 = \left(\frac{d\beta_1}{d\omega}\right) = -\frac{\lambda^2}{2\pi c}\,\frac{d\beta_1}{d\lambda}$$

$$\beta_2 = \frac{1}{c}\left(2\frac{dn}{d\omega} + \omega\frac{d^2n}{d\omega^2}\right) \qquad (2\text{-}10)$$

Where β_2 is called the group velocity dispersion (GVD) and this is responsible for the pulse broadening.

2.8.2 Nonlinearity of the Optical Fibre

In linear optics the refractive index of the medium is only the function of incident optical signal frequency whereas in nonlinear optics the refractive index of the medium is the function of both incident optical signal frequency and optical power as well, this can be explained by Kerr effect. The dielectric medium nonlinear response can be related to the harmonic motion of bound electrons to the incident optical field. The induced electric polarization (P) inside any material in the presence of intense optical filed can be written as follows.

$$\tilde{P} = \varepsilon_0 \{ \chi^1 . \tilde{E} + \chi^2 : \tilde{E}\,\tilde{E} + \chi^3 \vdots \tilde{E}\,\tilde{E}\,\tilde{E} + \cdots \} \quad (2\text{-}11)$$

Where χ^2 , χ^3 are the higher order susceptibilities of the optical medium which are responsible for the nonlinear effects in optical fibre but for the pure silica or glass fibre the second order susceptibility (χ^2) is negligible due to the symmetrical molecule structure of silica, so the lowest–order susceptibility responsible for nonlinear effect in optical fibre is third order nonlinear optical susceptibility χ^3 . This third order susceptibility is responsible for the nonlinear effects in optical fibre through four-wave mixing (FWM), third-harmonic generation (THG) and nonlinear refractive index. TGH and FWM are negligible in normal fibres where as in PCF, HNLF, ZBLAN fibre and tapered fibres these effects are responsible for new frequency generation along with nonlinear refractive index. In most of the cases the nonlinear effect is highly dominated by the nonlinear refractive index under the high intense optical field, which can represent as:

$$n(\omega, |E|^2) = n_0(\omega) + N_2 |E|^2 \quad (2\text{-}12)$$

Here $n_0(\omega)$ is the linear refractive index of the fibre which is a function of frequency and $N_2 |E|^2$ is nonlinear refractive index of fibre which is a function incident optical power intensity, this nonlinearity is called Kerr-Nonlinearity and the effect is called Kerr-effect. The nonlinear refractive index is a function of third order susceptibility and is given as follows.

$N_2 = \frac{3}{8 n_0} \chi^3$, for glass N_2= $3.2^{*}10^{-12}$ m²/W

Here N_2 represents the intensity-dependent refractive index which is responsible for the number of interesting nonlinear effects, most significant and widely investigated nonlinear effects are SPM and cross-phase modulation (XPM). SPM refers to the self-induced phase shift

experienced by an optical pulse while propagating through the nonlinear optical medium, the phase of optical pulse after propagating through such optical medium is changed by

$$\varphi = n(\omega, |E|^2)\, k_0\, L = (n_0(\omega) + N_2 |E|^2) k_0\, L \qquad (2\text{-}13)$$

Where *L* is the fibre length and $k_0 = 2\pi/\lambda$. The phase shift caused by self-phase modulation is given as:

$$\varphi_{NL} = N_2 |E|^2 k_0\, L$$

This nonlinear phase-shift φ_{NL} caused by self-phase modulation plays an important role in the spectrum broadening through new frequency generation. SPM is the self-induced phase shift where as XPM refers to the phase shift of an optical field induced by another optical field whose polarization, direction and wavelength are different. The nonlinear phase shift of optical field can be expressed as:

$$\varphi_{NL} = N_2 (|E_1|^2 + 2|E_2|^2) k_0\, L \qquad (2\text{-}14)$$

Here there are two terms in which first term represents the phase induced due to SPM and the second term represents the phase shift induced by XPM, which is responsible for the asymmetric spectral broadening.

2.8.3 Optical Pulse Propagation in Single-Mode Fibres

An optical fibre is a shallow cylindrical waveguide that confines optical signal within the core region (n_1) through total internal reflection, where core region is covered by cladding with lower refractive index (n_2) and followed by a plastic shielding for mechanical support and for protection from the environmental disturbances. The total internal reflection is possible in the optical fibre due to the refractive index variation of the core and cladding *i.e.*

the refractive index of core is slightly higher than refractive index of cladding ($n_2 < n_1$). The basic optical fibre structure and its refractive step index profile can be seen in the Figure 2.11.

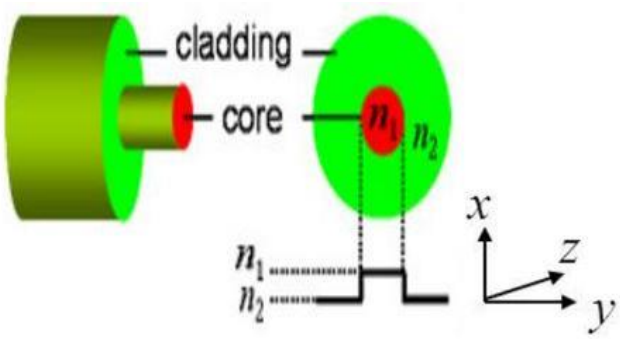

Figure 2. 11 Structural representation of optical fibre and its refractive step index profile. [58]

The optical fibre can be characterized by the two parameters: V number which decides the number modes that can be supported by the optical fibre and core-cladding refractive difference (Δ) and that are given as:

$$V = k_0 a (n_1^2 - n_2^2)^{\frac{1}{2}} \quad (2\text{-}15)$$

$$\Delta = \frac{(n_1 - n_2)}{n_1} \quad (2\text{-}16)$$

Where a the core radius and $k_0 = 2\pi/\lambda$, λ the wavelength of the incident optical signal. V number can decide whether the optical fibre supporting single mode of operation or multimode mode operation through it i.e. an optical fibre can be treated as single-mode fibre (SMF), where it will support only fundamental mode of propagation if it satisfied the condition $V < 2.405$.

Based on the slowly varying envelop assumption the mathematical expression for electric field of optical pulse propagating along SMF can be treated as a separation of variables in the longitudinal and the transverse direction as shown in the Figure 2.12. So the overall electric field $E(r,t)$ will be the product of modes propagating along transverse direction of fibre and the slowly varying envelop along with the phase variation as shown in the below equation.

$$E(r,t) \approx F(x,y)\, A(z,t) exp[i(\beta_0 z - \omega_0 t] \quad (2\text{-}17)$$

The first term *F(x, y)* in the right-hand side of the equation (2-16) represents the modes propagation distribution in transverse direction and the 2nd term *A(z, t)* represents the longitudinal directional propagation of slowly varying pulse envelop and the 3rd term $exp[i(\beta_0 z - \omega_0 t]$ represents the phase variation as a function of fibre length, incident optical pulse frequency and time. Where β_0 is the wavenumber corresponding to the centre wavelength ω_0. The optical spectrum $\tilde{A}(z, \omega - \omega_0)$ of pulse envelop can be derived by applying Fourier transform to it.

$$\tilde{A}(z, \omega - \omega_0) = \frac{1}{2\pi} \int_{-\infty}^{\infty} A(z,t) exp[\, i(\omega - \omega_0)t] dt \quad (2\text{-}18)$$

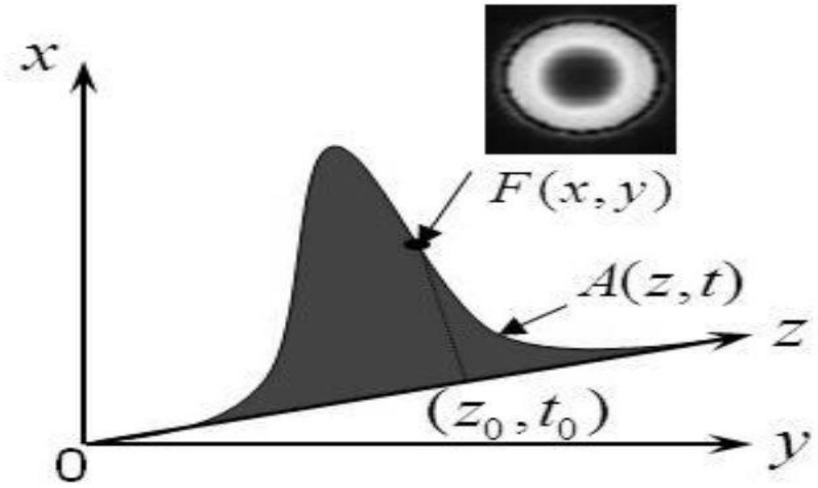

Figure 2. 12 Graphical representation of an optical pulse electric field. [51]

As the transverse mode distribution of *F(x, y)* is almost constant with the time when the fibre geometrical parameters are present. So the optical pulse electric field in frequency-domain can be simplified as follows:

$$\tilde{\mathrm{E}}(r, \omega - \omega_0) \approx F(x, y)\, \tilde{A}(z, \omega - \omega_0)\, exp(i\beta_0 z) \qquad (2\text{-}19)$$

As the above optical pulse has many frequency components and intensity variation, it will experiences chromatic dispersion and nonlinear effects during the propagation along the optical fibre which leads to the change of pulse both in time domain *A(z, t)* and spectral domain $\tilde{A}(z, \omega - \omega_0)$.

2.8.4 The Nonlinear Schrödinger Equation

The primary purpose of the passive fibres is to support optical signal propagation through it. There are various kinds of passive fibres which serve this basic purpose like silica fibres of single-mode and multi-mode type and special type of passive fibres like photonic crystal fibres (PCFs) and highly nonlinear fibres (HNLFs) which will support new frequency generation through nonlinear refractive index change. In the previous section, the simple case of optical signal propagation scenario in SMF is studied, where fibre dispersive effects and nonlinear effects are not included. But when high intense pulse is launched into fibre it will experience both dispersive effects and nonlinear effects, where simple pulse propagation equation through SMF can't explain it. So there is necessity to analyze general equation which includes both dispersive effects and nonlinear effects, this problem can be solved through the nonlinear Schrödinger equation (NLSE). NLSE is capable of explaining simultaneously both the effects such as dispersive and nonlinear effects experienced by the optical pulse when propagating through the passive optical fibre.

Investigation of pulse propagation inside the optical fibre starts with Maxwell's equations which gets modified due to the nonlinear polarization terms.

$$\nabla \times \tilde{E} = -\frac{\partial B}{\partial t} = -\mu_0 \frac{\partial \tilde{H}}{\partial t} \quad (2\text{-}20)$$

$$\tilde{B} = \mu_0 \tilde{H}$$

Where M is the magnetic polarization which is zero for optical fibres as they are nonmagnetic.

$$\nabla \times \tilde{H} = \frac{\partial \tilde{D}}{\partial t} \quad (2\text{-}21)$$

Where J is the conductivity of the medium which is zero for optical fibres as there is no free charge densities (ρ=0) in the optical fibre and the displacement (D) in the optical fibre can be written as:

$$\tilde{D} = \varepsilon_0 \tilde{E} + \tilde{P} \, (\tilde{P}_L + \tilde{P}_{NL})$$

Where P is the induced polarization in the optical fibre under the presence of intense optical field which includes the both linear polarization (P_L) and nonlinear polarization (P_{NL}) terms. By substituting P value from the equation 2-11 the displacement is modified as follows. Here the 2nd order polarization is negligible which is very small for glass fibres.

$$\tilde{D} = \varepsilon_0 \, [\tilde{E} + \chi^1 . \tilde{E} + \chi^3 \vdots \tilde{E} \, \tilde{E} \, \tilde{E}]$$

$$\nabla . \tilde{D} = 0 \quad \text{As } \rho=0 \text{ for optical fibres} \quad (2\text{-}22)$$

$$\nabla . \tilde{B} = 0 \quad (2\text{-}23)$$

In order to get the wave equation in terms of only electric field *E* and induced polarization *P.* By applying curl to the equation 2-20 and substituting all the values from the equations 2-21, 2-22 and 2-23 the wave equation in time domain looks as follows:

$$\nabla^2\tilde{E} - \frac{1}{c^2}\frac{\partial^2\tilde{E}}{\partial t^2} = \mu_0\frac{\partial^2\tilde{P}_L}{\partial t^2} + \mu_0\frac{\partial^2\tilde{P}_{NL}}{\partial t^2} \quad (2\text{-}24)$$

The wave equation in frequency domain which satisfies Helmholtz equation looks as follows, where $\tilde{\mathrm{E}}(r, \omega - \omega_0)$ is the Fourier transform of slowly varying time function *E(r, t)* from equation 2-19.

$$\nabla^2\tilde{\mathrm{E}} + \varepsilon(\omega)k_0^2\,\tilde{\mathrm{E}} = 0 \quad (2\text{-}25)$$

Where $\varepsilon(\omega)$ the frequency dependent effective dielectric constant which includes both linear and nonlinear effects. As the equation 2-25 satisfies Helmholtz equation under the slowly varying envelop assumption therefore the above equation can be separated using the variable separable method into transverse component *F(x, y)* which gives field distribution and longitudinal component which gives slowly varying envelop $\tilde{A}(z, \omega - \omega_0)$, as the pulse envelop is slowly varying the second order derivative of the pulse envelop with respect to fibre length is negligible $(\frac{\partial^2\tilde{A}}{\partial z^2} \cong 0)$ [57]. The following two equations can be further simplified under the following assumptions, nonlinear effects ($\mathrm{P_{NL}}$) are weak when compared with the linear effects ($\mathrm{P_{NL}}$), along the entire fibre length the polarization is assumed to be constant and the light bandwidth $\Delta\boldsymbol{\omega}$ *is* very narrow when compared with the centre frequency ω_0 *i.e.* $\Delta\boldsymbol{\omega} << \omega_0$ [57].

$$\nabla_\perp^2 F + \left[\varepsilon(\omega)k_0^2 - \tilde{\beta}^2\right]F = 0 \quad (2\text{-}26)$$

$$\frac{\partial\tilde{A}}{\partial z} + j\left(\tilde{\beta} - \beta_0\right)\tilde{A} = 0 \quad (2\text{-}27)$$

The $\tilde{\beta}$ is not same throughout the propagation rather it is a function of frequency as shown in the below and the dielectric constant $\varepsilon(\omega)$ is also given below:

$$\varepsilon = (n + \Delta n)^2 \approx n^2 + 2n\Delta n \quad (2\text{-}28)$$

Where $\Delta n = n_2 \left| E \right|^2 - j \frac{\alpha}{2k_0}$ and α is loss due to absorption in the fibre.

$$\tilde{\beta}(\omega) = \beta(\omega) + \Delta\beta(\omega) \tag{2-29}$$

Where $\beta(\omega)$ and $\Delta\beta(\omega)$ can be expanded as shown in the equations 2-7 and 2-8.

$$\Delta\beta(\omega) = k_0^2 \frac{n(\omega)}{\beta(\omega)} \frac{\iint \Delta n(\omega) \left| F \right|^2 dxdy}{\iint \left| F \right|^2 dxdy} \tag{2-30}$$

By substituting equation 2-29 in equation 2-27 and applying inverse Fourier transform the equation 2-26 can be re-written as follows:

$$\frac{\partial A}{\partial z} + \beta_1 \frac{\partial A}{\partial t} - j \frac{\beta_2}{2} \frac{\partial^2 A}{\partial t^2} + \frac{\alpha}{2} A = j\gamma(\omega_0) \left| A \right|^2 A \tag{2-31}$$

Where γ is the parameter which denotes the Kerr nonlinear effects and given as below:

$$\gamma(\omega_0) = \frac{n_2(\omega_0)\omega_0}{cA_{eff}} \tag{2-32}$$

Where A_{eff} the effective mode area given by the field distribution F(x, y) as follows:

$$A_{eff} = \frac{(\iint \left| F \right|^2 dxdy)^2}{\iint \left| F \right|^4 dxdy} \tag{2-33}$$

In order to simply more a new time is defined, where pulse envelop travels at a speed of group velocity, therefore, the 1st derivative of the envelope in new frame domain will be zero.

$$T = t - \frac{z}{v_g} = t - \beta_1 z \tag{2-34}$$

Equation 2-31 can be further simplified as:

$$\frac{\partial A}{\partial z} - j \frac{\beta_2}{2} \frac{\partial^2 A}{\partial T^2} + \frac{\alpha}{2} A = j\gamma \left| A \right|^2 A \tag{2-35}$$

The above equation is known as generalized nonlinear Schrödinger equation (NLSE), which explains the pulse propagation in passive fibres including all the effects such as fibre dispersion ($-j\frac{\beta_2}{2}\frac{\partial^2 A}{\partial T^2}$), fibre loss ($\frac{\alpha}{2}\ A$) and nonlinear effects ($-j\ \gamma\ \left|A\right|^2\ A$). By defining two operators such as dispersion operator ($\widehat{D}$) and nonlinear operator ($\widehat{N}$).

$$\widehat{D} = -j\ \frac{\beta_2}{2}\ \frac{\partial^2 A}{\partial T^2}$$

$$\widehat{N} = \ j\ \gamma\ \left|A\right|^2 \qquad (2\text{-}36)$$

As the group velocity varies with respect to the frequency so dealing the dispersion operator in frequency domain is easier and dealing the nonlinear operator in time domain is easier as the envelope varies w.r.to the time. This can be explained simultaneously by making use of Split-Step Fourier method [57], however different pulse propagation scenarios can be investigated in the next chapter under the section of different regimes of pulse propagation inside the optical fibre

2.9 Different Regimes of Pulse Propagation inside the Optical Fibre

In order to analyze the optical fibre effects on optical pulse two characteristics lengths need to be defined they are, one dispersion length L_D over which fibre dispersion effects are significant in modifying the optical pulse properties and the 2nd one is nonlinearity length L_{NL} over which nonlinear effects shows significant effect in modifying the optical pulse properties.

$$L_D = \frac{T_0^2}{\left|\beta_2\right|} \qquad (2\text{-}37)$$

$$L_{NL} = \frac{1}{\gamma P} \qquad (2\text{-}38)$$

Where T_0 refers to the optical pulse width, P is the pulse power. Based on the fibre length comparable to the above two lengths there are different regimes of pulse propagation along

the fibre length. The different regimes of pulse propagation along the length of the fibre as follows. Let assume fibre physical length is *L.*

The fibre physical length is very small when compared with both fibre lengths *i.e.* $\boldsymbol{L \ll L_D}$ and $\ll \boldsymbol{L_{NL}}$, in this regime fibre acts just like a bare medium and allow the pulse propagation without any significant changes to it.

The physical length of the fibre is significantly large when compared with dispersion length and significantly small when compared with nonlinearity length *i.e.* $\boldsymbol{L \gg L_D}$ and $\boldsymbol{L \ll L_{NL}}$, in this regime fibre acts as dispersive medium and which causes pulse broadening as pulse travels along the fibre. This regime is called *Dispersive regime*. From the equation 3-6, if the launched optical pulse is short enough then the dispersive effect plays a prominent role even if the physical length of the fibre is small.

The physical length of the fibre is significantly small when compared with dispersion length and significantly large when compared with nonlinearity length *i.e.* $\boldsymbol{L \ll L_D}$ and $\boldsymbol{L \gg L_{NL}}$, in this regime, fibre acts as nonlinear medium and optical pulse undergoes self-phase modulation as the different frequency components of pulse experiences different refractive indexes along the fibre length due to incident pulse intensity variation. This regime is called Nonlinearity regime*;* this can be easily achieved with the optical pulses with high input power as shown in the equation 2-35.

The physical length of the fibre is significantly large enough when compared with the both fibre lengths i.e. $\boldsymbol{L \gg L_D}$ and $\boldsymbol{L \gg L_{NL}}$, in this case, both dispersion as well as nonlinear effects plays an important role in modifying the optical pulse properties. This regime is called Soliton regime and this can be observed when the launched optical pulse width is short enough and the pulse power is large enough.

2.9.1 Dispersive Pulse Propagation Regime ($L \gg L_D$ and $L \ll L_{NL}$)

Dispersive regime is the pulse propagation regime over which pulse undergoes continuous pulse broadening as it travels along the length of the fibre due to the group velocity dispersion (GVD). The detailed description of how the optical pulse evolves along the length of the fibre can be explained with the help of solving NLSE for the given dispersive regime case *i.e.* where nonlinear effects are completely insignificant and fibre loss is considered to be negligible for simplifying the NLSE solution.

The different frequency components in the optical pulse travel with different group velocities, known as GVD. As the group velocity of each component varying with the frequency, so it is easy to solve GVD effects in frequency domain. Let's consider normalized amplitude *U (z, T)* and the pulse envelop looks as follows:

$$A\,(z,T) = \sqrt{P}\, e^{-\alpha z/2}\, U\,(z,T) \tag{2-39}$$

From equations 2-35 and 2-39, the NLSE can be written as follows by neglecting loss term,

$$\frac{\partial U}{\partial z} - j\,\frac{\beta_2}{2}\,\frac{\partial^2 U}{\partial T^2} = -j\,\frac{e^{-\alpha z}}{L_{NL}}\,\left|U\right|^2 U \tag{2-40}$$

by neglecting the nonlinearity terms as in the dispersive regime nonlinear effects are very week and hence solution to the equation 3-40 in dispersive regime is as follows:

$$\tilde{U}(z,\omega) = \tilde{U}(0,\omega) e^{-j\frac{\beta_2}{2}\omega^2 z} \tag{3-41}$$

The above equation represents the evaluation of pulse in frequency domain along the length of the fibre in dispersive regime, from this, it is clear that the amplitude spectrum of the pulse throughout the entire length won't change whereas the phase changes proportional to the

square of the frequency. This can be further understood in deep by taking a simple Gaussian pulse as input pulse.

Gaussian pulse $U(0,T) = e^{-\frac{T^2}{2T_0^2}}$ at z=0 and $T_{FWHM} = 1.66\,T_0$ (2-42)

The Fourier transform of Gaussian pulse is also a Gaussian pulse and looks as follows:

$$\tilde{U}(0,\omega) = \sqrt{2\pi}\,T_0 e^{-\frac{T_0^2}{2}\omega^2} \quad (2\text{-}43)$$

applying inverse Fourier transform to the equation 2-41 gives the dispersive propagating pulse properties in time domain.

$$U(z,T) = \frac{1}{2\pi}\int_{-\infty}^{\infty}\tilde{U}(z,\omega)\,e^{-j\frac{\beta_2}{2}\omega^2 z}\,e^{j\omega T}\,d\omega \quad (2\text{-}44)$$

By substituting equation 2-43 in equation 2-44 gives the dispersive pulse in time domain as follows:

$$U(z,T) = e^{-\frac{T^2}{2T_1^2}}.e^{j\varphi} \quad (2\text{-}45)$$

Where $$T_1(Z) = T_0\left\{1 + \left(\frac{z}{L_D}\right)^2\right\}^{1/2} \quad (2\text{-}46)$$

From equation 2-46, at $z = L_D$ the $T_1 = \sqrt{2}\,T_0$ *i.e.* dispersion length L_D is the fibre length over which propagating pulse becomes $\sqrt{2}$ times of the initial pulse width T_0 .

Phase component $$\varphi = \frac{sgn(\beta_2)(Z/L_D)}{1+(Z/L_D)^2}\,\frac{T^2}{2T_0^2} - \frac{1}{2}\tan^{-1}(Z/L_D) \quad (2\text{-}47)$$

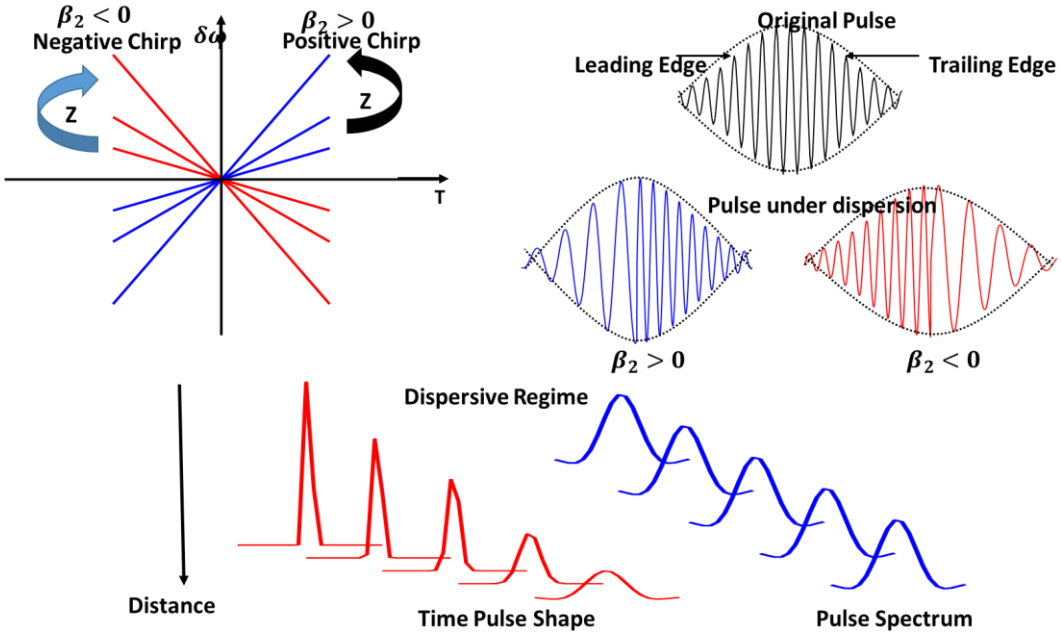

Figure 2. 13 Schematic illustration of pulse propagation through fibre in dispersive regime [59].

From the equation 2-41 it is clear that envelop of the amplitude spectrum doesn't change with the time but the frequency components inside envelop itself travel with different speeds due to the frequency modulation w.r.to time because of dispersion effect, therefore the change in frequency w.r.to time is called chirping and it is given as follows:

$$\delta\omega = \frac{d\varphi}{dT} = \frac{sgn\,(\beta_2)(^{Z}/_{L_D})}{1+(^{Z}/_{L_D})^2}\,\frac{T}{T_0^2} \qquad (2\text{-}48)$$

Where frequency change $\delta\omega$ is directly proportional to the time varying T *i.e.* $\delta\omega \propto T$.

From the above Figure 2.13, it is clear that the spectrum of the pulse in dispersive regime almost unchanged throughout the length of fibre, however, the different spectral components inside the pulse travel with different velocities based on the sign of β_2 . Suppose if β_2 is positive then the region in which pulse is launched is called normal dispersion region and in this regime low frequency components travel faster than the high frequency

components, this phenomenon is called positive frequency chirping and if β_2 is negative then the region in which pulse is launched is called anomalous dispersion region and in this regime high frequency components travel faster than the low frequency components, this phenomena is called negative frequency chirping but the spectrum envelop remains same, however, the pulse in time domain starts broadening with the length of the fibre as shown in the above Figure 2.14.

2.9.2 Nonlinear Pulse Propagation Regime ($L \ll L_D$ and $L \gg L_{NL}$)

This is the regime of pulse propagation inside the fibre in which nonlinearity effects are dominant over the dispersion effects *i.e.* physical length of the fibre is significantly large when compared with nonlinearity length and significantly small when compared with the dispersion length. In this case, as the pulse travels along the fibre experiences different refractive index values at different places of the pulse *i.e.* center of the pulse experiences large refractive index value when compared with the other parts of the pulse which causes change in velocity. The change in velocity of the pulse leads to the phase change called as SPM. The evolution of the pulse along the fibre in nonlinearity regime can be seen more in detailed by solving NLSE in nonlinearity regime conditions. From equation 2-40, by removing dispersion effects the NLSE in nonlinearity regime looks like as follows:

$$\frac{\partial U}{\partial z} = -j \frac{e^{-\alpha z}}{L_{NL}} \left| U \right|^2 U \tag{2-49}$$

The solution to the above equation 3-18 is looks like as follows;

$$U = V e^{j\varphi_{NL}} \tag{2-50}$$

Where φ the nonlinear phase change w.r.to length of the fibre and the solution after solving equations 2-49 and 3-50 looks as follows:

$$\frac{\partial U}{\partial z} = 0 \tag{2-51}$$

$$\frac{\partial \varphi_{NL}}{\partial z} = -\frac{e^{-\alpha z}}{L_{NL}} \left| V \right|^2 \tag{2-52}$$

From the equation 2-51, it is clear that the pulse amplitude in time domain is unaffected w.r.to the length of fibre *i.e.* envelop of the pulse in time domain is intact *V = U (z, T) = U (0, T).* Whereas phase of the pulse changes with distance as in the equation 2-52.

The phase evolution along the length of the fibre is given as follows:

$$\varphi_{NL} = -\left| U(0,T) \right|^2 \frac{L_{eff}}{L_{NL}} \tag{2-53}$$

Here L_{eff} the effective length of the fibre over which nonlinear effects can be seen inside the optical fibre, and it is given as:

$$L_{eff} = \frac{1-e^{-\alpha z}}{\alpha} \tag{2-54}$$

In this regime of pulse propagation also there is a frequency change $\delta\omega$ w.r.to the time and it depends on the intensity as shown below, here the intensity dependent frequency chirp is always positive *i.e.* frequency always increases with time irrespective of the sign of the dispersion co-efficient β_2 .

$$\delta\omega = -\frac{d\varphi_{NL}}{dT} = \frac{L_{eff}}{L_{NL}} \left| U(0,T) \right|^2 \tag{2-55}$$

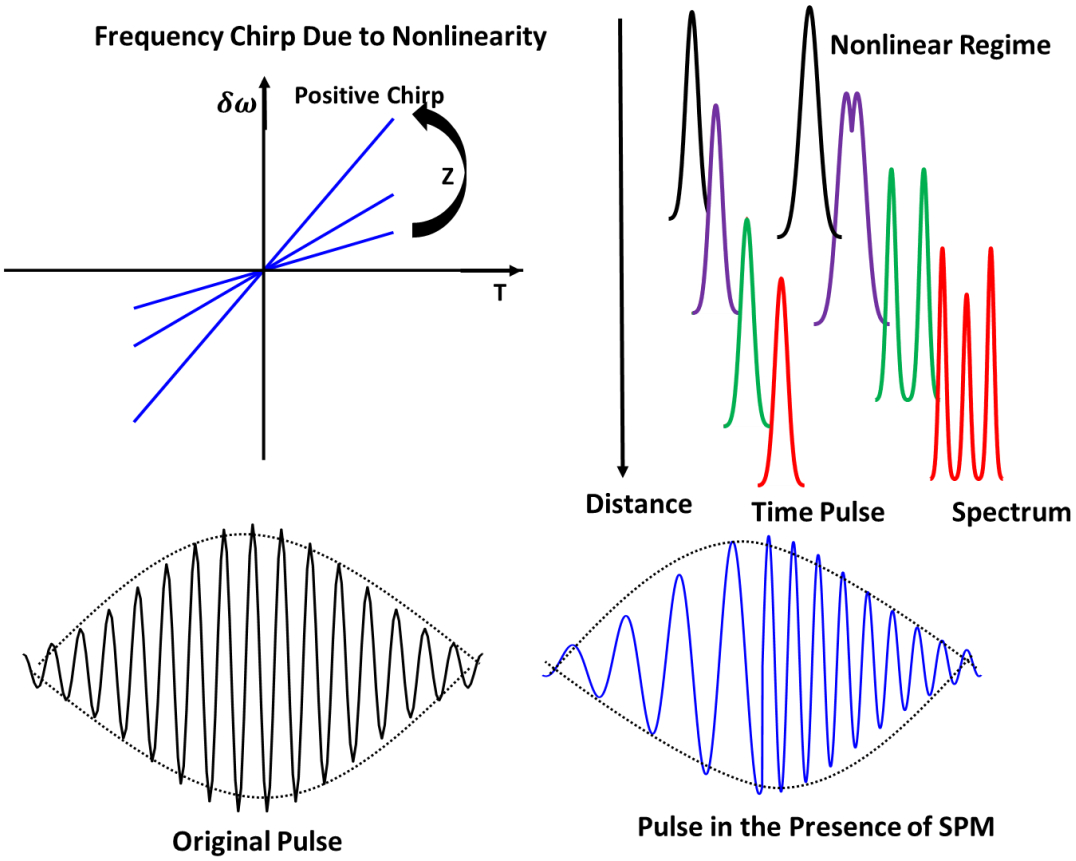

Figure 2. 14 Schematic illustration of frequency chirping phenomena and spectral broadening phenomena of pulse in nonlinearity regime [59].

The frequency chirp phenomena and spectral broadening phenomena can be explained schematically as shown in the Figure 2.14. As the frequency increases w.r.to the time there is change in the spectrum *i.e.* leading edge undergoes redshift and trailing edge undergoes blue shift through which spectral broadening phenomena take place in the nonlinearity regime of pulse propagation. Here in this regime, the new frequency generation can be seed due to the nonlinear phase change caused by the intensity of the pulse i.e. due to the SPM. This property of the fibre can be used to generate broad continuous spectrum. This nonlinear effect can be enhanced further by using the dispersion effect in normal dispersion regime through which broad continuous spectrum can be achieved. In the same way, the dispersion effect on the pulse can be nullified by operating pulse in anomalous region where negative frequency chirp

due to dispersion will be canceled by positive frequency chirp due to nonlinearity effect, where an undistorted pulse and same frequency through the entire pulse can be achieved.

In conclusion, the pulse in time domain is unchanged and spectral broadening phenomena takes place due to SPM effect when pulse propagates in nonlinearity regime, whereas in dispersion regime the spectrum of the pulse intact and the pulse in time domain keeps broadening along the length of the of the fibre due to the GVD effect as shown in the Figure 2.15.

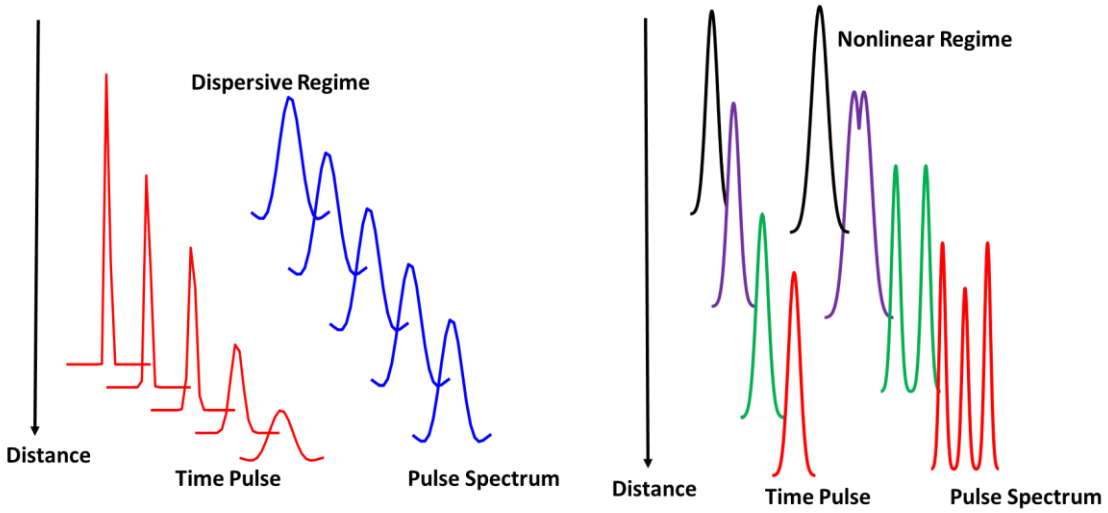

Figure 2. 15 Schematic illustration of pulse evolution in dispersive and nonlinearity regime [59].

2.9.3 Soliton Pulse Propagation Regime ($L \gg L_D$ and $L \gg L_{NL}$)

Here the fibre length is significantly large enough when compared with the both dispersion and nonlinear lengths, so both GVD and SPM acts together on the pulse during this regime of propagation. Based on the region in which pulse is launched decides the how pulse evolves along the length of the fibre. Suppose if the pulse is launched in normal dispersion region then the GVD and SPM act together on the pulse to form broad continuous spectrum through

nonlinear spectral broadening phenomena, which is useful to generate supercontinuum (SC) and pulse in time domain intact. Whereas if the pulse is launched in anomalous region then SPM effect will be balanced by the GVD effect which can be called as soliton propagation which gives undistorted pulse throughout the length of the fibre only when the fundamental soliton is maintained.

The NLSE will be expressed as in equation 2-49 such that the distance and time are normalized as $\xi = z/L_D$ and $\tau = T/T_0$. The parameter N is defined as in equation 2-57 and it represents the relative importance of the effects on the pulse propagation. When $N \ll 1$, GVD dominates and when $N \gg 1$, SPM dominates. N can also be described as the soliton number.

$$\frac{\partial U}{\partial \xi} - j\frac{sgn(\beta_{2)}}{2}\frac{\partial^2 U}{\partial \tau^2} = N^2|U|^2U \tag{2-56}$$

$$N = \frac{L_D}{L_{NL}} \tag{2-57}$$

The wave equation for the fundamental soliton looks like as follows:

$$U(\xi, \tau) = sech(\tau)\, e^{-j\xi/2} \tag{2-58}$$

The phase changes due to dispersion and nonlinearity is given as below:

$$\varphi_{NL}(L, T) = -sech^2(\tau)\xi \tag{2-59}$$

$$\varphi_D(z, T) = -\left(\frac{1}{2\, sech(\tau)}\frac{\partial^2\, sech(\tau)}{\partial \tau^2}\right)\xi \tag{2-60}$$

The addition of the above nonlinear and dispersive phases will cancel each other and the pulse adjusts itself to produce a chirp-free pulse, where the pulse shape and spectrum remains unchanged and this will support soliton generation. However, this is possible only if

the fundamental soliton is maintained throughout the entire length of fibre. Even though fundamental soliton maintained initially but as the pulse propagates, it's difficult to maintain as the pulse power reduces, GVD starts dominating SPM. In case of high power pulses such as ultra-short pulses, soliton dynamics plays a dominant role in SC generation through new frequency generation. Soliton-self-frequency shift (SSFS) is the dominant soliton related nonlinear phenomena responsible for the new frequency generation.

When short-pulses are pumped in the anomalous dispersion region of the optical fibre, then the interaction of soliton with Raman nonlinearity causes the SSFS. The interaction of soliton with Raman nonlinearity increases the red-shifting of soliton center frequency as the pulse propagates over the distance of the optical fibre. This can be understood as continuous transfer of energy from the blue side of the soliton spectrum to the red side of the soliton spectrum that is assisted by Raman interaction. This SSFS nonlinear phenomenon is of great interest in case of SC generation towards mid-IR region [8,61-63].

2.9.4 Four-Wave Mixing (FWM)

The four-wave mixing phenomenon in the optical domain is analogous to the inter-channel mixing or the inter-modulation products in the electronic systems. When an electronic amplifier goes into saturation, applications of two distinct frequencies result in the generation of new frequencies which may be either the sum or the difference between the applied frequencies, this happens due to the non-linearity in the amplifier performance. Exactly similar situation occurs inside an optical fibre in the presences of the third order non-linear susceptibility χ^3 [64]. Figure 2.16 schematically illustrates the new frequencies generation as the multiple frequency components travel along the non-linear fibre.

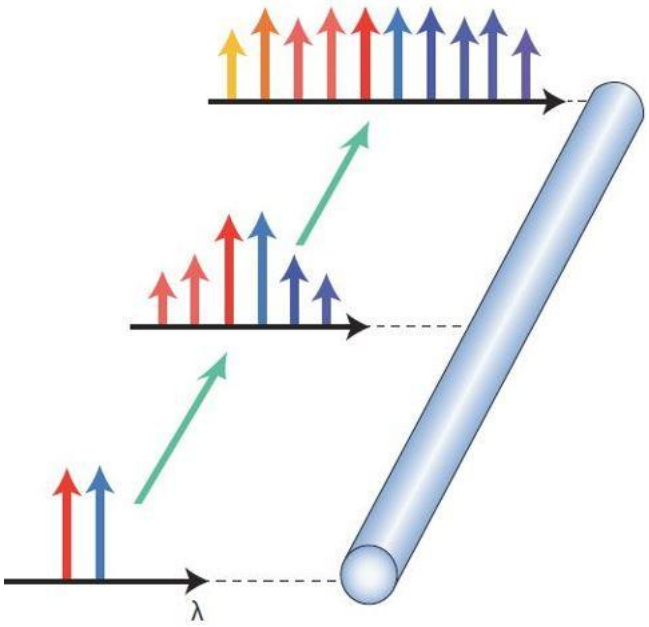

Figure 2. 16 Schematic illustration of new frequency generation in HNLF through FWM phenomena [65].

Suppose let's consider three different signals E_1, E_2 and E_3 are travelling inside the optical fibre, then the nonlinear polarization P_{NL} to the third order susceptibility is given as follows:

$$P_{NL} = \varepsilon_0 \chi^3 \vdots E_1 E_2 E_3 \tag{2-61}$$

As these three frequency components travel together inside the optical fibre, fourth frequency component will get generated due to the inter-modulation and is given by:

$$\omega_4 = \omega_1 \pm \omega_2 \pm \omega_3 \tag{2-62}$$

From the equation 2-62, it is observed that when three different frequency signals launched into nonlinear medium, new frequencies will get generated, so the generation of new frequencies through non-linear interaction between the parent signals is known as FWM.

2.9.5 Stimulated-Raman Scattering (SRS)

SRS is an important nonlinear phenomenon that can turn the optical fibres into broadband Raman laser sources and Raman amplifiers. In any material, some fraction of energy can be transferred from one state to another molecular state, whose wavelength is upshifted by an amount decided by the vibrational states of the material. This phenomenon was discovered in 1928 by Raman and it was named after him as Raman effect [66]. The stokes waves generated from the incident light through wavelength-shifting was observed in 1962 [67]. In case of high power pump, the stokes waves grow rapidly and produces higher order stokes which assist the continuum generation from an optical fibre medium. The initial observation of SRS in the optical fibres was made in 1973 [68] since then the SRS effect in optical fibres was studied intensively in a situation corresponding to the CW, quasi-CW, and short-pulse regime [57]. Quasi-CW is the regime in which the input pump pulse width to the fibre falls in the range of 1 – 100 ns. Short-pulse is the regime in which the input pulse width to the fibre falls in the range of below 100 ps and above 100 fs. In case of short-pulse regime, the SRS effect was intensively studied in the case of normal and anomalous dispersion GVD regime of optical fibre [57].

Figure 2.17 shows the illustration of new wavelength generation from a SRS process inside a fibre material having energy states such as ground state, vibrational or intermediate state, and the virtual state. SRS process can generate a new wavelengths such as stokes waves at a wavelength λ_s on the long-wavelength side of pump and anti-stokes waves at a wavelength λ_a on the short-wavelength side of pump. Here the location of stokes and anti-stokes wavelengths depends upon the fibre material, pump wavelength and, the pump power. The stokes-shift wavelength is decided by the Raman gain, in case of silica fibres it can vary up to

40 THz with a broad peak locating at 13 THz which is 100 nm away from the pump wavelength. If the pump power is high enough then the fibre supports the cascaded SRS processes and leads to the continuum generation. Depending upon the GVD region, the SRS processes and SPM, FWM, XPM, soliton effects and modulation instability influences each other and effects the SC spectral dynamics.

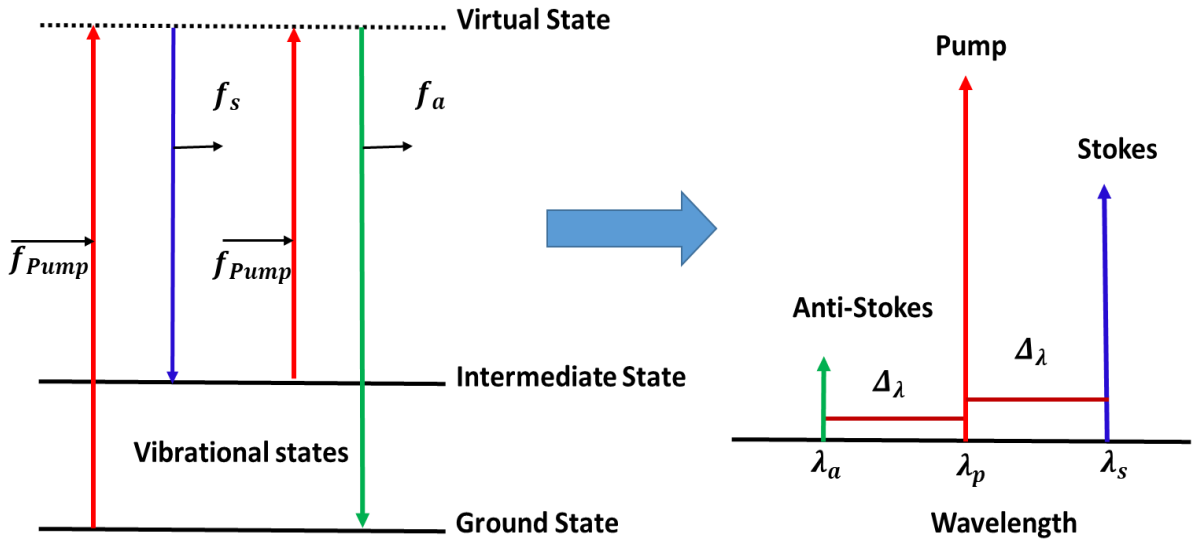

Figure 2. 17 Illustration of Stimulated Raman Scattering (SRS).

2.10 Background of Supercontinuum Sources

The above discussed all the nonlinear properties have the capability of generating new frequencies within the pump pulse spectrum when it propagates inside the nonlinear fibre medium, which then produces the output spectrum bandwidth more times greater than the pump pulse bandwidth. Depending upon the pump pulse characteristics and the nonlinear media nature, different nonlinear phenomena contributed in new frequency generation as discussed in the above sections. In the following, focused more on the progress of SC sources

using optical fibres with a different pumping mechanisms starting from CW or quasi CW (pulse width >1ns), picosecond pulses and femtosecond pulses pumping.

The first SC generation phenomenon was observed in around 1970 for the first time in gaseous and solid nonlinear media [1-2, 69-70]. In 1976, SC generation phenomenon in optical fibre was observed for the first time in a 20-m-long optical fibre medium by launching a Q-switched laser pulses having a pulse width of ~10 ns from a dye laser [71]. The output SC spectrum of ~180 nm was generated from the 20-m-long optical fibre at an input pulse peak power of > 1kW. Since then it was an interesting topic for many researchers till date. Later on, in 1987, a 50 nm bandwidth of SC spectrum was observed from a 15-m-long fibre by launching a picosecond pulse having 25 ps at the input wavelength of 532 nm [72]. The 50 nm band was generated due to the combined nonlinear effects of SPM, SRS, XPM and the FWM. Similar kind of nonlinear effects was expected to contribute for SC generation when a SMFs were used [73]. In the same year, a SC spectrum bandwidth of over 200 nm was observed from a 1-km-long SMF at an input pulse peak power of 530 W by launching a femtosecond laser pulses having pulse width of 830 fs [74]. Later on similar kind of SC spectral bandwidth is generated with a longer pulse [75, 76]. in 1994, a SC spectrum of bandwidth >40 nm was generated by launching a 3.8 W peak power of 6 ps pulse in the 4.9-km-long fibre and by 1995, 200 nm SC spectrum was produced with the same technique [77]. Until 2000, the SC sources was realized using very long fibres (~ 1km), later realized that the very short length of highly nonlinear fibres also can produce reasonable SC provided the input pulses with sufficient peak powers. In the same year, a SC spectrum bandwidth of 140 nm around 1.55 μm region was generated from a dispersion-shifted 4.5-m-long fibre having nonlinearity co-efficient γ = 2.3 (1/W-km), when a laser pulse with a pulse width of 1.3 ps is launched. The SC spectrum bandwidth is increased from 140 nm to 250 nm when the fibre is replaced with

a 4-m-long fibre with high nonlinearity co-efficient γ = 9.9 (1/W-km) [78]. Due to the availability of nano-core microstructured fibres whose ZDW close to 800 nm and having low dispersion around 700 nm, the SC laser sources covering whole visible region and even extending into near infrared region is realized by launching picosecond pulses [79]. Most of the SC generation experiments during the initial days was carried out using picosecond pulses. Later on, due to the availability of femtosecond laser pulse sources such as tunable Ti: sapphire lasers and mode-locked lasers, SC generation using femtosecond lasers was explored and now days it becomes common for realization of SC laser source in any wavelength region. the femtosecond broadband laser source was realized in the year of 2000, by launching a 100-fs laser pulse into a microstructured fibre of 75-cm-long at 770 nm wavelength region [80]. At an input pulse peak power of 7 kW, an SC output spectrum extending from 400 nm to 1600 nm was observed. The similar kind of SC spectrum was observed in a relatively very small tapered fibre of 9-cm-long with a core diameter of 2 µm [81]. Since 1970, the first SC generation phenomenon was observed, in all most all the SC generation experiments, quasi-CW or picosecond or femtosecond laser pulses as pump to the nonlinear medium. In early 2003, in experiment, researcher realized that the SC generation is possible with even CW lasers if achieve sufficiently high enough power from CW lasers and therefore, the SC generation using CW laser was demonstrated in the same year [82].

Figure 2.18 shows the summary of available SC sources and the corresponding pumping mechanisms. The SC source was realized with both silica and non-silica based fibres. Here in this survey, the SC generation with pump wavelength below 1600 nm is realized using silica-based fibres. Each and everything is color-coded to understand the available SC sources at different pumping mechanisms. Ytterbium, Erbium, and Thulium are the fibre-laser materials.

Whereas YAG: frequency-doubled or frequency- tripled or neodymium-doped yttrium aluminum garnet and Ti: titanium-doped sapphire are the solid-state lasers.

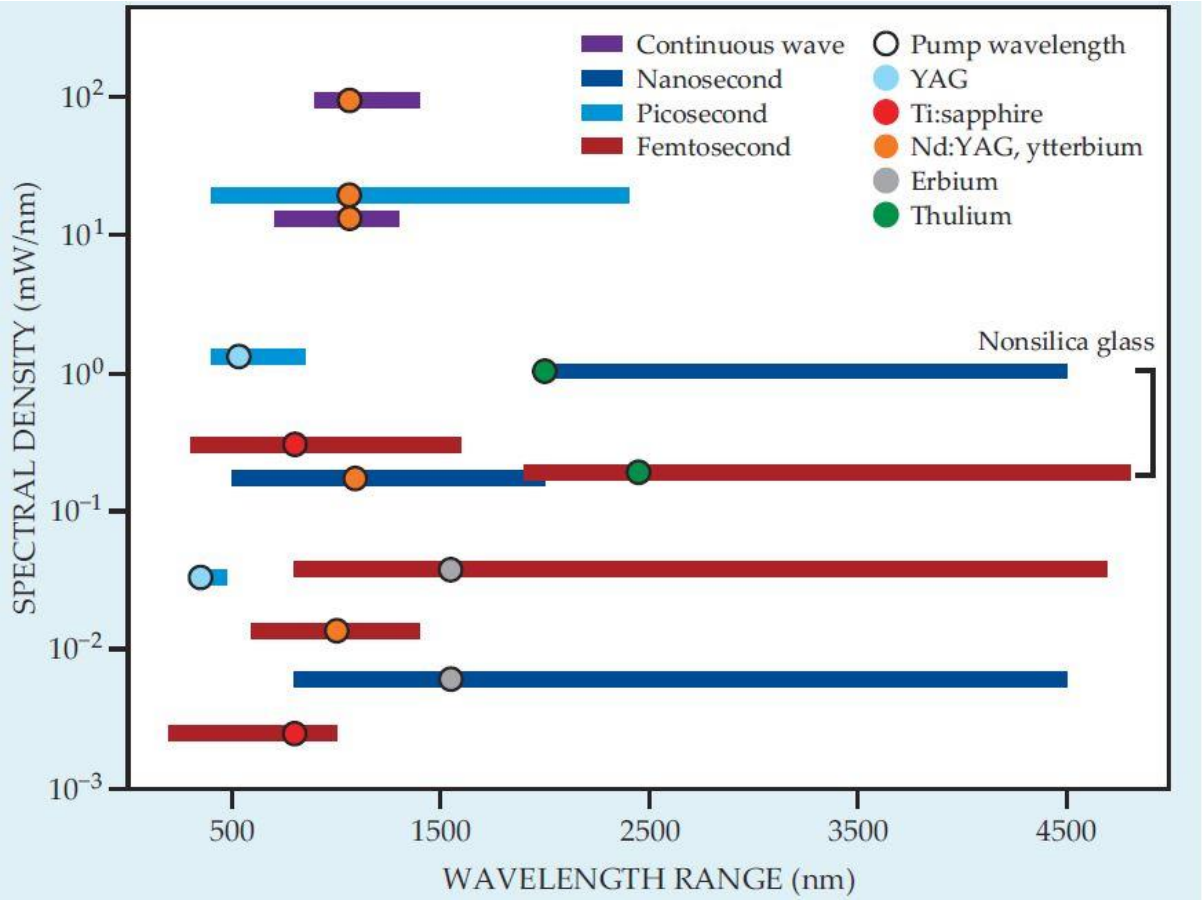

Figure 2. 18 Summary of SC sources available [83].

In 1970 Since the first observation of SC generation phenomenon, numerous study has been done and produced the broadband SC laser sources covering a wide range of spectral region starting from visible region to near-infrared and recently mid-IR region also due to the availability of transparent soft-glass fibre in mid-IR region. In this project, the specialty fibres such as highly nonlinear PCF, HNLF, and soft-glass fibre ZBLAN were used to study the input pulse power variation and the variation of fibre length and tapering effect on SC spectral dynamics. CNT-SA based passively mode-locked femtosecond EDFL is used as a seed laser to generate broadband SC spectrum from PCF, HNLF and, ZBLAN. Comparatively, SC generation

setup kept as very simple and compact. The background of each specialty fibre and the brief literature of SC sources using these fibres was given in the following corresponding chapters and the significance of my study is also explained.

2.11 Specialty Fibres

In general, the basic function of optical fibre medium is to transport light from one end to other end with a little or no loss. Specialty fibres are the optical fibres that are having at least one specialty when compared to standard optical fibres. One of the many applications of the specialty fibres is the new frequency generation through nonlinear conversion. The nonlinear properties that are possessed by the specialty fibre can cause new frequency generation. They occur either due to intensity dependence of the refractive index of the fibre or due to the inelastic scattering phenomenon. The specialty fibres differ with normal fibres in terms of core size, fibre diameter, dispersion properties, host material such other than silica and having air holes in the core region etc. PCF, HNLF, dispersion shifted fibres, soft-glass fibres, and tapered fibres are the some of the examples for the specialty fibre. These specialty fibres are often used for broadband SC generation starting from visible region to Mid-infrared region. In my experiments, highly nonlinear PCF, dispersion shifted HNLF, tapered fibre and ZBLAN fibre were used as the nonlinear media to generate broadband SC. A detailed background and corresponding SC sources based on these fibres are explained in the following respective chapters.

Chapter-3 Carbon –Nanotube-Based Passively Mode-Locked Laser Pulse Generation

Generation of broadband SC laser sources consists of two major parts: the seed laser and the nonlinear medium. Throughout my experiments, CNT-SA-based passively mode-locked femtosecond erbium-doped fibre laser (EDFL) was used as a pump laser to generate the SC from all the specialty fibres that was used in this project. This chapter introduces the generation of femtosecond pulse from passively mode-locked EDFL using CNT-SA.

3.1 Introduction

3.1.1 CNT-SA background

There are two types of CNTs: single-walled CNTs and multi-walled CNTs. The applications of single-walled CNTs are mostly explored in the fields of photonics and electronics. Single-walled CNT can be regarded as allotropy of carbon which means rolling up of an atom-thick layer of carbon with a cylindrical nanostructure. The cylindrical nanostructure has a typical length scale of ~ 1 μm and diameter of ~ 1 nm. Therefore, it can be considered as an ideal one-dimensional element in the world. Rolling diameter and angle decide the behavior of CNTs, depending on these parameters CNTs act as either materials or semiconductors [84]. The semiconducting CNTs have the capability of absorbing light starting from UV wavelength to near-infrared with direct energy band-gap [85].

For the first time, the optical switching properties of CNTs at the wavelength of 1.55 μm was discovered in 2002 by Y. Chen *et al* [86]. After two years in 2004, S. Y. Set *et al* for the first time demonstrated the passively mode-locked fibre laser incorporating CNT-SAs that produced the pulse train with a pulse width of 1.1 ps and 3.7 nm of spectral bandwidth [87].

CNT-SA based passively mode-locked fibre lasers can operate at different center wavelengths depending upon the gain mediums employed in the laser cavity. The center wavelengths covered by the CNT-SA passively mode-locked fibre lasers are 1 µm, 1.3 µm, 1.55 µm and 1.9 µm where the gain fibres employed are ytterbium-doped fibre, praseodymium-doped fibre, erbium-doped fibre, and thulium-doped fibre, respectively [88-91]. The schematic representation of CNT-SA based passively mode-locked fibre laser at different center wavelengths is shown in the Figure 3.1. The center wavelength of the mode-locked pulse can be tuned within the gain bandwidth of the gain fibre by inserting suitable gain fibre in the laser cavity [92].

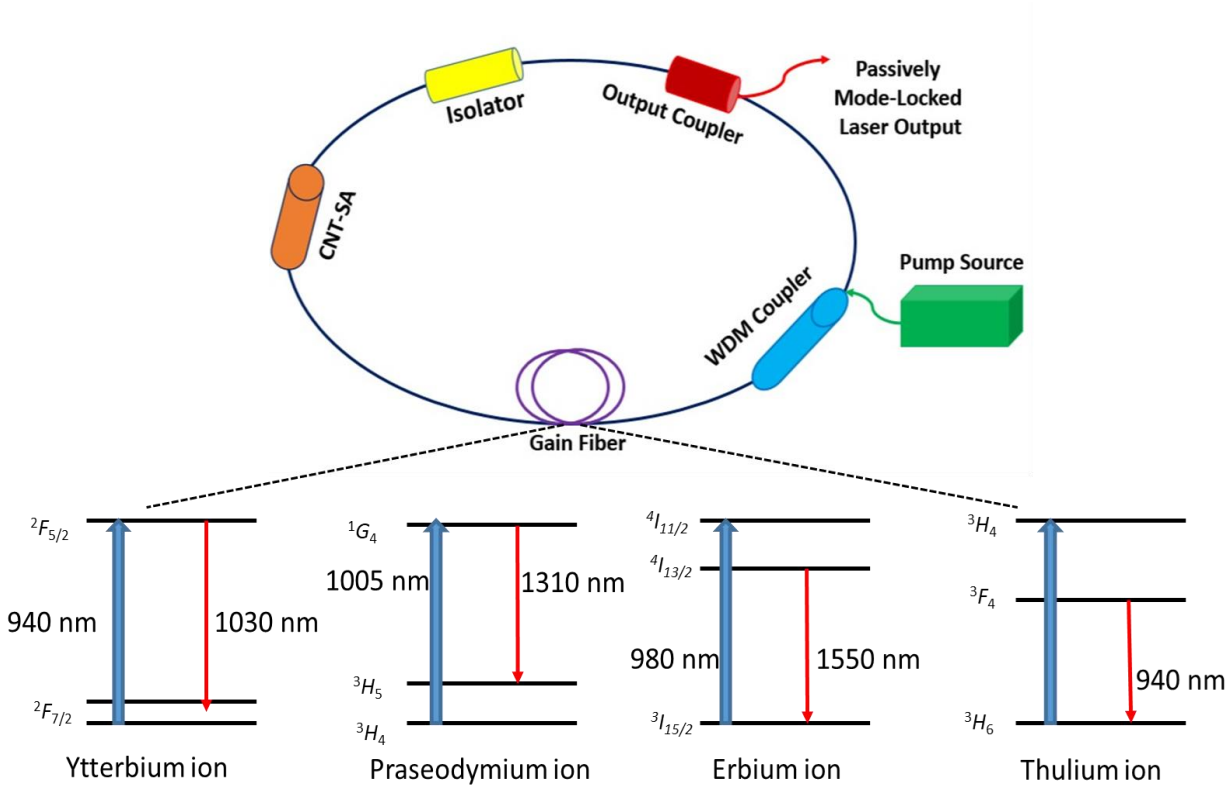

Figure 3 .1 Schematic of CNT-SA based passively mode-locked fibre lasers operating at different center wavelengths incorporating different gain fibres.

3.1.2 Mode-locked Fibre Laser Characterization

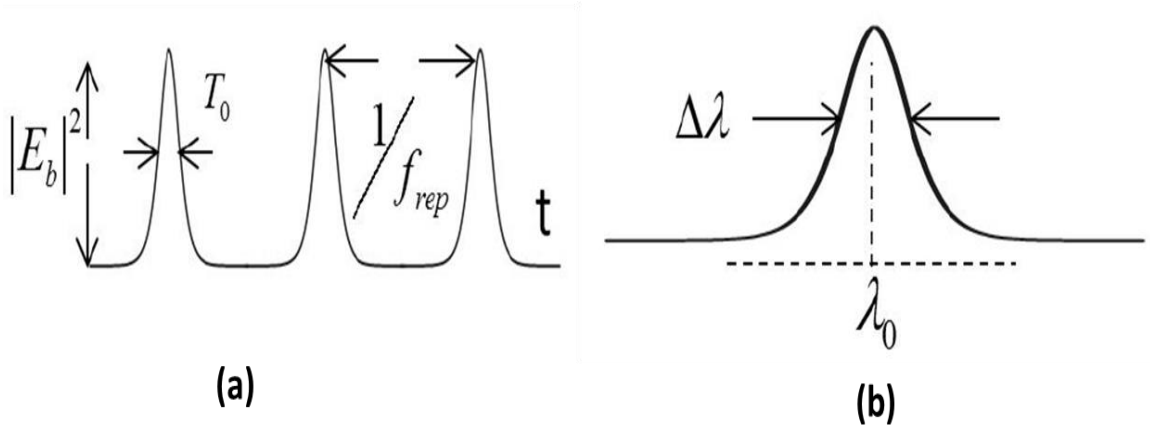

Figure 3 .2 Mode-locked fibre laser pulse key performance parameters: (a) mode-locked laser pulse output in time-domain, (b) mode-locked laser pulse output in frequency-domain.

The key performance parameters of any passively mode-locked fibres lasers are illustrated in the Figure 3.2. Figure 3.2 (a) illustrates the mode-locked laser output in time-domain with laser pulse width of T_0, fundamental repetition rate of pulse train f_{rep} ($1/\tau_{rep}$), and pulse peak power of $|E_b|^2$ (P_{peak}) . Figure 3.3 (b) illustrates the optical spectrum of mode-locked laser pulse with centre wavelength locating at λ_0 and 3 dB spectral bandwidth of $\Delta\lambda$. From the knowledge of pulse width, pulse repetition rate and the average power (P_{avg}), the pulse peak power and pulse energy (P_{Energy}) can be estimated as follows:

$$P_{peak} = \frac{P_{avg} * \tau_{rep}}{T_0}$$

$$P_{Energy} = P_{avg} * T_0$$

Ultra-short and high energy optical pulses generation in fibre lasers using mode-locking technique have emerged as one of the best-pulsed light sources for wide range of applications including micromachining, sensing, frequency metrology and nonlinear applications such as SC generation [93]. Such high energy optical pulses with ultra-short duration can be achieved through the fibre lasers by applying passive mode-locking technique [94]. Among passive mode-locking techniques, NALM, NPR, NOLM and SAs, SA-based mode-locking technique is preferred to be more efficient and environmentally stable [95]. Widely used SAs are SESAMs, CNTs and recently graphene. Among these, CNTs have emerged as promising SAs because of their cost-effective production, saturable absorption, ultrafast recovery time, wide absorption wavelength and ease of fibre integration [95, 96]. CNTs are highly suitable for femtosecond laser pulse generation because of ultrafast recovery time (< 1 ps), which helps to stabilize the laser mode locking; whereas slower recovery time could facilitate the laser self-starting [97].

In this chapter, a CNT-SA based passively mode-locked femtosecond EDFL is generated. The generated EDFL has a pulse train with a repetition rate of 18 MHz, pulse width of 620 fs and a center wavelength at ~1565 nm with a 3 dB bandwidth of ~ 5 nm.

3.2 Passively Mode-Locked Femtosecond Laser Pulse Generation Incorporating CNT-SA

In passive mode-locking, the random phase relations of the many longitudinal modes of the laser cavity are locked by means of applying intensity-dependent loss on the laser signal in each cavity round trip. Resulting an emission of single pulse with a fixed repetition rate. The repetition rate depends on the cavity length and it is equal to the inverse of the cavity

round trip time. In order to achieve the stable mode-locked pulse operation from laser cavity, many aspects such as dispersive and nonlinear properties of the intra-cavity components need to be balanced. The basic mode-locking mechanism can be easily understood by considering the intensity-dependent transmission of SA during the time span of pulse width. When an optical pulse propagates through a SA, the optical pulse wings experience more loss due to less intensity than the central part of the pulse, which is intense enough to saturate the SA. Due to pulse wings experiencing high loss in each roundtrip, the pulse continues to shorten until it becomes short enough which is comparable to the gain bandwidth. Thus a specific pulse width at a stable output pulse operation could be achieved. In the following sections, a femtosecond laser pulse from a passively mode-locked EDFL is achieved using CNT-SA.

3.2.1 Experimental Setup

Figure 3.3 shows the experimental setup of passively mode-locked fibre laser incorporating a CNT-SA. A 0.6 m-long erbium-doped fibre (EDF) is pumped by a 976 nm laser diode through a 980/1550 nm wavelength-division-multiplexing (WDM) coupler. A polarization controller (PC) is inserted in the cavity to adjust and optimize the mode-locking condition and an optical isolator is also inserted in the cavity to avoid reflections and to ensure optical signal propagation only in one direction in the cavity. 10% of the optical power is extracted from the cavity through the 90/10 optical coupler as the mode-locked pulse laser output. The EDF which is used in this experiment is a commercial product (LIEKKI Er110) with a peak core absorption of 110 dB/m and a mode-field diameter around 6.5 μm at 1530 nm. The modulation depth and the non-saturable absorption of CNT-SA used in this experiment at 1560 nm are 8% and 27% respectively. The remaining all fibres used in the cavity are standard

single-mode fibres and the overall length of the cavity is around 5 m. The spectral and temporal characteristics of the mode-locked laser pulse are analyzed by optical spectrum analyzer (OSA) at a resolution of 0.01 nm and 2 GHz photodetector (PD) followed by 350 MHz oscilloscope respectively.

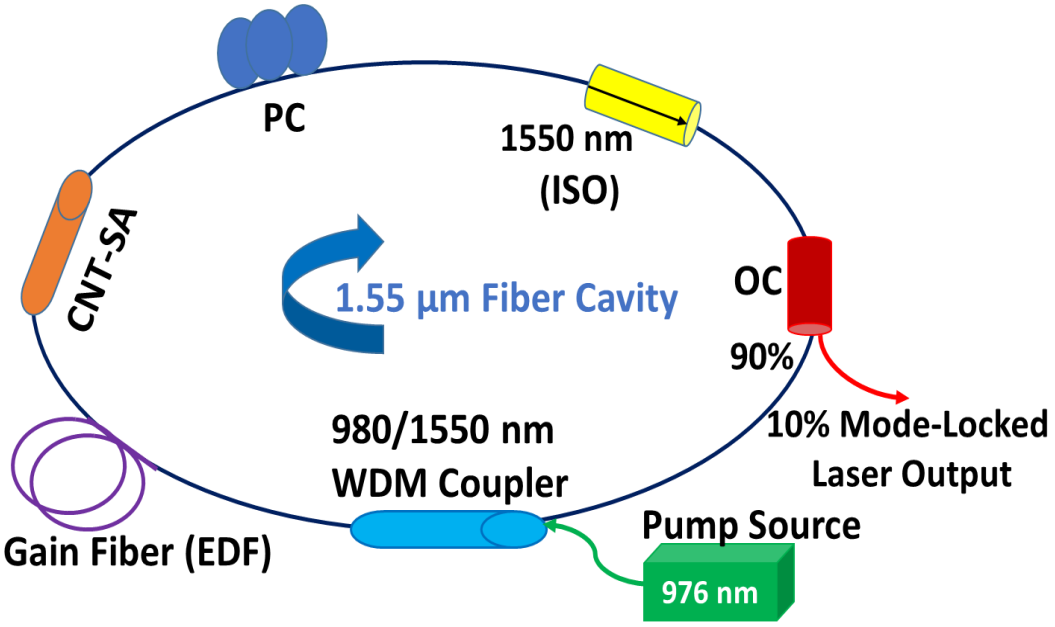

Figure 3. 3 Experimental setup of passively mode-locked fibre laser incorporating CNT-SA.

The active fibres and passive fibres are spliced with optical components using the standard fusion splicing technique. The commercially available CNT-SA has termination with the UPC type fibre connectors, therefore, in the cavity, two UPC type fibre connectors are spliced at the end of EDF termination and at the beginning of PC. Fibre connectors were used to insert the CNT-SA in the ring cavity. Figure 3.4 shows the picture of CNT-SA used in the experiment and Figure 3.5 shows the experimental setup picture that was taken in the laboratory.

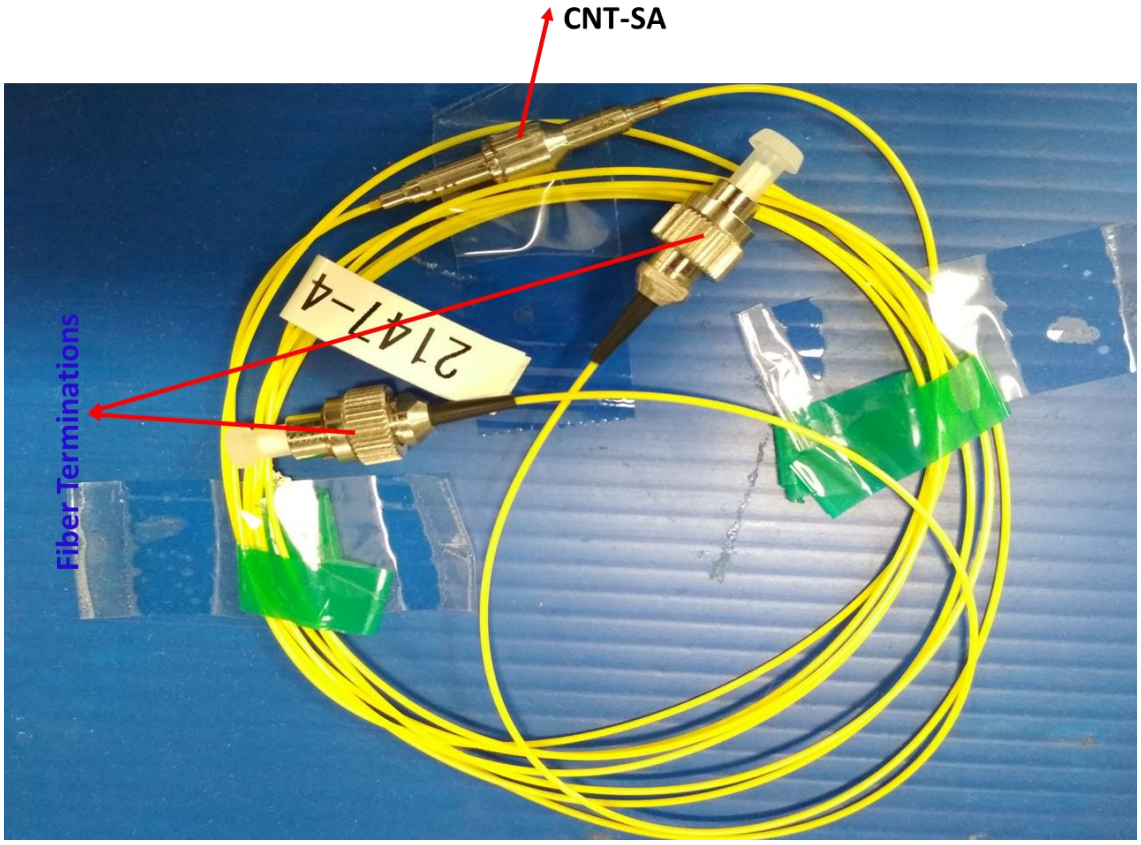

Figure 3. 4 CNT-SA used for the passive mode-locking.

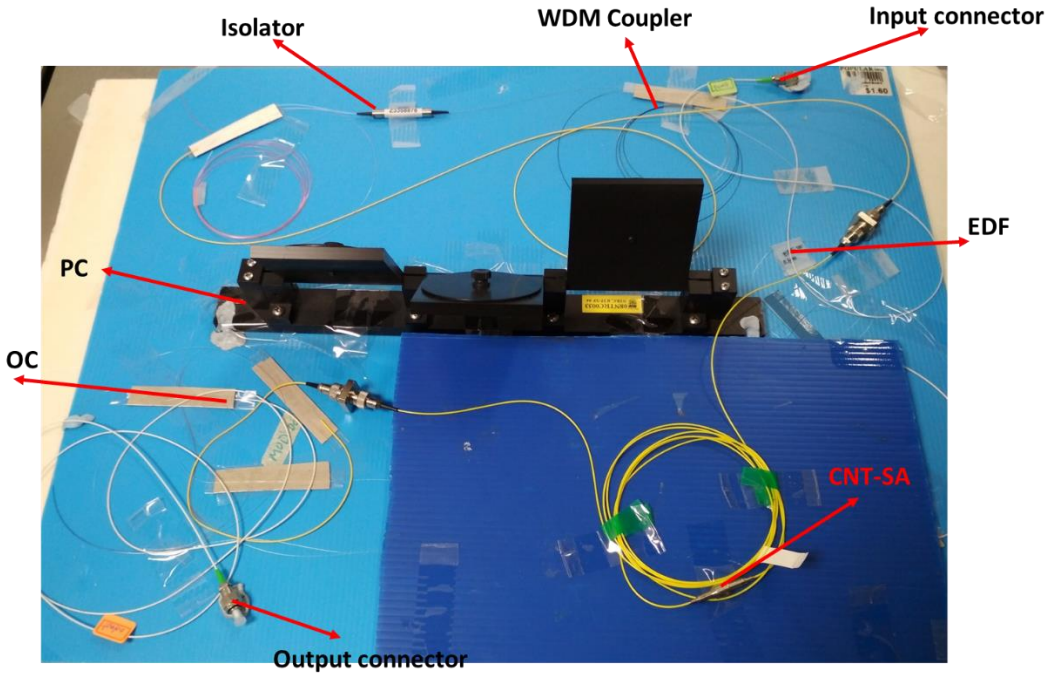

Figure 3. 5 Ring-cavity setup in the laboratory.

3.2.2 Experimental Results and Discussion

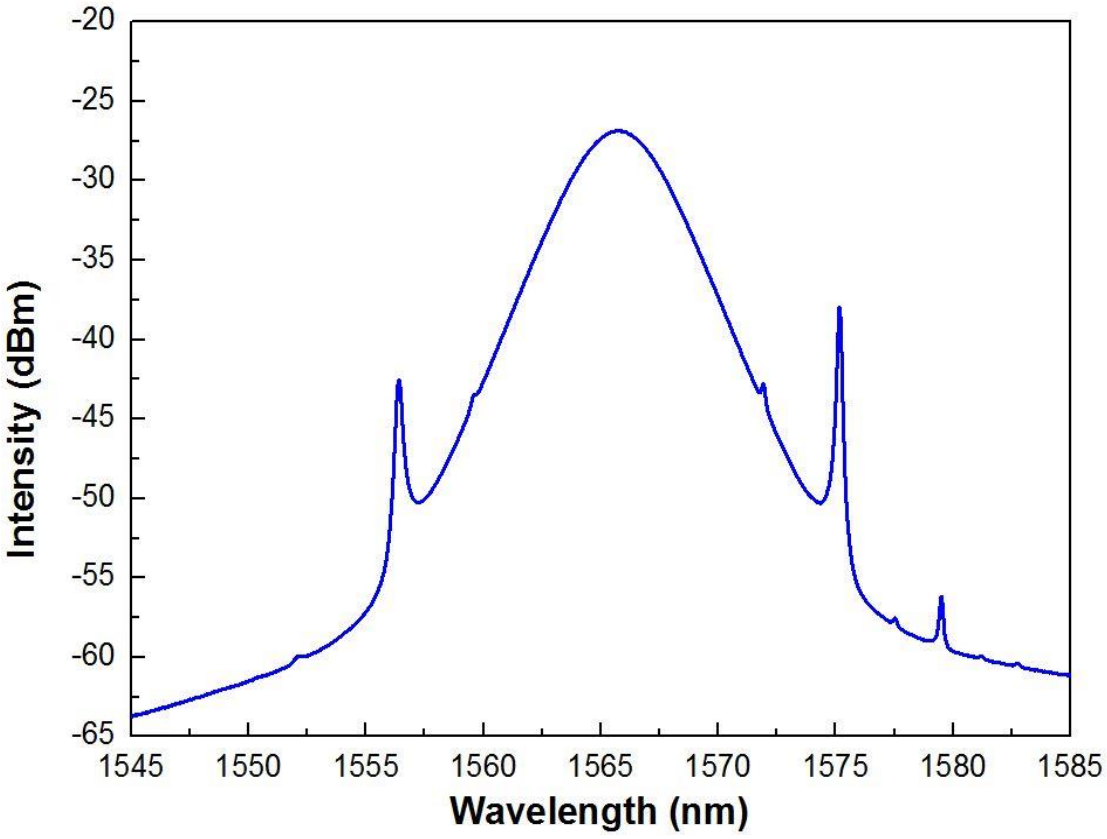

Figure 3. 6 Output spectrum of mode-locked laser pulse.

In this experiment, the cavity starts emitting self-started mode-locked pulses at an input pump power of 50 mW, but the pulse observed at this input power is highly unstable which is undesirable for SC generation applications. In order to achieve stable mode-locked pulse emission, the input pump power is increased in steps and achieved the stable mode-locked pulse at around 126 mW. Further increase of input pump power to the cavity pushes the cavity into unstable mode-locked pulse operation. It is observed that the output pulse power increased linearly with the input power. The cavity is maintained at an input pump power of 126 mW to maintain the stability of mode-locked pulse emission. Figure 3.6 shows the passively mode-locked laser pulse optical spectrum with a 3dB bandwidth of 5 nm at center

wavelength of 1565 nm, which is measured using OSA at a resolution of 0.01 nm and measured 10% output average pulse power is observed as 0.21 mW and the corresponding pulse peak power, pulse energy is 19 W and 11.76 pJ respectively. Initially, at the stable mode-locked pulse operation, two pairs of strong spectral peaks are observed on both sides of the center wavelength, one pair close to the center wavelength is minimized by adjusting the PC. Whereas 2nd pair of peaks is fixed irrespective of the adjustment of PC, indicates that the soliton-like pulse propagates inside the cavity [98]. The shape and strong spectral peaks are called Kelly-side bands which arises from the soliton-like pulse propagation inside the laser cavity.

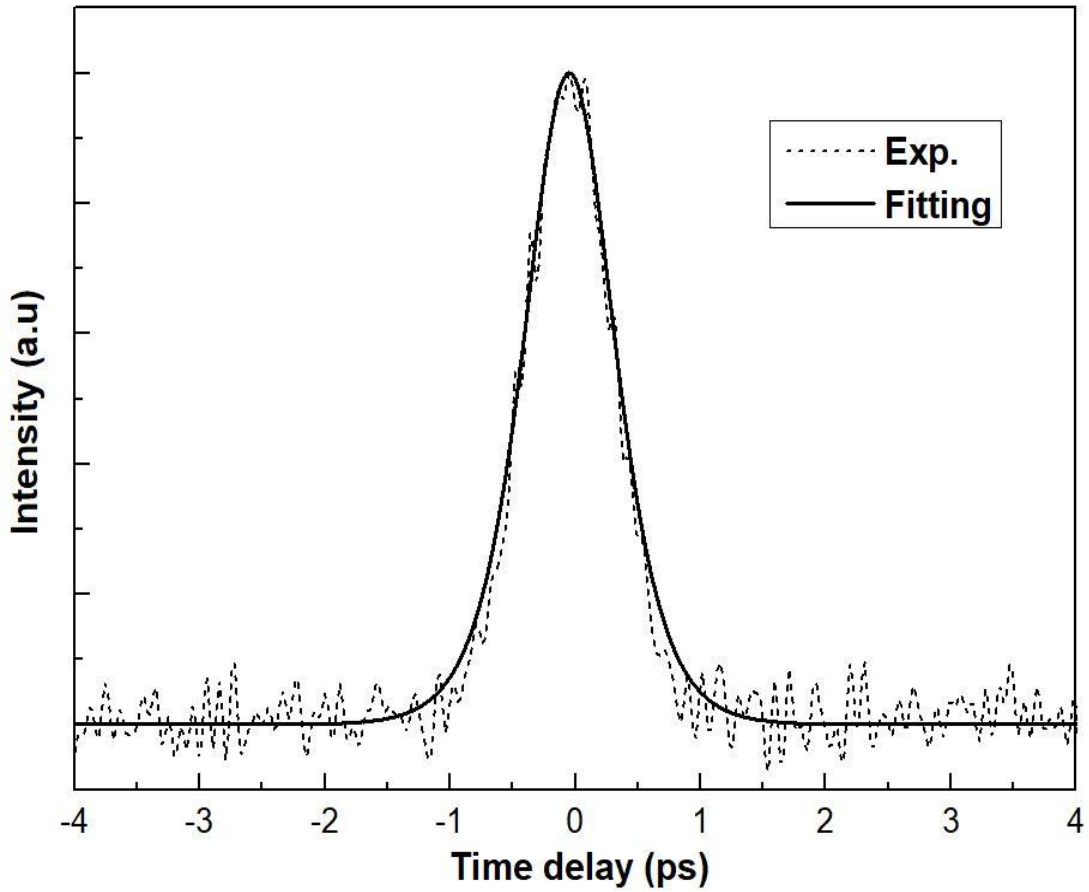

Figure 3 7 Autocorrelation trace of passively mode-locked fibre laser pulses.

Figure 3.7 shows the autocorrelation trace of passively mode-locked laser pulse output along with $sech^2$ curve fitting which is measured using second harmonic generation (SHG) auto-correlator. It is observed that my experimental data fits well with the $sech^2$ pulse profile and the measured pulse width at full width half maximum (T_{FWHM}) of the autocorrelation trace is 620 fs. The time-bandwidth product ($\Delta f * T_{FWHM}$) of the mode-locked pulse is observed to be ~0.379, which is close to the transform-limited $sech^2$-pulse with time-bandwidth product of 0.315, indicating that the generated mode-locked laser pulse is nearly chirp-free.

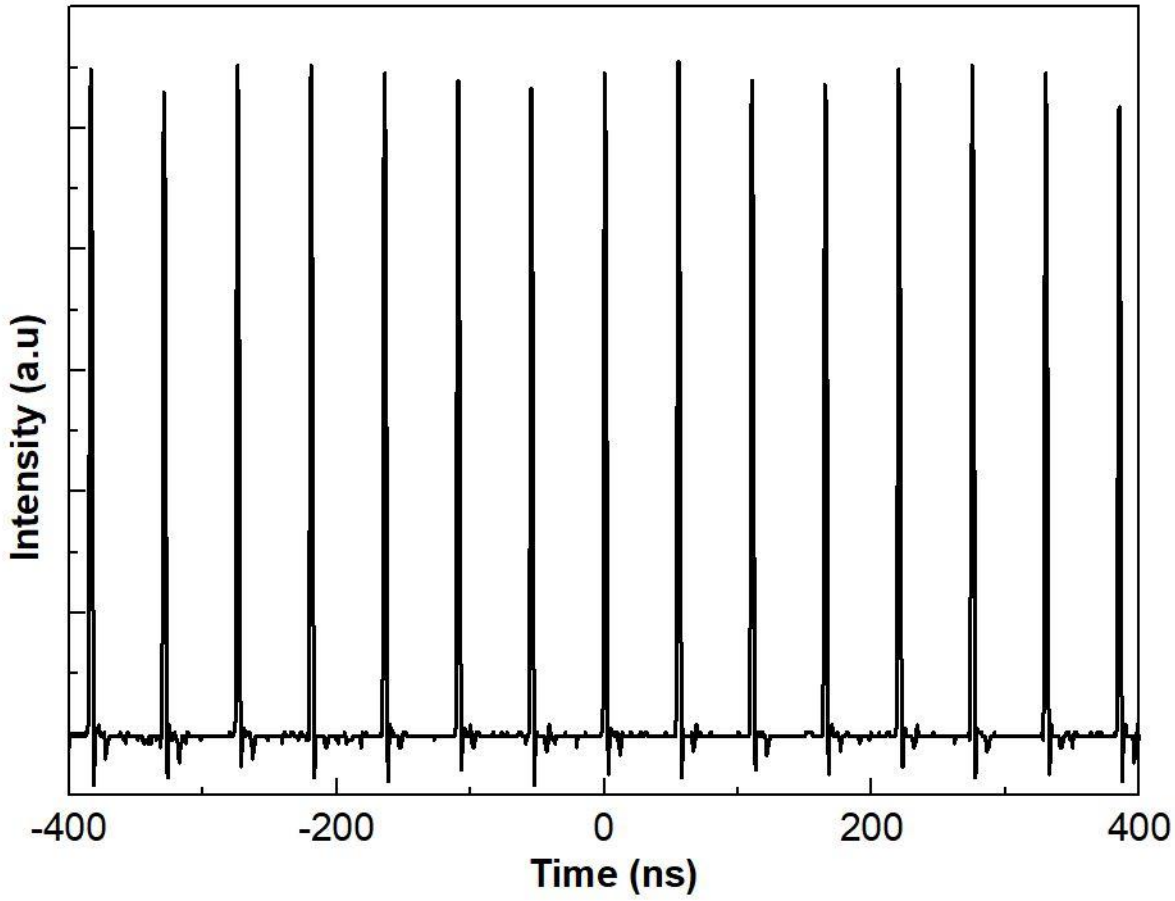

Figure 3 8 Optical pulse train of the mode-locked laser.

Figure 3.8 shows the output wideband RF spectrum which is recorded using 2 GHz photodetector followed by 350 MHz oscilloscope, gives the pulse train of passively mode-

locked laser. The observed pulse repetition rate of the mode-locked laser is measured at 18 MHz which is corresponding to the total cavity length ~5 m, indicating that the laser operates at fundamental mode-locking state.

3.3 Summary

In this chapter, the passively mode-locked EDFL pulse train is generated. The mode-locking is achieved using CNT-SA and the generated mode-locked laser pulse has a pulse width of 620 fs, 3 dB bandwidth of 5 nm at a center wavelength of 1565 nm. The CNT-SA used in this experiment for mode-locking is a commercial available product with a modulation depth of 8% and a non-saturation absorption of 27%. The laser is mode-locked at fundamental mode-locking frequency at a pulse repetition rate of 18 MHz. The generated mode-locked pulse is nearly chirp-free transform-limited $sech^2$-pulse having time-bandwidth product of 0.379. The average output power observed from the mode-locked laser cavity is 0.21 mW and the corresponding pulse peak power and pulse energy is 19 W and 11.76 pJ respectively. The above conditions are maintained through-out the SC spectral variation study from the PCF, DS-HNLF and ZBLAN fibre with respect to the variation in the input pulse power. The pulse mode-locked output pulse power is amplified using EDFA.

Chapter 4 Supercontinuum Generation in PCF and HNLF

In this chapter. the broadband SC is generated using highly nonlinear PCF as nonlinear medium and the 620 fs laser pulse as seed. Here the seed laser pulse power is boosted using a commercially available EDFA and then the effect of input pulse power variation on SC spectral dynamics inside the PCF is observed. Also, the variation of SC spectral dynamics and the SC bandwidth from a HNLF with respect to the variation in pump pulse power is investigated. Further, the length of the HNLF fibre is varied and observed the SC spectral dynamics at different input powers. The effect of spectral broadening is studied by applying tapering to the HNLF. Throughout the investigation SC spectral variation in the silica-based solid-core highly nonlinear PCF and DS-HNLF, the input pulse power is limited to 20 dBm due to the EDFA output power limitation.

4.1 Supercontinuum Generation in PCF

4.1.1 Introduction

In general, all the conventional optical fibres support the optical propagation inside the fibre through the total internal reflection which takes place at the core-cladding boundary, having high refractive index core surrounded by lower refractive index cladding. The PCF is a novel type of microstructured optical waveguide having periodic holes which run along the fibre length. The guiding mechanism in PCF was different from conventional fibres and it is decided by the PCF geometry. There are two mechanisms that support the optical guidance in the PCF: modified total internal reflection and photonic band-gap effect. Optical guidance through the modified total internal reflection mechanism was observed in PCFs having a solid core in the center of the fibre structure surrounded by array of air-holes along its fibre length.

The photonic band-gap mechanism was observed in the hollow core PCFs [99-104]. When compared to a standard fibre, PCF has the advantage of change the fibre parameters such as fibre dispersion, ZDW and fibre nonlinearity by varying cladding structure, which makes the PCF as one of the best fibres for optical sensing, particle trapping and novel applications in nonlinear optics [105-106]. PCFs, also commonly known as microstructured fibres or holey fibres. In my experiment commercially available solid-core 60-m-long highly nonlinear PCF is used.

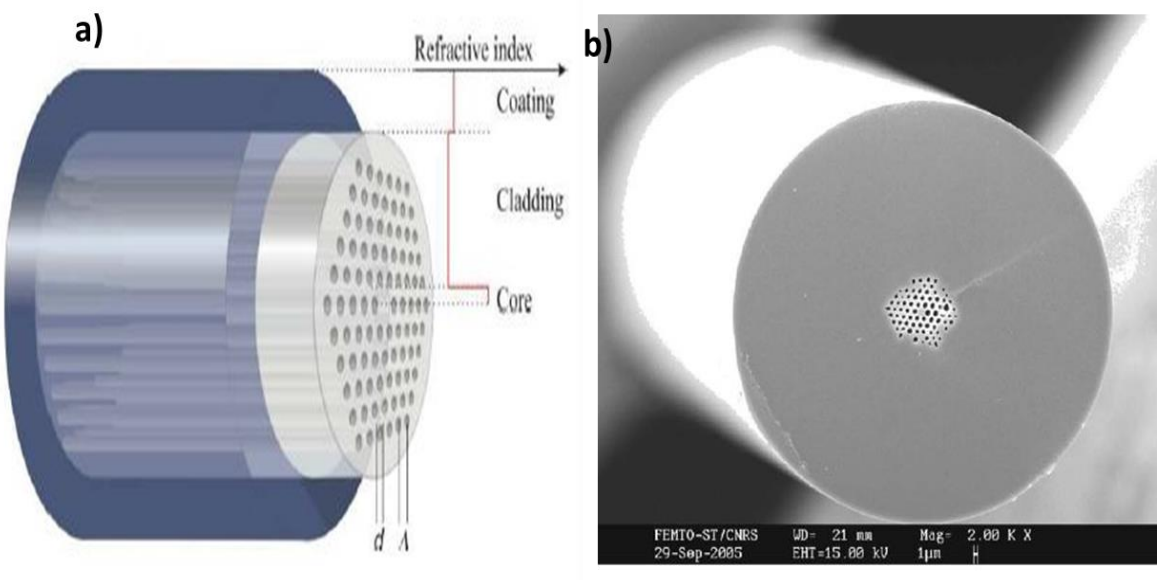

Figure 4. 1 Typical schematic of solid-core PCF [107], (b) Solid-core PCF that used for SC generation for the first time [108].

Figure 4.1 (a) shows the typical schematic of solid-core PCF having hole-size 'd' and hole-pitch 'ʌ'. Highly nonlinear PCFs, typically designed with a hole-pitch around 1-3 µm [107]. Figure 4.2 (b) shows the solid-core fibre that was used for the SC generation for the first time by Ranka, it has a hole-pitch ʌ = 1.6 µm and hole diameter of d = 1.4 µm [108].

The first demonstration of SC generation in PCF with femtosecond pump pulses was done by Ranka et al. in 2000, where he was able to achieve a SC spectrum of bandwidth over an

octave-spanning from 0.39 µm to 1.6 µm by pumping femtosecond pulses close to ZDW i.e. close to 800 nm [108]. Since then, broadband SC laser sources were realized using PCF and different pumping mechanisms. Where the pumping mechanisms involved a laser source with pulse widths varying over a wide range starting from nanosecond to femtosecond. The SC spectrum was generated spanning from 380 nm in visible spectrum to the extent of near-infrared region by pumping a laser pulse with widths varying from 25 fs to 0.8 ns having pump wavelengths in the visible or near infrared region [79,108-112]. In all the above demonstrations, SC generation using PCF have realized using a commercially available solid-state lasers or mode-locked pulsed fibres lasers. In this study, the SC generation in a commercially available 60-m-long solid-core highly nonlinear PCF by pumping CNT-SA based passively mode-locked femtosecond EDFL is demonstrated. To our best knowledge, this the first demonstration of 1080 nm wide SC spectrum with a CNT-SA based passively mode-locked femtosecond EDFL and PCF as nonlinear media. In this section, the spectral broadening phenomena inside PCF is observed at different input pulse powers and the bandwidth variation with respect to the input pulse power variation is also presented.

4.1.2 Experimental Setup

Figure 4.2 shows the experimental setup of SC generation from a CNT-SA based passively mode-locked EDFL and PCF. In order to activate the nonlinear properties of PCF efficiently for broadband SC generation and to study the effect of input pulse power variation on the SC spectral dynamics, an EDFA is used to boost the input pulse power before launching into PCF. to protect the mode-locked laser pulse stability and to protect the EDFA from back reflection from PCF, on both sides of the EDFA high power isolators are used. The output spectrum from PCF is observed with OSA. Here two OSAs (450 - 1750 nm & 1200 - 2400 nm) were used to

cover the whole wavelength range of SC spectrum generated from PCF. A 60 meters' (60-m) length of commercially available (NL-1550-POS-1) solid-core PCF is used to observe the SC spectral variation with respect to the input pulse power variation. The PCF has numerical aperture (NA) of 0.4 µm and mode-field-diameter (MFD) of ~2.8 µm respectively, at 1550 nm and an average core diameter of ~2.1 µm [113]. It has two ZDWs close to 1475 nm and 1650 nm [107]. The attenuation of the PCF is < 9 dB/ km.

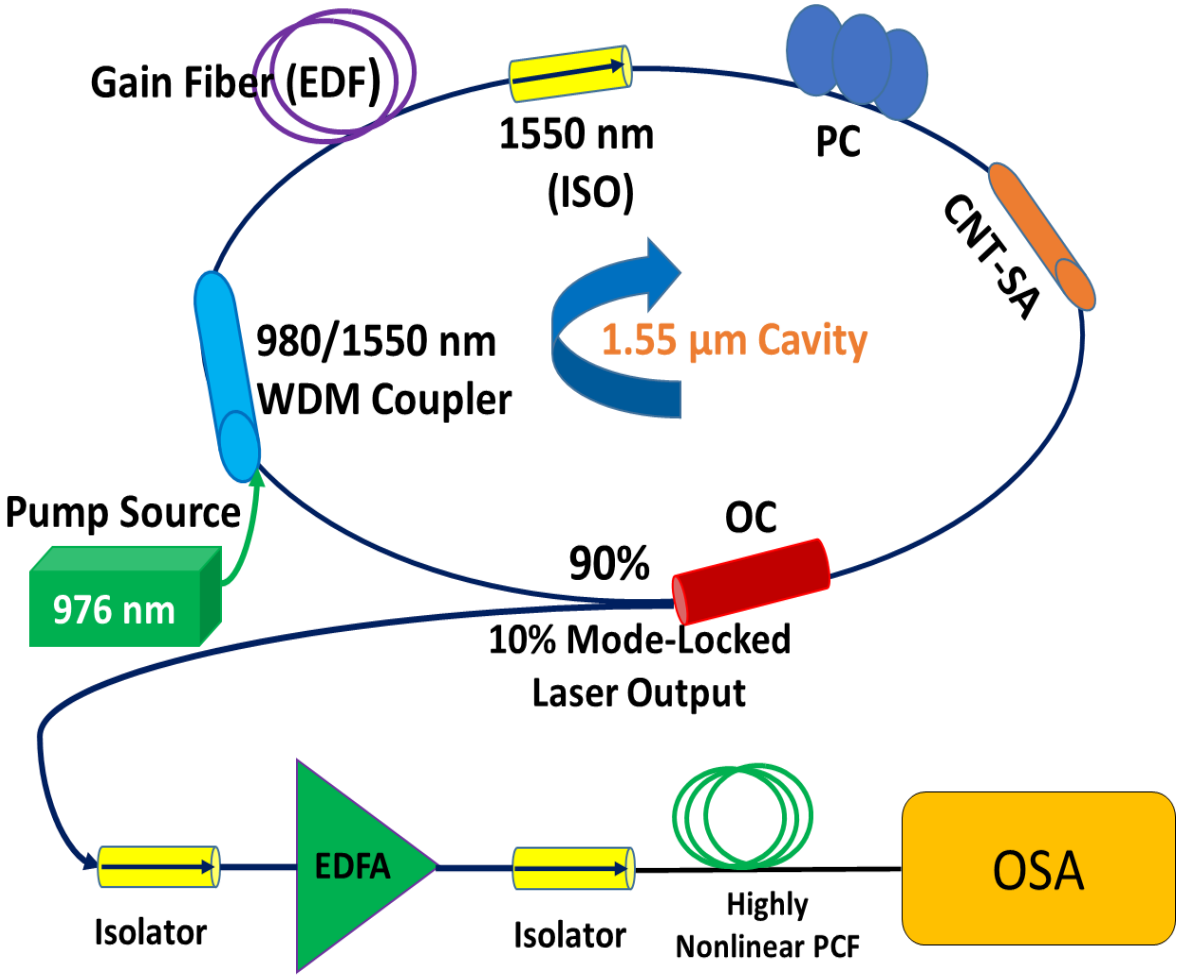

Figure 4. 2 Experimental setup of SC generation from a PCF using passively mode-locked fibre laser.

4.1.3 Results and Discussion

Figure 4.3 shows the SC spectrum output from PCF at different input pulse powers. An amplified 620 fs pulse is launched into 60-m-long PCF. The femtosecond pulse has a 3 dB bandwidth of ~5 nm at a center wavelength of 1565 nm. The input pulse power is amplified in steps starting from 0 dBm to 20 dBm and the output SC spectral variation is observed. From the SC spectral variation, the SC spectrum bandwidth increases with the increase in input pulse power. The seed pulse center wavelength falls into the middle region of the ZDWs wavelengths of the PCF. Therefore, it is difficult to draw a conclusion on the SC spectral dynamics from the seed pulse launching region into PCF. However, from the SC spectral output, the nonlinear phenomena that are responsible for the spectral broadening with the increase in input pulse power are clearly understandable.

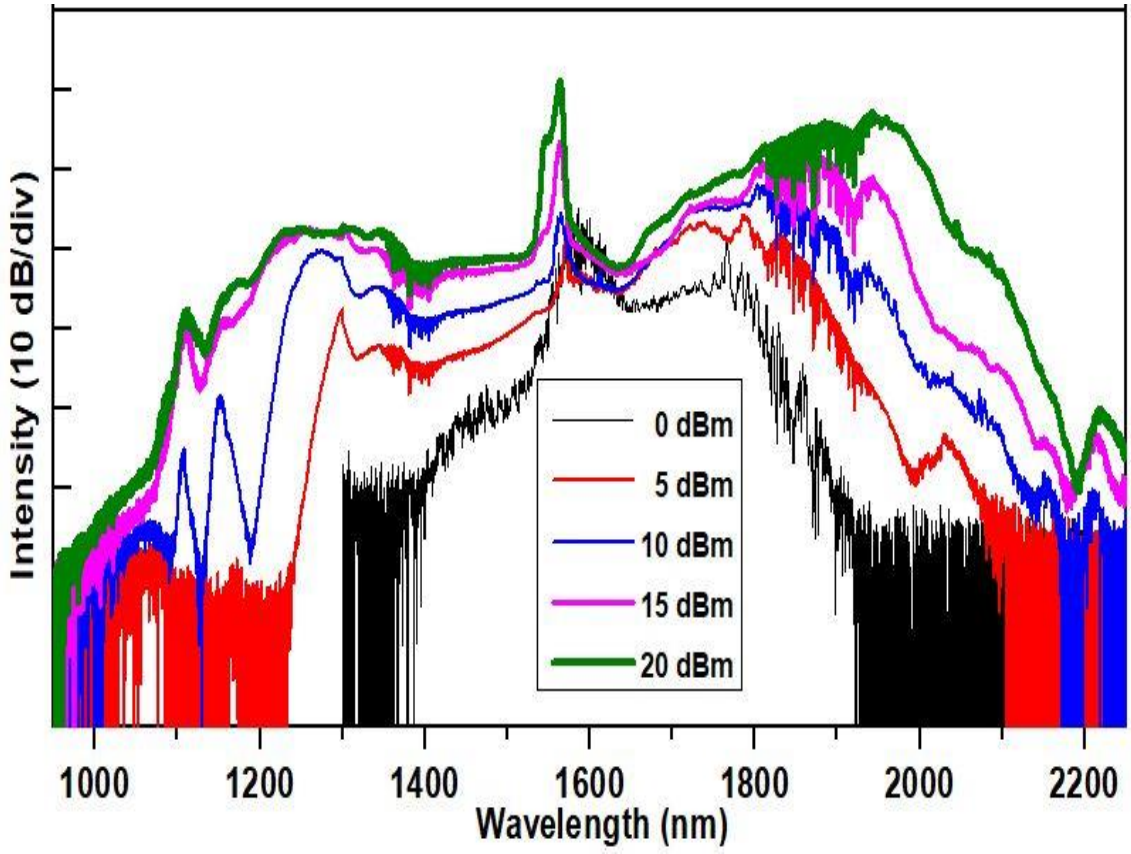

Figure 4. 3 SC spectrum output from PCF at different input pulse powers.

At 0 dBm input pulse power, the SC spectrum is broadened more towards longer wavelength side which means that the SRS effect plays a dominant role in generating new frequency components through the strong strokes generation from the seed signal. As the input pulse power increases the SC spectrum starts broadening on the both sides of the seed pulse center wavelength which is evident that the both SPM and SRS are responsible for the new frequency generation inside the PCF. The strong spectral components in the long wavelength region suggest that the SRS is plays a dominant role in the generation of long wavelength components in SC generation process inside the PCF. The strong residual peak at the center wavelength suggests that the SPM effect is weak in the SC generation process. The residual peak at the center wavelength can be reduced by pumping very ultra-short pulses making SPM very strong, which distribute the pump energy towards the long and short wavelength sides leads to the depletion of pump residual peak. An average power loss of 8 dBm is observed at the output of 60-m-long PCF.

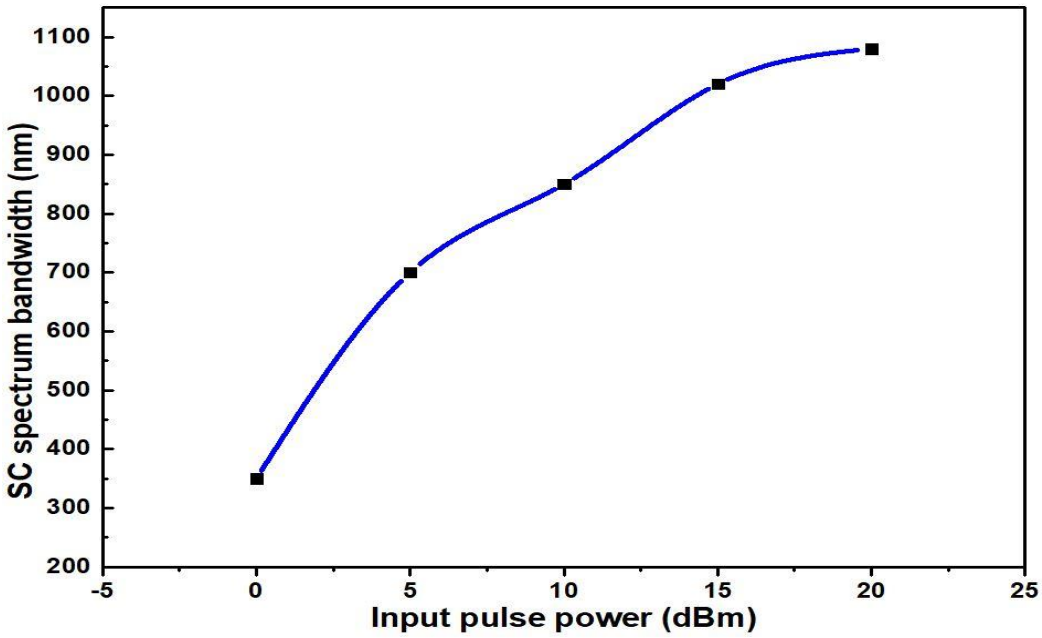

Figure 4. 4 PCF output SC bandwidth variation with respect to the input pulse power.

Figure 4.4 shows the PCF output SC bandwidth variation with respect to the input pulse power. It is observed that the SC bandwidth is increased with the input pulse power, however, the improvement in the SC bandwidth at high power i.e. at 20 dBm is less than the improvement in the SC bandwidth at 5 dBm and 10 dBm. This is due to the nature of the fibre i.e. the PCF used in this experiment is of silica-based which experiences more loss beyond 2 µm. Due to high fibre loss beyond 2 µm, a clear observation was made that the SC spectrum broadening towards longer wavelength is very minimal at higher powers when compared to shorter wavelength side. A maximum SC spectrum bandwidth of 1080 nm spanning from 1090 nm – 2170 nm is achieved at 20 dB below the residual peak with power fluctuations less than 8 dB. The power fluctuations in the spectrum is mainly arises from constructive and destructive interference of the SPM-induced chirp frequency components [57].

4.2 Supercontinuum Generation in HNLF

In the previous section, for the first time 1080 nm, wide SC spectrum from a solid-core highly nonlinear PCF using CNT-SA-based passively mode-locked femtosecond EDFL as pump is demonstrated. In order to extend the SC spectrum further into mid-IR region and to achieve broad SC spectrum bandwidth, the dispersion-shifted HNLF (DS-HNLF) is chosen. In this section, the spectral broadening variation inside the 1-km-long DS-HNLF by varying the input pulse power is demonstrated. Here the CNT-SA-based passively mode-locked femtosecond EDFL used as the pump to the 1-km-long DS-HNLF. In this section, demonstrated a SC spectrum spanning from 1100 nm to 2470 nm at an input pulse power of 20 dBm. The DS-HNLF is a commercially available nonlinear silica fibre, where the dispersion is shifted in order to launch the input pulse near the ZDW to achieve broad and flat spectrum. Variation of fibre

length and tapering effect on SC spectral broadening phenomenon is also studied in the subsequent sections.

4.2.1 Introduction

The fibre nonlinearity can be measured by calculating the fibre nonlinearity co-efficient γ , defined in equation 2.32, can be written as $\gamma = \frac{2\pi n_2}{\lambda A_{eff}}$, where A_{eff} is the effective mode area as defined in equation 2.33, λ is the wavelength of the optical signal and n_2 is the nonlinear-refractive index of the material. In general, conventional fibres has γ values ~ 1 (1/W-km), therefore the nonlinear effects are almost negligible and need to give very high input power to observe any nonlinear phenomena in such fibres. In order to reduce the input pulse power to activate the nonlinear phenomenon inside the SMF, there is an alternative such as modifying the fibre parameters to achieve high nonlinearity. For a particular glass fibre n_2 is fixed, therefore, in case of silica-based optical fibres, high nonlinearity can be achieved by reducing the effective mode area. Effective mode area depends on both the core size and the doping levels [114]. For a silica-based fibre, the reduction of effective mode area can be achieved by reducing the core-size. Therefore, high nonlinearity can be achieved. Fibres that are having γ > 10 (1/W-km) can be considered as HNLF [57]. Other ways to achieve high nonlinearity is by changing the refractive index n_2 , this can be done by varying the doping levels in non-silica fibres and through the microstructured design of fibre. In this experiment commercially available silica-based 1-km-long HNLF having γ >15 (1/W-km) was used. the high nonlinearity can also be achieved by applying tapering on the fibre which then reduce the fibre core size there by reducing the effective mode area. Tapering effect on SC spectral variation is also studied by applying tapering ratio of 2 on short-length of HNLF. In this case

the DS-HNLF is used in order, to launch the input pulse in the region of ZDW of the fibre to attain flat and broad SC spectrum.

Silica-based HNLF fibres are preferred over the microstructured (PCF) fibres due to its low splicing loss and easy to splice with standard SMF. Till date, many researchers demonstrated the SC generation using HNLFs, where they have used the CW, sub-microsecond to femtosecond pulses as pump in a relatively long length of HNLFs, which varies from few 10's of meters to over 5 km and also the SC generation setup was quite complex [115-126]. In all the mentioned previous studies, a hybrid kind of fibre structure is used such as cascaded structure of SMF and HNLF with multiple-amplifications stages of input pump pulses is used for SC generation. Most recently, a CNT-SA-based passively mode-locked EDFL setup is used to generate broadband SC generation in a 100-m-long HNLF by pumping 70 fs pulses [116]. A SC spectrum spanning from 1130 nm to 2220 nm is achieved from the 100-m-long HNLF. In this study, relatively broad SC spectrum with a simple single stage amplification in a very short length of HNLF is generated.

In this study, the SC generation from a 1-km-long DS-HNLF is generated by pumping a CNT-SA-based passively mode-locked femtosecond EDFL. The variation of spectral dynamics and the SC spectrum bandwidth is observed with respect to the input pulse power variation. Further, the study is extended to HNLF length variation effect on SC spectral dynamics. At the end of this section, a tapering ratio of 2 is applied on short-length of HNLF to study the tapering effect on the SC spectral dynamics and bandwidth variation.

4.2.2 Experimental Setup

Figure 4.5 shows the experimental setup of SC generation from a HNLF using CNT-SA based passively mode-locked femtosecond EDFA. In order to observe the spectral broadening i.e. SC generation phenomena inside the HNLF at different input pulse powers, the 10 % of the mode-locked pulse output is amplified using a commercially available pulsed EDFA. Isolators are connected at both the input and output of the EDFA in order to maintain the stability of the mode-locked laser cavity and to protect the EDFA from back reflections. The output of EDFA is connected to the HNLF through isolator.

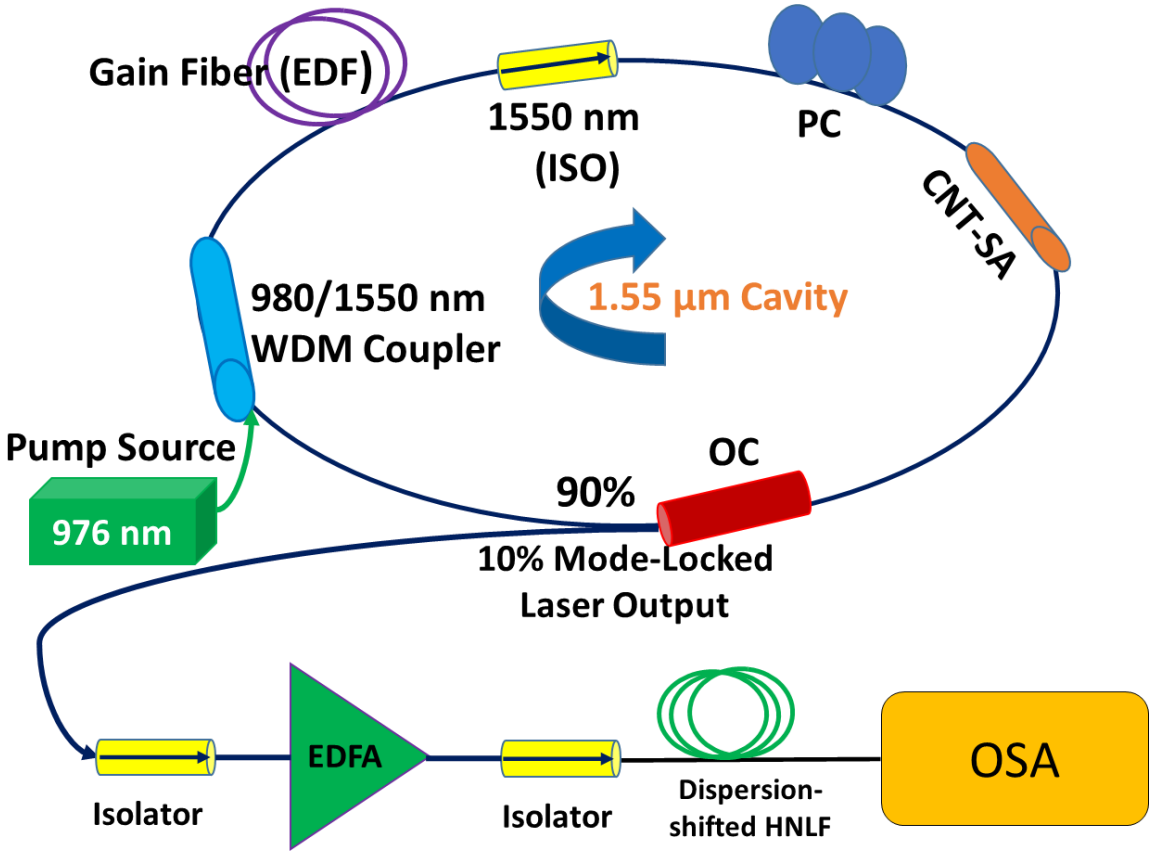

Figure 4. 5 Experimental setup of SC generation from a HNLF using passively mode-locked fibre laser.

The characteristics of the HNLF used in this experiment are, loss α = 0.7 dB/km, dispersion of -0.23 ps/(nm.km), and a dispersion slope of 0.03 ps/(nm^2.km) at 1550 nm and Kerr

nonlinearity coefficient of $\gamma > 15$ $(W.km)^{-1}$. The ZDW of the DS-HNLF is located at ~1560 nm which is close to the pump wavelength. Here the HNLF length is varied from 1 kilometer to 30 cm to study the effect of length variation on SC spectral dynamics. Apart from the length variation, tapering is also applied on HNLF to investigate the tapering effect on SC spectral dynamics. The above experimental setup is maintained through-out the study of HNLF length variation and the tapering effect study.

4.3.1 SC Generation from 1 km Length of HNLF

The input pulse power to the 1-km-long DS-HNLF is varied from 0 dBm to 20 dBm and the output SC spectrum is observed using OSAs of different wavelength range. The input femtosecond EDFL has achieved through the passive mode-locking by incorporating CNT-SA in the EDF ring cavity. The generated EDFL has a pulse train with a repetition rate of 18 MHz, pulse width of 620 fs and a center wavelength at ~1565 nm with a 3 dB bandwidth of ~ 5 nm. These pulse characteristics are maintained through-out the SC generation study in the DS-HNLF.

4.3.1.1 Experimental Results and Discussion

Figure 4.6 shows the SC spectrum variation from the output of 1-km-long DS-HNLF for the input pulse power variation from 0 dBm to 20 dBm. The maximum input pulse power to the fibre is limited by the EDFA output power limitation. From the spectral broadening trend, it is observed that the SC spectral bandwidth is increased with the increase in the input pulse power. The nonlinear physical phenomena are reasonable for the input pulse spectrum broadening inside the DS-HNLF is decided by the pump pulse wavelength and the ZDW of the fibre. The pump pulse has its spectrum center wavelength at ~1565 nm and the DS-HNLF has

its ZDW at around ~1560 nm. Therefore, the femtosecond pulse is launched closed to the ZDW of the fibre and in the normal dispersion region of the fibre. As the femtosecond pulse falls into normal dispersion regime of the fibre, the SPM is the dominant nonlinear physical phenomena responsible for the input pulse spectrum broadening inside the fibre and generates the broad SC spectrum from the output of DS-HNLF. The symmetrical broadening nature of SC spectrum and the spikes in the spectrum depict the SPM dominance over the spectral broadening inside the fibre for the input powers varying from 0 dBm to 10 dBm. As the input pulse power increases beyond 10 dBm, the spectrum starts shifting more towards longer wavelength side than the shorter wavelength, which explains the dominant role of SRS related nonlinear physical phenomena responsible for the spectrum broadening more towards longer wavelength side at the high input powers (15 dBm and 20 dBm). At the input pulse power of 15 dBm and 20 dBm, the spectrum broadened more towards long wavelength making it asymmetric with respect to the center wavelength of the input pulse. The asymmetric nature of SC spectrum is more red-shift of SC spectrum than the blue-shift which is caused by SRS

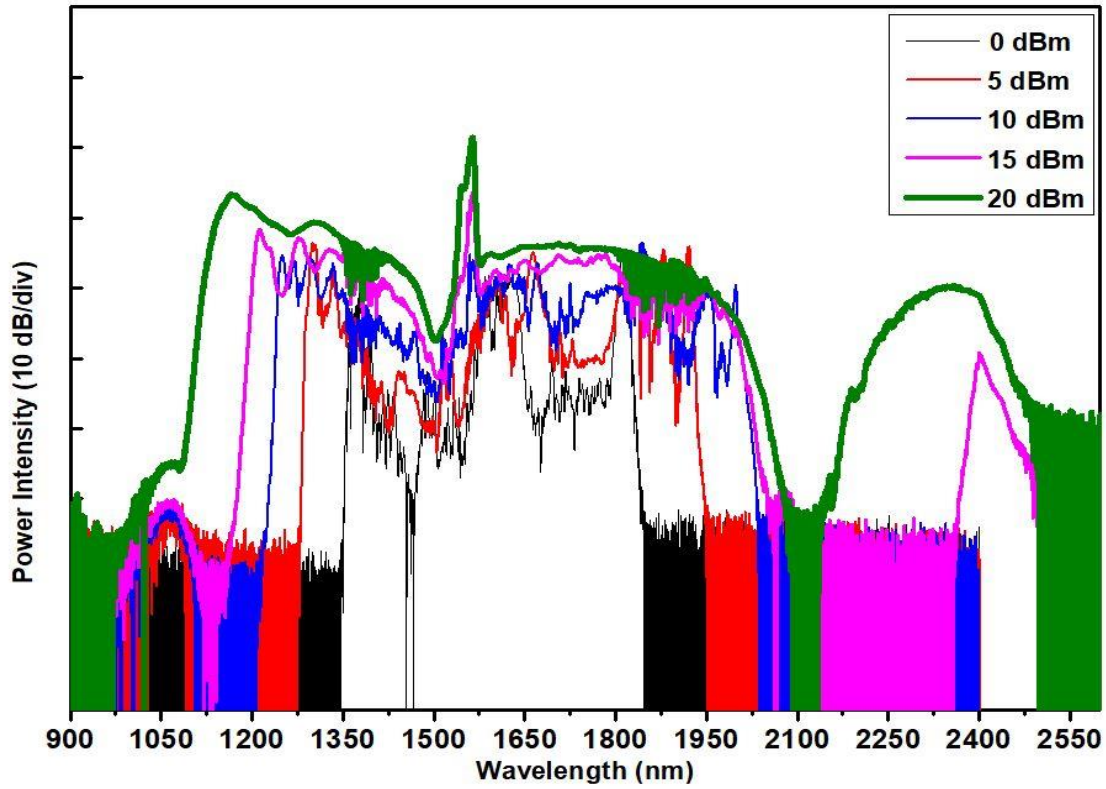

Figure 4. 6 SC spectrum output from DS-HNLF for different input pulse powers.

At the input pulse powers of 15 dBm and 20 dBm, the SC spectrum extended more towards longer wavelength side but there is a dip in the spectrum which breaks the continuity of the spectrum which is undesirable for broadband laser applications. The appearance of dip in the spectrum at around 2.1 µm -2.3 µm may be due to the length of the fibre. This dip in the spectrum can be reduced by increasing the input pulse power to the fibre or by reducing the fibre length. As the input pulse power is limited in this case, opted for the variation of HNLF length study in order to minimize the dip in the spectrum and to achieve flat and possible broad spectrum with the minimal length of HNLF at an available maximum power of 20 dBm.

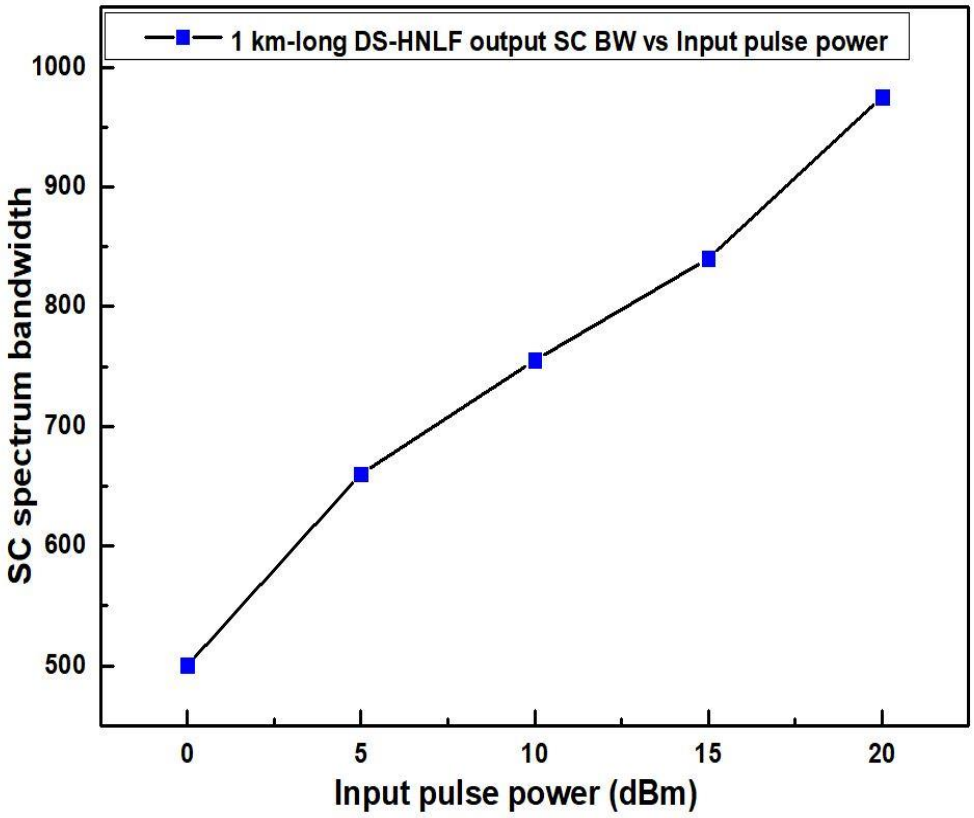

Figure 4. 7 SC spectrum bandwidth variation with respect to input pulse power variation.

Figure 4.7 shows a 20 dB flat output SC spectrum bandwidth variation from 1-km-long DS-HNLF with respect to the variation in the input pulse power. Only the continuous-part of SC spectrum is considered to calculate the 20 dB flat spectral bandwidth. Almost a linear trend of spectral bandwidth is observed with respect to the input pulse power variation due to the symmetrical nature of spectrum. The SC spectrum beyond the 2.1 µm is not considered due to dip in the spectrum. At an input pulse power of 20 dBm, an SC spectrum bandwidth of 975 nm spanning from 1100 nm to 2075 nm is observed at the output of 1-km-long Ds-HNLF. Even though the spectrum is extended up to 2475 nm on the longer wavelength side but the continuous part of the SC spectrum is considered. At all the input pulse powers, an average loss of 9 dB is observed.

In the following section, the length of the fibre is varied in order to generate possible flat and broad SC spectrum by removing the dip in the SC spectrum generated by 1-km-long DS-HNLF. At the end of the following section, a comparative conclusion is included to discuss the spectral bandwidth and spectral flatness variation of SC spectrum with respect to the fibre length variation.

4.3.2 Study of SC Spectrum Variation with respect to the HNLF Length.

In order to achieve the flat and broad SC spectrum from the available DS-HNLF, the length of the fibre is varied to study the effect of input pulse power variation at each different length of DS-HNLF. The fibre length is chosen based on the nonlinearity length (L_{NL}) calculation.

$$L_{NL} = \frac{1}{\gamma P}$$

Where γ is the nonlinearity co-efficient of the fibre and the P is the pulse peak power. The L_{NL} is calculated by considering the $\gamma = 15$ (1/W-km) and the pulse power is varied from the o dBm to 20 dBm. Where the peak power (P) is at all the input power while using the same pulse width (620 fs) here the effect of EDFA on pulse width variation is neglected for easy calculation. Based upon the fibre nonlinearity and the available input pulse power, the L_{NL} is varied from 1 cm to 75 cm. Taken this length as reference and have chosen a fibre length of 30-cm-long, 50-cm-long and 100-cm-long to study the effect of length variation on SC spectral dynamics. In each case, the input pulse power is varied from 0 dBm to 20 dBm and compared the results. These fibres segments are cut from the 1-km-long fibre and then spliced to the fibre connectors. The same experimental setup was utilised for the study of SC generation from 30-cm, 50-cm and 100-cm-long DS-HNLF, just replaced each fibre segment in the place of 1-km-long fibre with the help of fibre connectors.

4.3.2.1 SC spectrum variation in 30 cm Length of HNLF

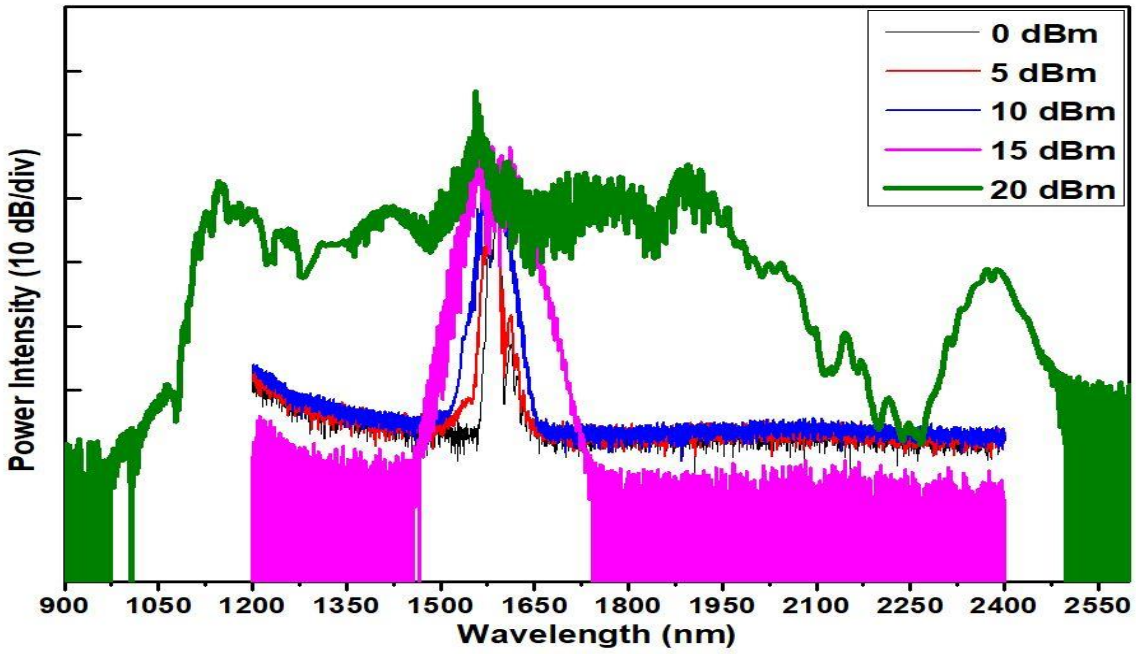

Figure 4. 8 Output SC spectral variation from 30-cm-long DS-HNLF for different input powers.

Figure 4.8 shows the SC spectral variation from the 30-cm-long DS-HNLF at different pulse powers varying from 0 dBm to 20 dBm. The spectral broadening observed for the input pulse powers of 0 dBm to 15 dBm was very nominal when compared to the spectral broadening observed at the input pulse power of 20 dBm. The spectral smoothness is degraded when compared to the SC spectrum obtained from 1-km-long fibre. whereas, the fibre loss in the region of 2.1 µm to 2.3 µm is relatively reduced. The further discussion is given in the comparative study section.

4.3.2.2 SC spectrum variation in 50 cm Length of HNLF

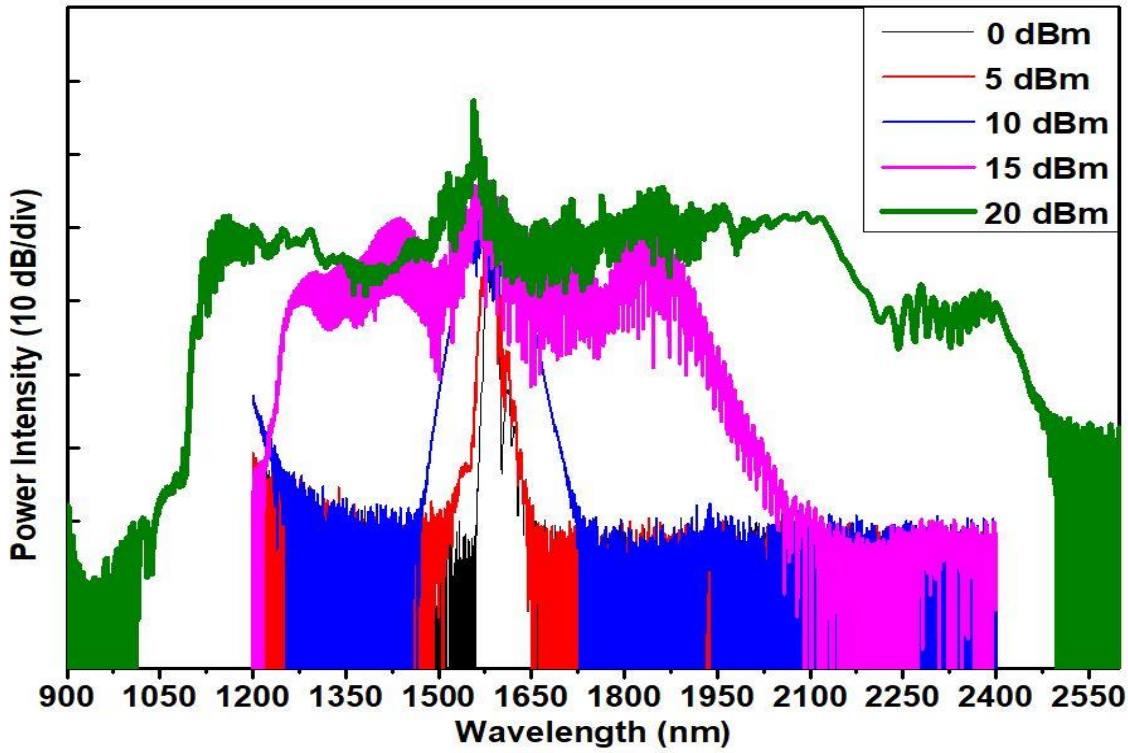

Figure 4. 9 Output SC spectral variation from 50-cm-long DS-HNLF for different input powers.

Figure 4.9 shows the output SC spectral variation from the 50-cm-long DS-HNLF with respect to the variation in the pulse powers from 0 dBm to 50 dBm. When compared to the SC spectrum obtained from the 30-cm-long DS-HNLF, the SC spectrum obtained from the 50-cm-long DS-HNLF exhibits the similar kind of spectral broadening phenomena for the input powers varying from 0 dBm to 10 dBm. When comes to 15 dBm input powers the spectrum shows very significant difference in terms of SC bandwidth more times greater than the SC spectrum bandwidth obtained from 30-cm-long DS-HNLF. whereas the spectral smoothness is degraded furthermore. The SC spectrum corresponding to the 20 dBm input power looks like more or less similar in both cases, whereas, the dip is further reduced and the SC spectrum is boosted in case of 50-cm-long DS-HNLF in the region from 2.1 µm to 2.3 µm. From 30-cm-

long fibre to 50-cm-long fibre, significant change in the spectral broadening is observed. Therefore, the fibre length is increased to 100 cm in order to achieve smooth and possible broad SC spectrum.

4.3.2.3 SC spectrum variation in 100 cm length of HNLF

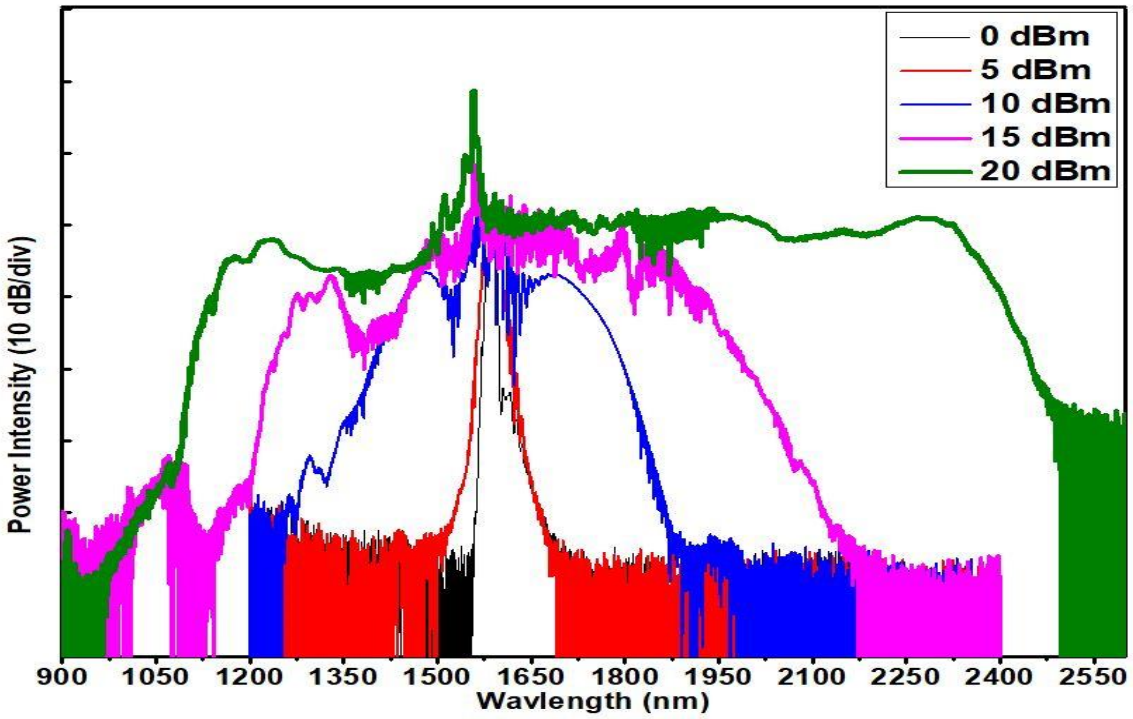

Figure 4. 10 Output SC spectral variation from 100-cm-long DS-HNLF for different input powers.

Figure 4.10 shows the output SC spectral variation from a 100-cm-long DS-HNLF for different input pulse powers varying from 0 dBm to 20 dBm. When compared to 30-cm-long and 50-cm-long fibre, the 100-cm-long fibre generated broader and smooth SC spectrum starting from the input power of 10 dBm. The corresponding SC spectrum bandwidth at the input power of 10 dBm is many times greater than the SC spectrum bandwidth obtained at the same input power from 30-cm-long and 50-cm-long fibre. the spectral smoothness is significantly improved when compared to the SC spectrum generated from 30-cm-long and 50-cm-long fibre. The spectral dip that was appeared in the region from 2.1 µm to 2.3 µm, in

the case of 1-km-long fibre is completely disappeared when comes to the SC spectrum generated from100-cm-long fibre. In the following section, a comparative explanation is given for all the SC spectrums generated from 1-km-long, 30-cm-long, 50-cm-long and 100-cm-long DS-HNLF in terms of spectral smoothness and spectral bandwidth.

4.4 Comparison of SC spectrum generated from different lengths of DS-HNLF

Table.1 summarize the SC spectral bandwidth obtained from different lengths of DS-HNLF and the Figure 4.11 shows the SC spectral bandwidth variation from all the different lengths of DS-HNLFs with respect to the input pulse power variation.

Table 1 Summary of SC spectral bandwidth obtained from different lengths of DS-HNLF.

Input pulse power (dBm)	**20-dB SC spectral Bandwidth (nm) from HNLF**			
	30-cm	50-cm	100-cm	1-km
0	15	15	15	500
5	30	60	70	660
10	80	150	440	755
15	170	700	810	840
20	1000	1350	1360	975

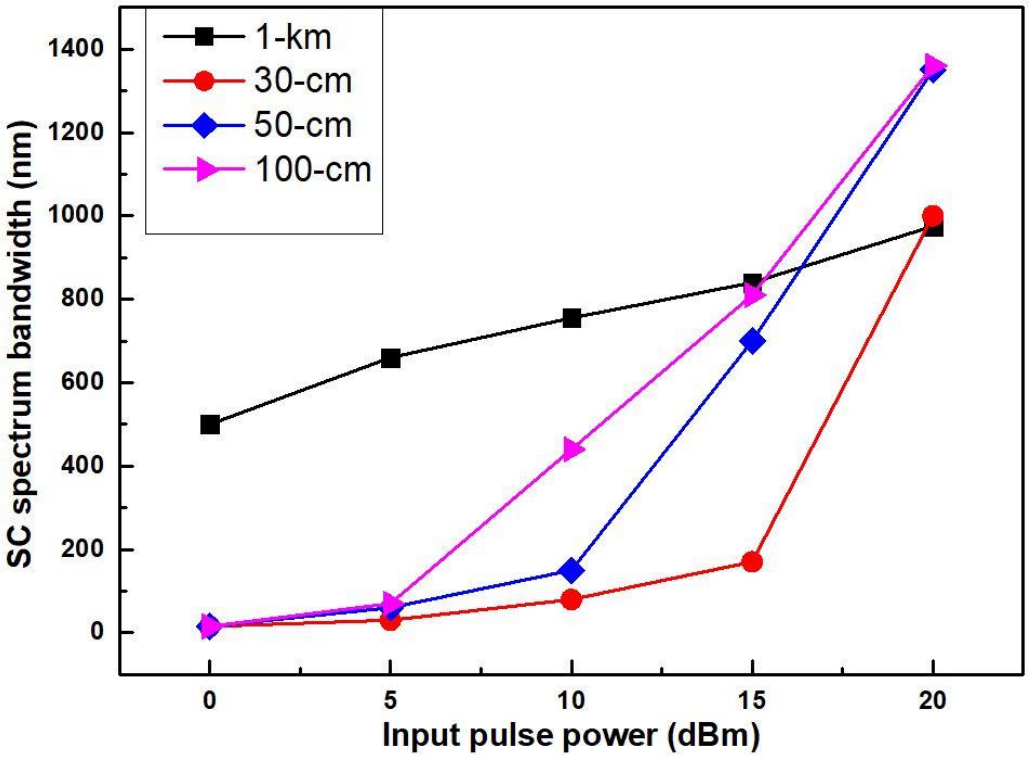

Figure 4. 11 SC spectral bandwidth variation from 30-cm, 50-cm, 100-cm and 1-km-long DS-HNLF with respect to the input power variation.

As per the literature, broad SC spectral bandwidth is obtained from 1-km-long fibre at low input power of 0 dBm when compared to all other length of HNLF. At 0 dBm, a SC spectral bandwidth of 500 nm is observed which is extending from 1350 nm to 1850 nm, where as in all other cases, minimal spectral broadening is observed having SC spectral bandwidth of 15 nm. As the length of the fibre increases the SC spectral bandwidth, as well as the spectral smoothness, is increased. Whereas, in the case of very long fibre such as in 1-km-long fibre, the spectral bandwidth is decreased due to pulse experiencing the huge loss inside the fibre in the region of 2.1 µm to 2.3 µm as shown in the Figure 4.12, which shows the transmission spectrum of 1-km and 100-cm-long DS-HNLF measured over a wavelength range of 1125 nm to 2475 nm. This is due to the OH ions absorption of the silica material in that region. This may be minimized at the high input pulse powers, however, the input pulse power is limited

in this case. Therefore, length variation study is performed and obtained a maximum SC spectral bandwidth of 1360 nm from 100-cm-long DS-HNLF spanning from 1100 nm to 2460 nm as shown in the Figure 4.13, which shows the SC spectrum obtained from 30-cm, 50-cm, 100-cm and 1-km-long HNLF at an input pulse power of 20 dBm.

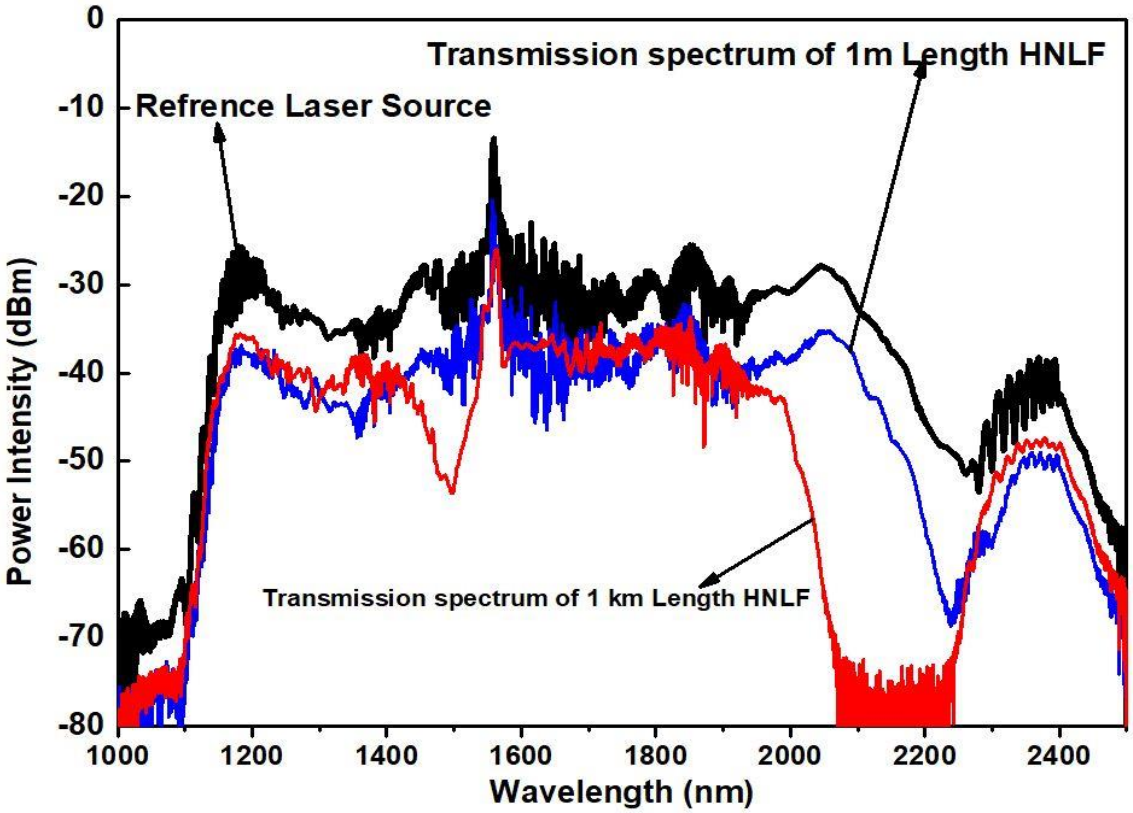

Figure 4. 12 Measured transmission spectrum from 1-km and 100-cm-long DS-HNLF over a wavelength range of 1125 nm to 2475 nm.

Figure 4.12 shows the transmission spectrum of 1-km and 100-cm-long DS-HNLF measured over a wavelength range of 1125 nm to 2475 nm. The SC generated from 50-cm-long DS-HNLF at an input pulse power of 20 dBm is used as laser source in order to estimate the loss profile of 100-cm and 1-km-long DS-HNLF. From the transmission spectrum, it is clearly visible that 1-km-long fibre is experiencing very high loss in the wavelength region of 2.1 µm to 2.3 µm and also in the region close to the pump wavelength i.e. around 1.5 µm when compared to 100-cm-long fibre.

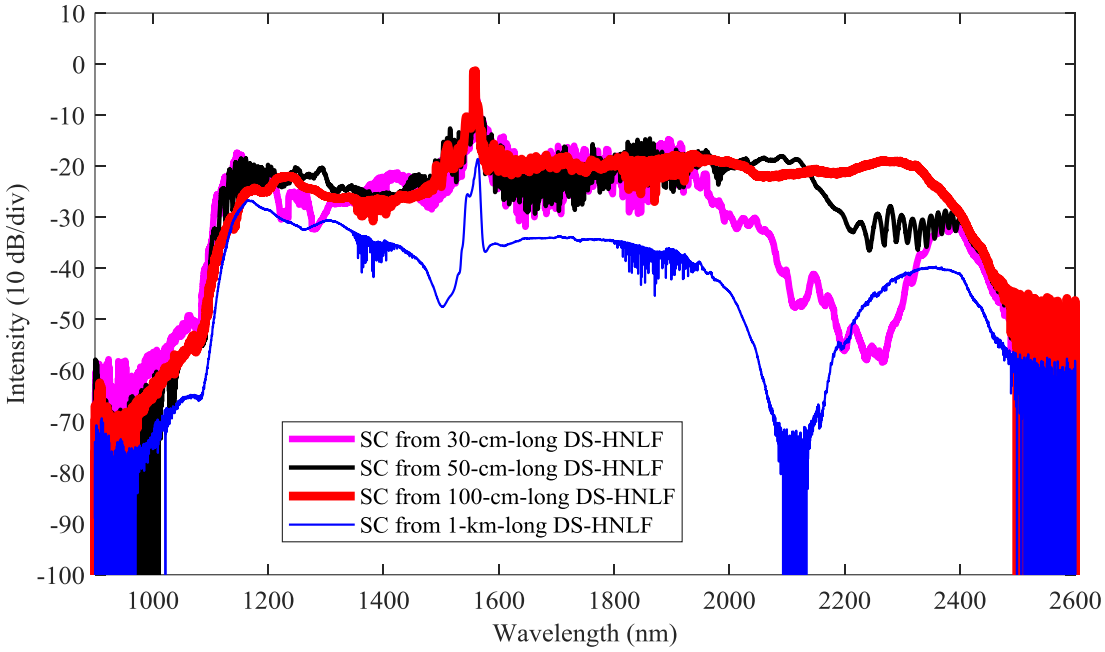

Figure 4. 13 SC spectrum from 30-cm, 50-cm, 100-cm and 1-km-length HNLF at 20 dBm input pulse power

4.5 Effect of HNLF Tapering on SC spectrum

From the above study, a broad SC spectrum with a bandwidth of over 1360 nm spanning from 1100 to 2460 nm is generated from a 100-cm-long DS-HNLF. Here the purpose of applying tapering of DS-HNLF is to study the possibility of extending the SC spectral bandwidth further at the available maxim input power of 20 dBm. In the following section, given a basic theory of tapering and observed the SC spectral variation from tapered DS-HNLF. Here tapering ration of 2 is applied on short segment of a 35-cm-long DS-HNLF.

4.5.1 Fibre Tapering

Tapering, altering fibre nonlinearity and dispersion by means of changing fibre core size. As core size decreases, effective area decreases which leads to significant increase in fibre

nonlinearity, which allow us to generate broad and wide SC spectrum from a very short length of fibres at relatively lower input pulse powers. The nonlinearity co-efficient of the fibre α 1/ effective mode area and effective mode area is α core diameter of the fibre.

Change of fibre core size leads to change in dispersion which shifts the zero dispersion wavelength. As the tapering ratio increases the nonlinearity of the fibre increases and the ZDW shifts towards shorter wavelength side [127-128]. Till date, numerous studies have been done on SC generation by applying tapering on different fibres starting from microstructured fibre to SMF [81, 129-133]. In my case, for the first time tapering on HNLF is applied and observed the SC spectral change and compared with the SC spectrums obtained from normal HNLF. The standard fusion splicer method is used for fibre tapering. The following terminology is used to describe the tapering fibre segment length and the length of the fibre segment after tapering. The tapering lengths are taken as 1 cm and 1.5 cm due to tapering machine limitation and considered only tapering ratio 2 as the other tapering ratios made the fibre very fragile.

In this study, two different tapering lengths are chosen i.e. L_1 =1 cm and 1.5 cm and applied taper ratio of 2 on L_1. The corresponding fibre length (L_2) after tapering a fibre segment of 1-cm and 1.5-cm with tapering ratio of 2 is 4-cm and 6-cm respectively. In both the cases overall fibre length is maintained at L = ~35-cm. Here, L_1= fibre tapering length, L_2 = fibre length after tapering and L =overall fibre length that is used for the SC generation experiment including tapered and untampered region of the fibre.

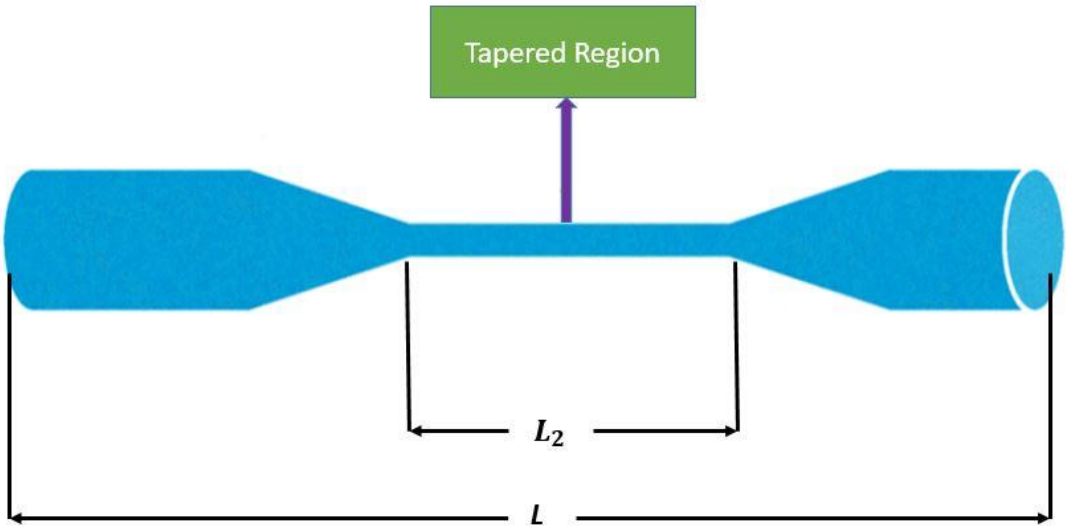

Figure 4. 14 Illustration of tapered fibre [133].

Figure 4.14 shows the schematic of fibre with tapered segment. Where L_2 is the tapered fibre segment length and L is the overall length of the fibre used for SC generation experiment.

4.5.2 SC Output from Tapered Fibre and Results Discussion

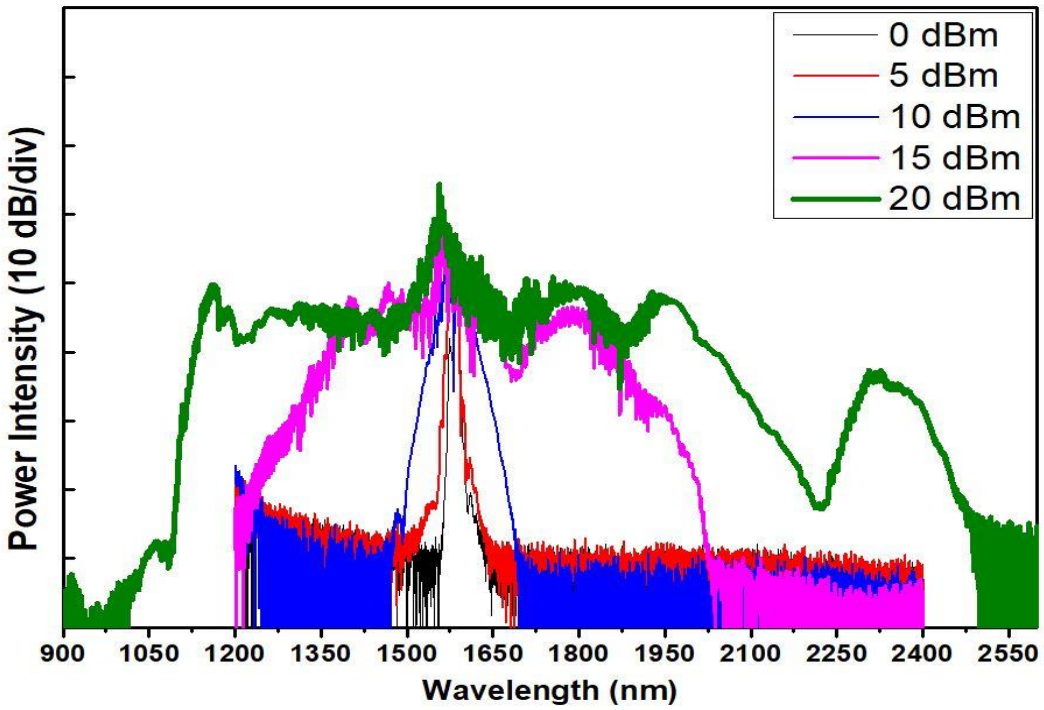

Figure 4. 15 SC spectral output from ~35-cm-long fibre (L1 =1 cm and L2 =4 cm).

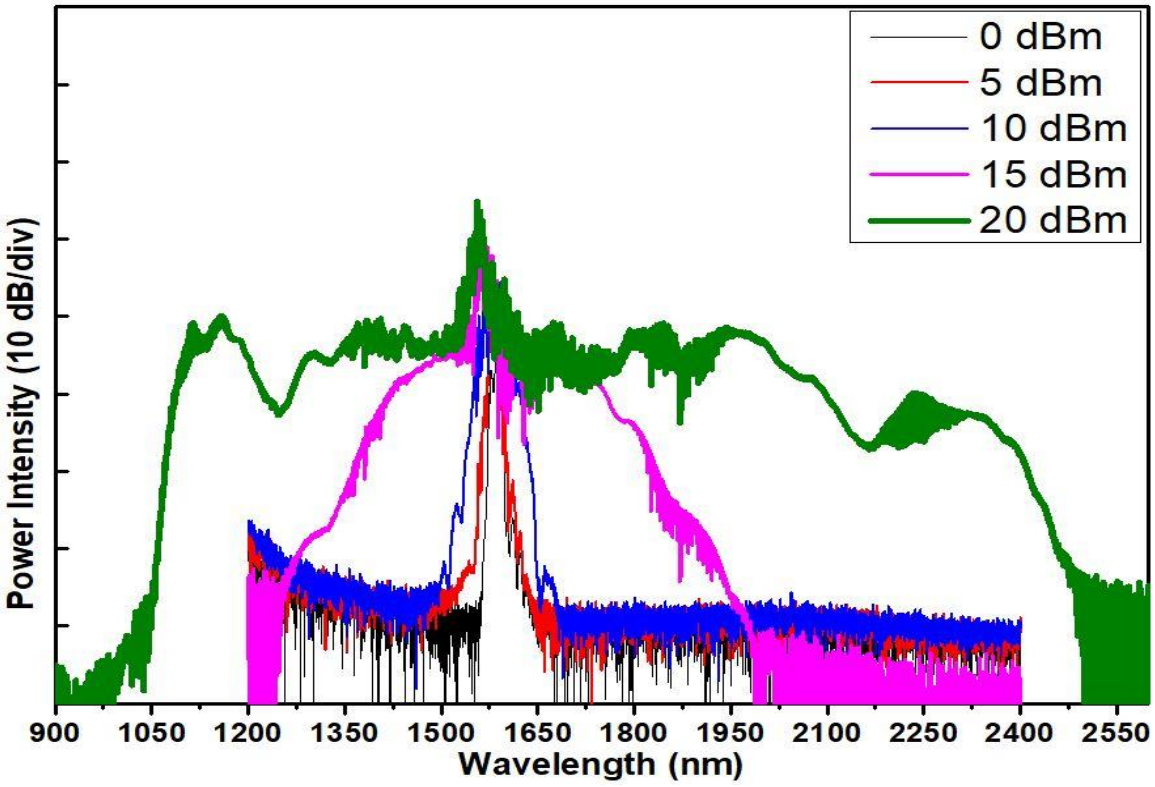

Figure 4. 16 SC spectral output from ~35-cm-long fibre (L1 =1.5 cm and L2 =6 cm).

Figures 4.14 and 4.15 show the output SC spectrum variation from the tapered fibre length of 4 cm and 6 cm where the overall length of the fibre used for the SC generation experiment if ~35-cm. Here also the similar observation i.e. the SC spectrum broadened with respect to the input pulse power. The SC spectral bandwidth variation of tapered HNLF is listed along the 30-cm, 50-cm, 100-cm and 1-km-long HNLF for comparison purpose in the table.2.

Table.2 shows the 20-dB flat SC spectral bandwidth variation from 30-cm, 50-cm, 100-cm, 4-cm tapered and 6-cm tapered DS-HNLF with respect to the variation in input pulse power. The notable achievements here are that the SC bandwidth achieved at an input pulse power of 15 dBm from 4-cm tapered fibre is many times greater than the bandwidth achieved from the 30-cm-long fibre at the same input pulse power, which is highlighted in the table.

Table 2 List of SC Spectral BW obtained from different lengths of HNLF

Input pulse power (dBm)	**20-dB SC spectral Bandwidth (nm) obtained from DS-HNLF**				
	30-cm	50-cm	100-cm	L_2 =4-cm	L_2 =6-cm
0	15	15	15	15	15
5	30	60	70	20	20
10	80	150	440	150	120
15	170	700	810	630	470
20	1000	1350	1360	740	1400

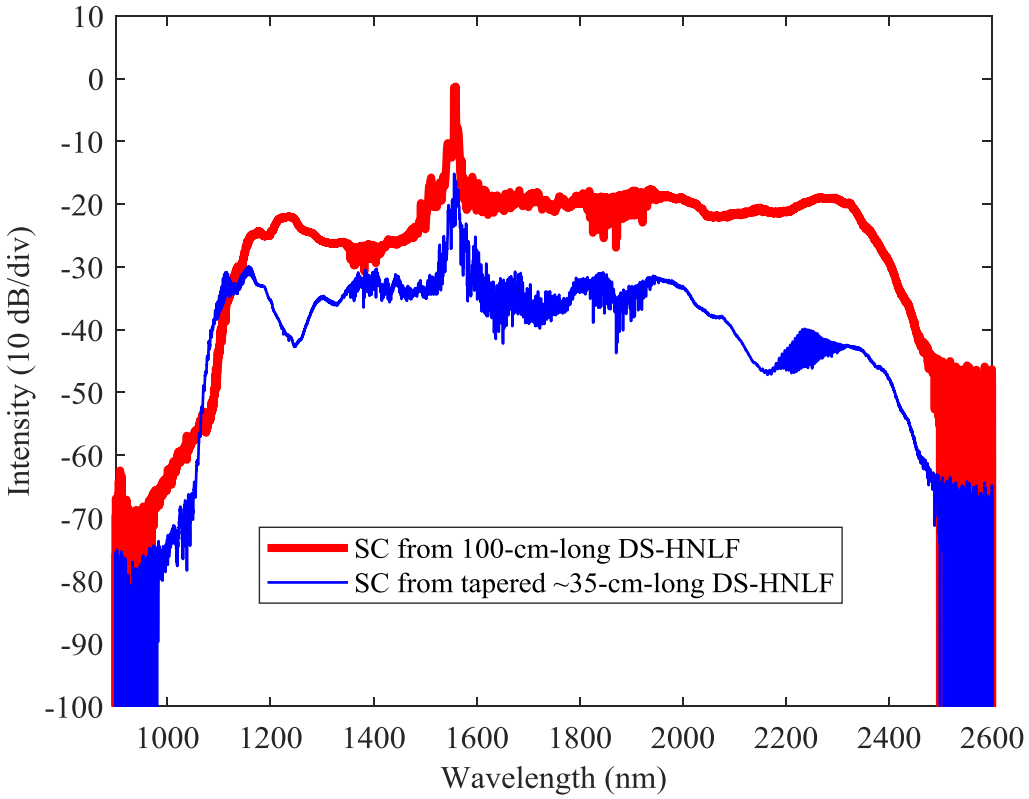

Figure 4. 17 SC spectrum from ~35-cm (6-cm-tapered) and 100-cm at the input pulse power of 20 dBm

The 20-dB flat SC spectrum bandwidth achieved from 6-cm tapered segment fibre is more than the bandwidth achieved from the 100-cm-long fibre and the shorter wavelength side of the SC spectrum is shifted further in case of 6-cm tapered fibre. The 20-dB flat SC spectral bandwidth at an input pulse power of 20 dBm is observed as 1360 nm from 100-cm-long DS-HNLF, whereas,40 nm broader i.e. 1400 nm SC spectral bandwidth spanning from 1060 nm to 2460 nm is observed from the 6-cm tapered fibre at the same input as shown in the Figure 4.17, which shows the SC spectrum obtained from 6-cm tapered ~35-cm-long and 100-cm-long DS-HNLF at an input pulse power of 20 dBm.

4.6 Summary

This chapter demonstrates the broadband SC spectrum generation from a 60 m long highly nonlinear PCF by pumping a CNT-SA based passively mode-locked EDFL having 620 fs pulse width. The SC spectral dynamics variation is observed with respect to the input pulse power variation by varying input pulse power from 0 dBm to 20 dBm. A 20 dB SC bandwidth of 1080 nm spanning from 1090 nm – 2170 nm is achieved from a 60-m-long PCF at an input pulse power of 20 dBm, where the SC spectrum exhibits some power fluctuations of less than 8 dB. The DS-HNLF fibre length variation study also demonstrated and achieved a maximum bandwidth of 1360 nm spanning from 1100 nm to 2460 nm from a 100-cm-long fibre at an input pulse power of 20 dBm. The SC spectral variation from tapered fibre at two different tapering lengths is observed and extended the SC spectral bandwidth further by 40 nm at the available maximum input pulse power of 20 dBm. In the next chapter, the SC spectrum is further extended towards mid-IR region using soft-glass ZBLAN fibre, where the same CNT-SA-based passively mode-locked femtosecond EDFL is used to pump the ZBLAN fibre.

Chapter 5 Supercontinuum Generation in ZBLAN Fibre

In this chapter, the non-silica based soft-glass fibre such as ZBLAN fibre is used to generate broadband SC towards mid-IR region. The CNT-SA based passively mode-locked femtosecond EDFL is used as seed laser to the non-doped single-mode ZBLAN fibre. The spectral broadening phenomena inside the ZBLAN fibre with respect to the variation in the input pulse power is studied.

5.1 Introduction

In these few decades, intensive researches are carried out on the fibre-based SC sources which mainly focuses on the silica-based fibres [135]. However, the SC spectrum is limited to 2.5 µm due to intrinsic losses of silica substrate [136]. Therefore, to generate mid-IR SC beyond 2.5 µm, fibres with low transmission loss in the mid-IR region such as soft glass fibres composed of tellurite, fluoride, and chalcogenide glasses are required and alternatively, there exists an approach called hollow-core fibre to reduce the silica material absorption significantly [135, 137-139].

Silica-based optical fibres are good candidates for SC generation in the visible and near-infrared regions, whereas these fibres experiences huge loss in the mid-IR region due to intrinsic losses [136]. This made it difficult to realize SC sources that covers wavelength from visible region to mid-IR region using silica-based fibre. To overcome this problem and to realize SC generation towards mid-IR region many researchers have opted for fluoride fibres due to drawing technology feasibility and its transmission window. Fluoride-glass-based fibre drawing is considered to be the 2nd most mature optical drawing technology after silica-based

drawing technology [140]. Heavy-metal fluoride has unique properties such as wide transmission window, relatively low loss in the 2 to 3 µm region when compared to silica glass, a low refractive index, low optical dispersion and the possibility of machining and polishing. All these attractive properties made fluoride glasses-based optical fibres are excellent candidates to choose as nonlinear media to generate SC in both the visible and in the mid-IR region. Figure 5.1 shows the transmission spectrum of different glasses-based fibres where the impurity incurred losses are not mentioned. Among all the soft-glasses, heavy-metal fluoride glass is preferred due to its technology maturity and attractive properties as mentioned above. Among all heavy-metal fluoride fibres, fluorozicronate glass, commonly known as ZBLAN has been adopted due to its high glass stability, technology maturity and transparency in mid-IR region [141].

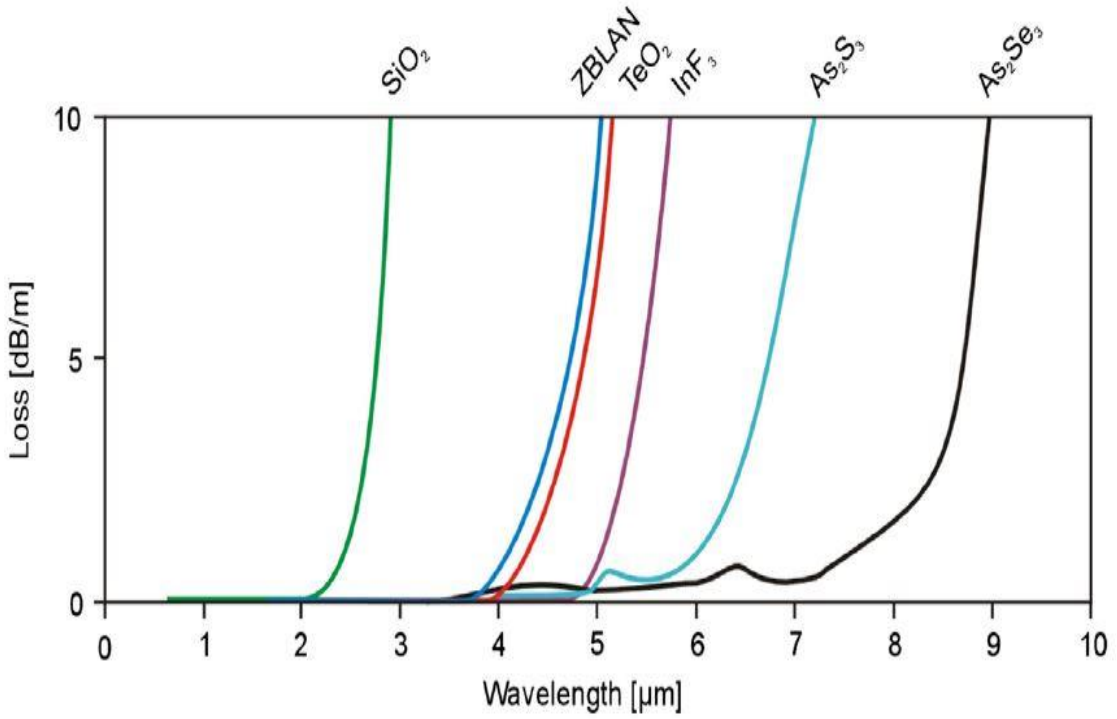

Figure 5. 1 Transmission curves for different optical fibres used for SC mid-IR SC generation [142].

ZBLAN (ZrF_4-BaF_2-LaF_3-AlF_3-NaF) is a mixture of ZrF_4 (53 mol%), BaF2 (20 mol%), LaF3 (4 mol%), AlF3 (3 mol%), and NaF (20mol%) and it is characterised by the maximum phonon energy of ~600 cm^{-1} [142-143]. The fluorozicronate glass, in its bulk form, has a transmission window from ~0.3 to 8 µm, whereas ZBLAN fibres are transparent in the region of 0.25 to 4.7 µm [144]. The typical ZDW of the ZBLAN fibre lies between 1.65 - 1.9 µm [146].

The most popular and commercially available mid-IR sources are amplifiers (OPA), quantum cascaded lasers (QCL) and optical parametric oscillators [147-149]. These systems have achieved very good performance in terms of important applications but these are very complex in nature and stability is very poor. These problems can be overcome by all-fibre-based SC generation towards mid-IR region using the soft-glass fibres as the nonlinear media. Till date mid-IR SC generation using ZBLAN fibre that involves multi-stage SC generation and multi-stage amplification is adopted widely [142]. The system, in general, is complex and suffers poor stability. Here, the complexity is reduced and the stability is improved and, compactness of the system by using single-stage SC generation approach. For the first time to my best knowledge, a CNT based passively mode-locked femtosecond EDFL based SC generation in ZBLAN fibre is demonstrated. The CNT based mode-locking has achieved a pulse width of 620 fs with a repetition rate of 18 MHz at a center wavelength of 1565 nm. A single stage amplification is employed on mode-locked pulses and the trend of spectral broadening inside the ZBLAN fibre is studied experimentally at different input pulse power levels. The study of SC generation inside the ZBLAN fibre at high input pulse powers is limited by the output power limitation of erbium-doped fibre amplifier (EDFA) and limitation of optical spectrum analyzer (OSA) wavelength measurement. Successfully demonstrated an SC spectrum generation from a ZBLAN fibre covering a bandwidth of 2100 nm extending from

1100 nm to 3200 nm at an input pulse power of 25 dBm. Achieved a smooth spectrum with spectral flatness of less than 8 dB. A piecewise linear relationship of SC spectrum bandwidth with the input pulse power is observed.

5.2 Experimental Setup

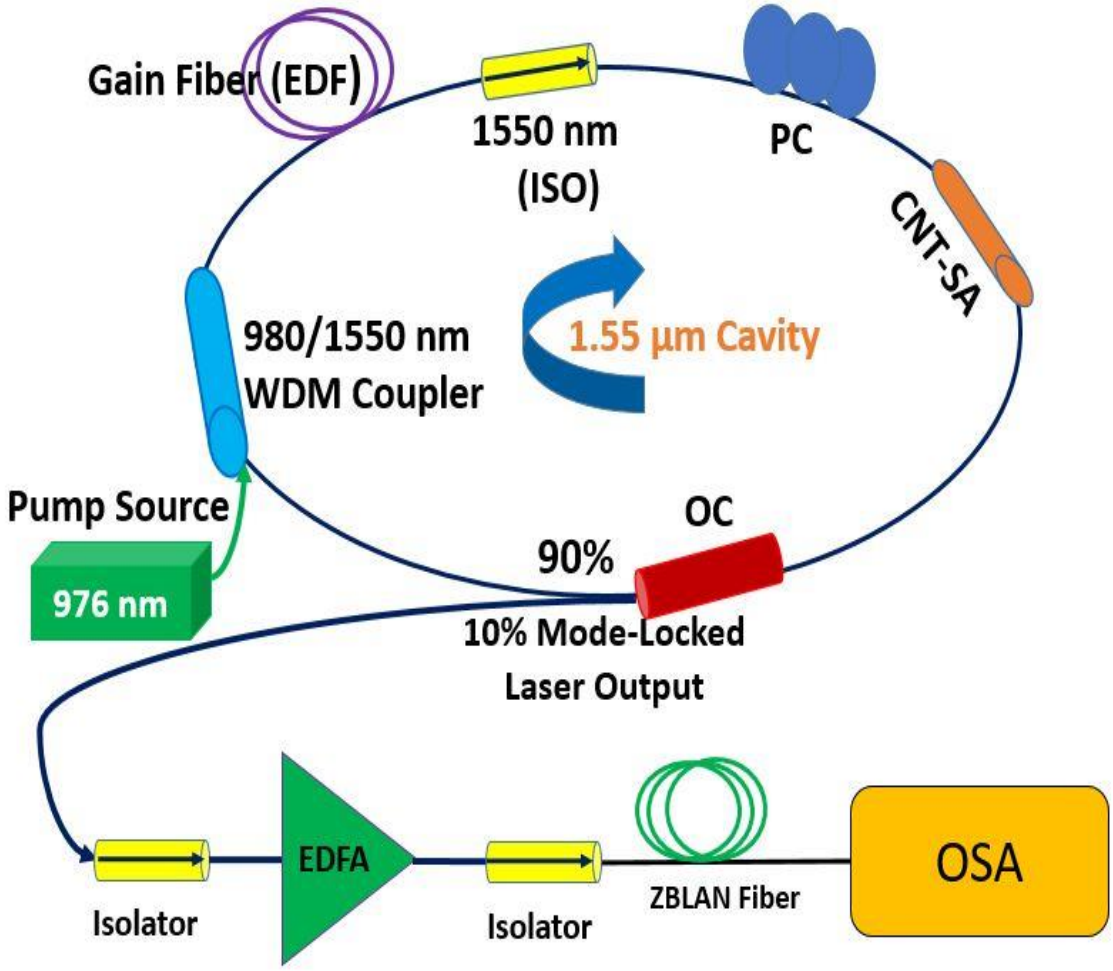

Figure 5. 2 Experimental setup of SC generation from a ZBLAN fibre using passively mode-locked fibre laser.

Figure 5.2 shows the experimental setup of SC generation from a CNT-SA based passively mode-locked EDFL and single-mode non-doped ZBLAN fibre. In order to activate the nonlinear

properties of ZBLAN fibre efficiently for broadband SC generation and to study the effect of input pulse power variation on the SC spectral dynamics, an EDFA is used to boost the input pulse power before launching into ZBLAN. to protect the mode-locked laser pulse stability and to protect the EDFA from back reflection from ZBLAN fibre, on both sides of the EDFA high power isolators are used. The output spectrum from ZBLAN fibre is observed with OSA. Here three OSAs (450 - 1750 nm, 1200 - 2400 nm and 1900 – 3200 nm) were used to cover the whole range of SC spectrum generated from ZBLAN. A 25-m-long commercially available single-mode non-doped ZBLAN fibre is used to observe the SC spectral variation with respect to the input pulse power variation. The ZBLAN fibre has a core/cladding diameter of 6/125 µm, NA of 0.26 and ZDW is at ~ 1.6 µm.

5.3 Results and Discussion

In order to observe the spectral broadening phenomena efficiently from ZBLAN fibre, the output of CNT-SA based passively mode-locked laser is amplified using a commercially available EDFA. As shown in the Figure 5.2, isolators are connected at both the input and output of the EDFA in order to protect the EDFA from back reflections and to maintain the stability of mode-locked laser ring-cavity. The output of EDFA is connected to the 25-m-long ZBLAN fibre through an isolator and the SC spectrum from ZBLAN fibre is observed by varying input pulse power from 10 dBm to 25 dBm. The multi-stage amplification and sub-band SC generation is avoided as reported in previous studies to generate broad SC generation towards mid-IR region [146]. In this approach, only a single stage of amplification is applied on the mode-locked laser pulse and generated SC directly by launching amplified pulse into ZBLAN fibre without any intermediate stages of SC generation like, first launching into a small

piece of HNLF or SMF or EDF and thereby launching into ZBLAN fibre, which makes my setup more environmentally stable, economical, and compact.

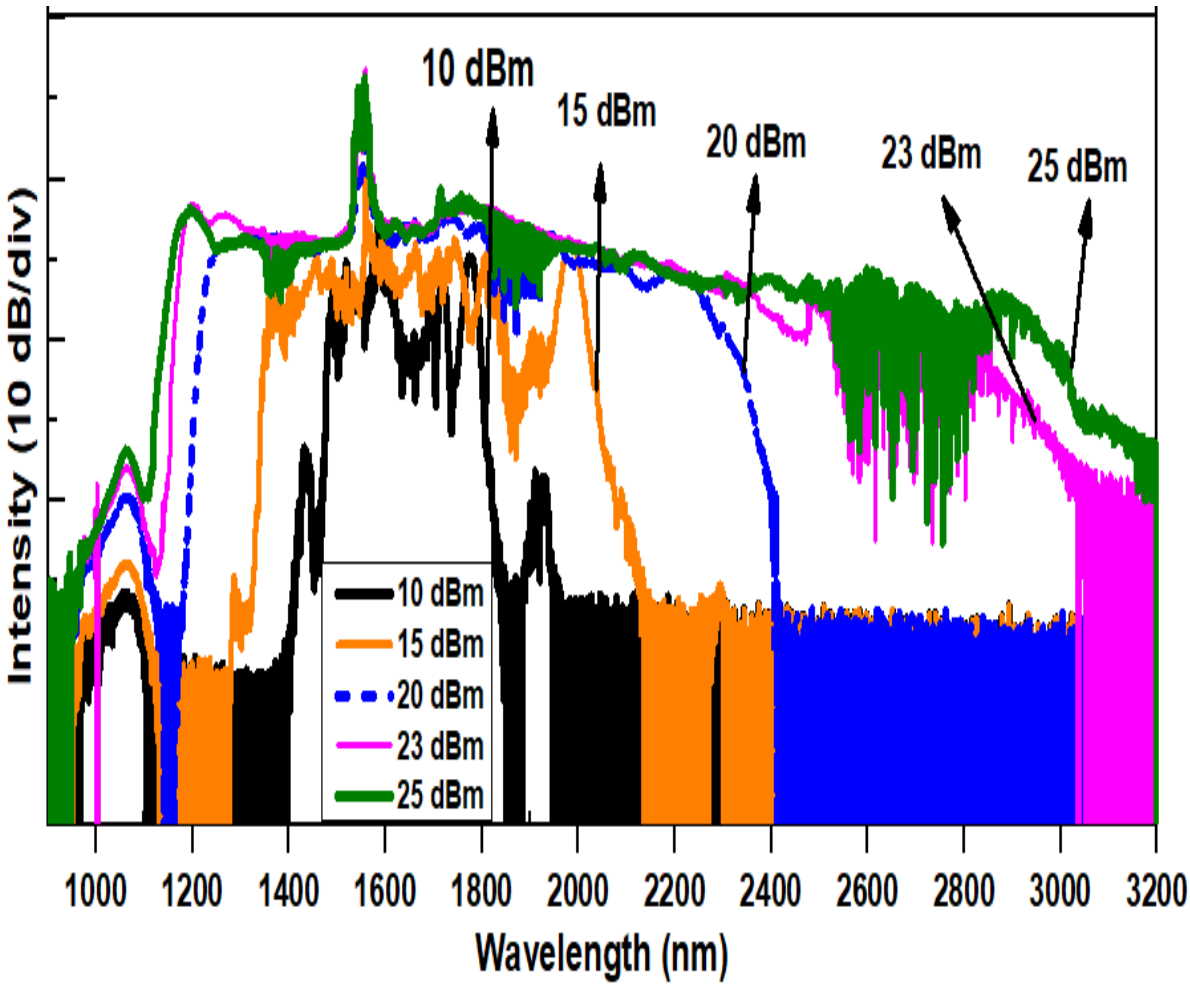

Figure 5. 3 SC spectrum output variation from 25-m-long ZBLAN fibre for different input pulse powers.

Figure.5.3 shows the variation of output SC spectrum from ZBLAN fibre for different input powers. To observe the spectral broadening phenomena and the bandwidth variation of SC generation from ZBLAN fibre with respect to input power variation, the pulse power is varied from 10 dBm to 25 dBm. Three different OSAs (450 - 1750 nm OSA1, 1200 - 2400 nm OSA2 & 1200 - 3400 nm OSA3) have been used to analyze the SC spectrum generated from ZBLAN

fibre. All the three OSAs are maintained at the same input conditions, and the intensity mismatch is minimized using subtraction method at the intersecting wavelength of the OSAs. It is observed that the spectral broadening followed by SC bandwidth increases with the increase in the input pulse power. Also, Over the variation of input pulse power from 10 dBm to 25 dBm, the observed average power loss in the 25-m-long ZBLAN fibre is ~7 dB. The flat and maximum SC bandwidth of 2100 nm extending from 1100 nm to 3200 nm is observed at an input power level of 25 dBm. For all the input powers the spectrum was bi-directionally broadened both to the near- and mid-IR region. The dip that was observed in the spectrum at around 2700 nm is corresponds to OH^{-1} ions absorption in the ZBLAN fibre and unpurged detection of long wavelength OSA. The further study of SC spectrum from ZBLAN fibre at higher powers is limited by the EDFA output power and OSA wavelength range.

The femtosecond pulses experience normal dispersion in the ZBLAN fibre as the seed pulse wavelength (1565 nm) is below the ZDW (1600 nm) of ZBLAN. Therefore, initially the spectral broadening inside the ZBLAN is dominated by the SPM and soliton-frequency shift, and as the pulse propagates further inside the fibre, the SC spectrum broadening towards longer wavelength side is dominated by the soliton fission assisted by SRS as discussed in the literature section. At all the input pulse powers there appears a residual peak in the output SC spectrum at around 1550 nm which is appearing from the amplification of seed pulse. When comes to the different peaks in the output SC spectrum corresponding to the input pulse powers at 10 & 15 dBm, is attributed by the weak SPM and soliton-frequency shift effect which disappears at high input pulse powers as the SPM and soliton-frequency shift phenomena becomes stronger. Strong SPM processes enhance the transfer of energy away

from pump peak and thereby decrease residual pump light in the spectrum. Thus, a flatter spectrum is generated by pumping femtosecond pulses in normal dispersion region.

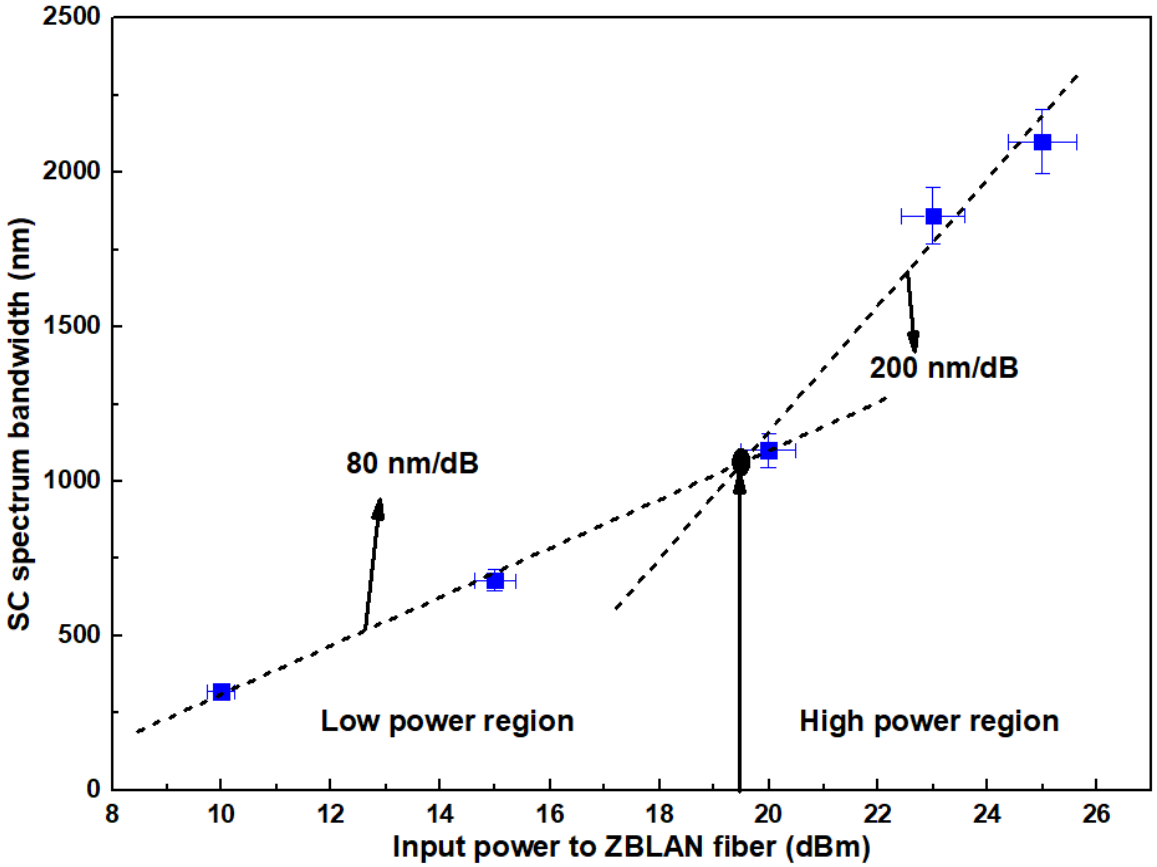

Figure 5. 4 SC spectrum bandwidth variation from 25-m-long ZBLAN fibre with respect to input pulse power variation.

Figure 5.4 shows the variation of SC spectrum bandwidth from ZBLAN fibre output with respect to the input pulse power. From the graph, a piecewise linear relationship of SC spectrum bandwidth increment with input power is observed and to make this relationship more reliable a 5 % error bar is added to the data points. This knowledge of bandwidth vs input power relationship helps us to estimate the amount of power that needs to be pumped to a ZBLAN fibre to generate a particular bandwidth of SC spectrum. Based on the piecewise linear relationship, it is observed that the ZBLAN generates a SC spectrum bandwidth at a rate

of ~ 80 nm/dB when the input power is < 19.5 dBm and ~ 200 nm/dB in high power region (input power > 19.5 dBm). In this case, the study of SC generation at further higher powers is limited by the EDFA maximum power limitation and the OSA wavelength range limitation.

5.4 Summary

In this chapter, for the first time to the best of my knowledge a flat and broad mid-IR SC generation with spectrum bandwidth of 2100 nm spanning from 1100 nm to 3200 nm in an un-doped single-mode ZBLAN fibre pumped by a 620 femtosecond EDFL pulses at an input power of 25 dBm is demonstrated. CNT-SA-based passive mode-locking technique has been used to achieve a femtosecond seed pulse to pump the un-doped single-mode ZBLAN fibre. The spectral broadening phenomena within the ZBLAN fibre is investigated for different input powers and also a piecewise linear relationship of SC spectrum bandwidth with input pulse power variation is observed. With this study, the SC spectral bandwidth is improved and extended further into mid-IR region.

Chapter 6 Conclusion and Future Work

6.1 Conclusions

In summary, this project focused on the study of spectral variation from specialty fibres such as from highly nonlinear PCF, DS-HNLF and ZBLAN fibre at different input pulse power using a CNT-SA based passively mode-locked femtosecond EDFL. The study mainly involves three parts including the generation of femtosecond seed pulse through CNT-SA based passive mode-locking technique, the study of spectral broadening phenomena inside silica-based nonlinear fibres such as PCF and HNLF and, the generation of SC towards mid-IR region using ZBLAN fibre.

SC generation involves two parts: the seed laser and the nonlinear medium. CNT-SA based passively mode-locked femtosecond EDFL is used as seed laser throughout the study and the PCF, DS-HNLF and ZBLAN are used as nonlinear medium. The major contribution and achievements of these research is summarized as follows:

- In order to study and achieve broad SC spectrum from specialty fibres, stable and high power seed laser is important. Therefore, to achieve stable and high power seed laser passive-mode locking technique is chosen. In the passive mode-locking technique, a CNT-SA is used as passive element in the EDFL ring cavity and achieved the stable mode-locking. The CNT-SA based passively mode-locked EDFL produced a pulses with pulse energy of 11.76 pJ. At stable mode-locked operation of passively mode-locked EDFL generates laser pulses at a repetition rate of 18 MHz and pulse width of 620 fs. The mode-locked laser pulse has a 3-dB bandwidth of ~5 nm at a center wavelength

of ~1565 nm. The average output power observed from the mode-locked laser cavity is 0.21 mW and the corresponding pulse peak power is 38 W. This CNT-SA based passively mode-locked femtosecond EDFL is used throughout this study and maintained all pulse parameters same in each case study of SC generation from different fibres. The femtosecond laser pulse power is further boosted using EDFA in order to study the spectral variation inside each fibre.

- The SC spectral variation inside the silica-based 60-m-long highly nonlinear PCF is observed by varying the input pulse power from 0 dBm and 20 dBm. Achieved a 20-dB flat SC spectral bandwidth of 1080 nm spanning from 1090 nm to 2170 nm at an input pulse power of 20 dBm. This is the first time demonstration of such as wideband SC generation from a CNT-SA based passively mode-locked femtosecond EDFL.

- The SC spectral variation studied with respect to the variation in the input pulse power is continued using the 1-km-long DS-HNLF. Similar kind of spectral broadening phenomena is observed from the DS-HNLF as in case of PCF. The long wavelength side of the SC spectrum is extended up to 2475 nm, due to the appearance of dip in the SC spectrum in the region of 2.1 µm to 2.3 µm, the 20-dB flat SC spectral bandwidth (975 nm) achieved from the 1-km-long DS-HNLF is relatively lower when compared to the SC bandwidth achieved from the 60-m-long PCF. In order to minimize loss of spectral components in the region of 2.1 µm to 2.3 µm, the length of the DS-HNLF is varied and studied the variations in SC spectral dynamics. Here DS-HNLF over PCF is chosen for length variation study because of its splicing compatibility with the standard SMF. The SC spectral variation is studied in the 30-cm, 50-cm and 100-cm-long DS-HNLF. The

length of the fibre has been chosen based on the theoretical calculation of nonlinearity length.

- The spectral variation at each different length is studied by varying the input pulse power from 0 dBm to 20 dBm. For the first time achieved a SC spectral bandwidth of 1360 nm extending from 1100 nm to 2460 nm from a 100-cm-long DS-HNLF using a CNT-SA based passively mode-locked femtosecond EDFL as the pump.

- The effect of tapering on the SC spectral variations also studied at the tapering ratio of 2 with at two different tapered lengths. With this study, achieved a SC bandwidth of 1400 nm which is 40 nm broader than the maximum bandwidth that have achieved from the 100-cm-long DS-HNLF. This is the first time demonstration of such wide SC spectrum generation from shortest length of DS-HNLF (~35-cm-long) using CNT-SA-based passively mode-locked femtosecond EDFL as pump. The 1400 nm wide SC spectrum is extended from 1060 nm to 2460 nm and the ~35-cm-long DS-HNLF has a tapered segment of 6 cm at a tapering ratio of 2.

- With the study of length variation and tapering effect on SC spectrum at different powers allow us to find the possible shortest length of the DS-HNLF to generate maximum SC bandwidth at the possible maximum power of 20 dBm.

- Further investigated the SC generation in non-silica based fibres in order to generate the broadband SC spectrum in the mid-IR region. The SC spectral variation from the output of 25-m-long ZBLAN fibre is studied at different input pulse powers varying from 0 dBm to 25 dBm. With a simple setup of single-stage amplification and direct launch of amplified CNT-SA based passively mode-locked femtosecond EDFL pulses

into 25-m-long single-mode ZBLAN fibre, and achieved a 2100 nm wide mid-IR SC spectrum extending from 1100 nm to 3200 nm.

6.2 Future Works

The broadband SC generation in speciality fibres study shows that the very broadband SC spectrum is possible in a short length of HNLF from the observations of SC spectral variation with respect to the variation in fibre length DS-HNLF and achieved broader SC spectrum towards mid-IR region from a soft-glass ZBLAN fibre at minimal input power by pumping CNT-SA based passively mode-locked femtosecond EDFL at 1.5 μm region.

- The above studies recommend a thorough investigation of fibre tapering technique to achieve flat and wider SC generation at relatively low powers from very short length of fibres.
- Future study also includes the tapering effect on SC spectral variation. Such as applying different tapering ratios on the same fibre by choosing different lengths. So far tapering is applied at one place or two places of the whole fibre and studied the SC spectral variation. The multiple tapering ratios at different lengths on the fibre has the capability of generating flattest SC spectrum due to the variation of nonlinearity along the fibre and laser pulse experiencing the multiple ZDWs when it propagated along different tapering ratio segments along the fibre
- When comes to soft-glass fibres, hybrid fibre structures, and multi-stage amplification is used to achieve flatter and broad SC spectrum towards mid-IR region. The cascade structure of PCF, HNLF, and ZBLAN at different pump wavelengths to realize the SC

spectrum extending from visible region to mid-IR using single stage of amplification which make the system compact and cost realiable is needs to be investigated.

- In general, multistage amplification is using to achieve high output power SC spectrum, instead of multi-stage amplification, need to explore the possibility of achieving high output power SC spectrum using the cascaded structure of passive fibre and active fibre, where the nonlinear passive fibres provide the spectral broadening of the input pulse whereas, active fibres give the distributed amplification along the whole fibre length which leads the generation of high output power SC spectrum.
- Future prospects of SC technology may also include the fabrication of different shapes combination of active and passive fibres with soft glass material in order to achieve the high output power along with broad SC spectrum.

Author's Publications

Journal Publications

[1]. **Sivasankara Rao Yemineni,** Wenn Jing Lai, Arokiaswami Alphones, Ping (Perry) Shum, "Mid-IR supercontinuum generation in a single-mode ZBLAN fiber by erbium-doped fiber laser," *Opt. Eng.* **57**(11), 111804 (2018), doi: 10.1117/1.OE.57.11.111804.

[2]. **Sivasankara Rao Yemineni,** W. J. Lai, A. Alphones and P. Shum a "Broadband supercontinuum generation in PCF, HNLF and ZBLAN fibre with a carbon-nanotube-based passively mode-locked erbium-doped fibre laser," [**Under Review:** Optics Communication]

[3]. **Sivasankara Rao Yemineni,** W. J. Lai, A. Alphones and P. Shum, "Broadband supercontinuum generation in sub-meter length of HNLF with a carbon-nanotube-based passively mode-locked femtosecond fibre laser," [**Under review:** Optics Communication]

Conference Publications

[1]. **Sivasankara Rao Yemineni,** W. J. Lai, A. Alphones, and P. Shum, "Mid-IR supercontinuum generation in a single-mode ZBLAN fibre pumped by a carbon-nanotube-based passively mode-locked erbium-doped femtosecond fibre laser ", *Proc. SPIE 10516, Nonlinear Frequency Generation and Conversion:* Materials and Devices XVII, 105160N (15 February 2018);

[2]. **Sivasankara Rao Yemineni,** W. J. Lai, A. Alphones, and P. Shum, "Flat broadband supercontinuum generation in a short length of highly nonlinear fibre pumped by a femtosecond carbon-nanotube-based passively mode-locked erbium-doped fibre laser", *Proc. SPIE 10516, Nonlinear Frequency Generation and Conversion*: Materials and Devices XVII, 105160A (15 February 2018);

[3]. **Sivasankara Rao Yemineni,** W. J. Lai, A. Arokiaswami, and P. Shum, "Broadband supercontinuum generation in photonic crystal fibre pumped by femtosecond carbon-nanotube-based passively mode-locked erbium-doped fibre laser," *2017 Progress in*

Electromagnetics Research Symposium - Fall (PIERS - FALL), Singapore, 2017, pp. 2993-2995.

[4]. **Sivasankara Rao Yemineni,** A. Alphones, and P. Shum, "Broadband supercontinuum generation in highly nonlinear fibre with carbon-nanotube-based passively mode-locked erbium-doped fibre laser," *2017 IEEE Photonics Conference (IPC),* Orlando, FL, 2017, pp.263-264.

[5]. **Sivasankara Rao Yemineni,** A. Alphones and P. Shum, "All-fibre femtosecond laser pulse generation at 1.55 μm and 2 μm using a common carbon-nanotube-based saturable absorber," *2017 Conference on Lasers and Electro-Optics Pacific Rim (CLEO-PR),* Singapore, 2017, pp. 1-2.

[6]. **Sivasankara Rao Yemineni,** H. H. Liu, and K. K. Chow, "Carbon-nanotube-based passively mode-locked erbium-doped fibre laser for broadband supercontinuum generation," *2015 10th International Conference on Information, Communications and Signal Processing (ICICS)*, Singapore,2015, pp.1-4.

[7]. **Sivasankara Rao Yemineni**, W. J. Lai, A. Alphones and P. Shum, “Tapered fibres for flat and broad supercontinuum generation”, *2017 IEEE Photonics Conference (IPC),* Orlando, Florida, USA-2017 [Non-Archived poster presentation].

[8]. **Sivasankara Rao Yemineni,** W. J. Lai, A. Alphones and P. Shum, “Broadband Supercontinuum Generation in PCF, HNLF and ZBLAN Fibre with Carbon-Nanotube-Based Passively Mode-Locked Femtosecond Erbium-Doped Fibre Laser (EDFL”, Photonics@SG 2018 Conference & Exhibition, Singapore-2018 [poster presentation].

[9]. **Sivasankara Rao Yemineni,** W. J. Lai, A. Alphones and P. Shum, “Broadband Supercontinuum Generation in Sub-Meter Length of HNLF using Carbon-Nanotube-based Passively Mode-Locked Erbium-Doped Fibre Laser (EDFL)”, Photonics@SG 2018 Conference & Exhibition, Singapore-2018 [poster presentation].

References

1. R. R. Alfano and S. L. Shapiro, “Emission in the region 4000 to 7000 Å via four-photon coupling in glass,” Phys. *Rev. Lett.* **24** (11), pp. 584-587, 1970.
2. R. R. Alfano and S. L. Shapiro, “Observation of self-phase modulation and small-scale filaments in crystals and glasses”, Phys. *Rev. Lett.* **24** (11), pp. 592-594, 1970.
3. Jacek Swiderski, Maria Michalska, and Gwenael Maze, "Mid-IR supercontinuum generation in a ZBLAN fibre pumped by a gain-switched mode-locked Tm-doped fibre laser and amplifier system," *Opt. Express.* **21 (7)**, pp. 7851-7857, 2013.
4. Kivanç Özgören, Bülent Öktem, Sinem Yilmaz, F. Ömer Ilday, and Koray Eken, "83 W, 3.1 MHz, square-shaped, 1 ns-pulsed all-fibre-integrated laser for micromachining," *Opt. Express.* **19** (18), pp. 17647-17652, 2011.
5. Sergey V. Smirnov, Sergey M. Kobtsev, and Sergey V. Kukarin, "Efficiency of non-linear frequency conversion of double-scale pico-femtosecond pulses of passively mode-locked fibre laser," *Opt. Express.* **22** (1), pp. 1058-1064, 2014.
6. Y. Chen, E. Räikkönen, S. Kaasalainen, J. Suomalainen, T. Hakala, J. Hyyppä, and R. Chen, “Two-channel hyperspectral LiDAR with a supercontinuum laser source,” *Sensors (Basel).* **10**(7), pp. 7057–7066, 2010.
7. Jacek Swiderski, “High-power mid-infrared supercontinuum sources: Current status and future perspectives," *Prog. Quantum Electron*. **38** (5), pp. 189-235, 2014.
8. John M. Dudley, Goëry Genty, and Stéphane Coen, “Supercontinuum generation in photonic crystal fibre,” *Rev. Mod. Phys*. **78** (4), pp-1135-1384, 2006.
9. Goëry Genty, Stéphane Coen, and John M. Dudley, "Fibre supercontinuum sources (Invited)," *J. Opt. Soc. Am. B.* 24 (8), pp. 1771-1785, 2007.
10. A. V. Husakou and J. Herrmann, “Supercontinuum Generation of Higher-Order Solitons by Fission in Photonic Crystal Fibres,” *Phys. Rev. Lett.* **87** (20), pp. 203901, 2001.
11. J. P. Gordon, "Theory of the soliton self-frequency shift," *Opt. Lett.* **11**(10), pp. 662-664, 1986.
12. D. Y. Tang and L. M. Zhao, "Generation of 47-fs pulses directly from an erbium-doped fibre laser," *Opt. Lett.* **32**(1), pp. 41-43, 2007.

13. L. Kuznetsova, A. Chong, and F. W. Wise, "Interplay of nonlinearity and gain shaping in femtosecond fibre amplifiers," *Opt. Lett.* **31**(17), pp. 2640-2642, 2006.
14. Sivasankara Rao Yemineni, H. H. Liu, and K. K. Chow, "Carbon-Nanotube-based Passively Mode-Locked Erbium-Doped Fibre Laser for Broadband Supercontinuum Generation", *in Proc. International Conference on Information, Communications, and Signal Processing,* Singapore, 2015.
15. V. J. Matsas, T. P. Newson, D. J. Richardson, and D. N. Payne, "Self-starting passively mode-locked fibre ring soliton laser exploiting nonlinear polarization rotation," *Electron. Lett.* **28**(15), pp. 1391–1393, 1992.
16. I. N. Iii, "All-fibre ring soliton laser mode locked with a nonlinear mirror," Opt. Lett. **16** (8), pp. 539–541 1991.
17. O. Okhotnikov, A. Grudinin, and M. Pessa, "Ultra-fast fibre laser systems based on SESAM technology: New moonzons and applications," *New J. Phys.* **6**(1), pp. 177, 2004.
18. S. Y. Set, H. Yaguchi, Y. Tanaka, and M. Jablonski, "Ultrafast fibre pulsed lasers incorporating carbon nanotubes," *IEEE J. Sel. Top. Quantum Electron*. **10**(1), pp. 137–146, 2004.
19. Venkatesh Mamidala, R. I. Woodward, Y. Yang, H. H. Liu, and K. K. Chow, "Graphene-based passively mode-locked bidirectional fibre ring laser", *Opt. Express*. **22**(4), pp. 4539-4546, 2014.
20. Q. L. Bao, H. Zhang, Y. Wang, Z. H. Ni, Y. L. Yan, Z. X. Shen, K. P. Loh, and D. Y. Tang, "Atomic-layer graphene as a saturable absorber for ultrafast pulsed lasers," *Adv. Funct. Mater.* **19**(19), pp. 3077–3083, 2009.
21. Z. Sun, T. Hasan, F. Torrisi, D. Popa, G. Privitera, F. Wang, F. Bonaccorso, D. M. Basko, and A. C. Ferrari, "Graphene mode-locked ultrafast laser," *ACS Nano.* **4**(2), pp. 803–810, 2010.
22. A. Martinez and S. Yamashita, "Carbon nanotube-based photonic devices: Applications in nonlinear optics," in Carbon Nanotubes Applications on Electron Devices, J. M. Marulanda, ed. Pp. 367–386, Intech, 2011.

23. T. Hasan, Z. Sun, F. Wang, F. Bonaccorso, P. H. Tan, A. G. Rozhin, and A. C. Ferrari, “Nanotube-polymer composites for ultrafast photonics,” *Adv. Mater.* **21**(38-39), pp.3874–3899, (2009).
24. X. Liu, D. Han, Z. Sun, C. Zeng, H. Lu, D. Mao, Y. Cui, and F. Wang, “Versatile multi-wavelength ultrafast fibre laser mode-locked by carbon nanotubes,” *Sci. Rep*. **3** (2718), 2013.
25. T. H. Maiman, "Stimulated Optical Radiation in Ruby," *Nature,* vol. 187, pp.493-494, 1960.
26. C. J. Koester and E. Snitzer, "Amplification in a Fibre Laser," Applied Optics, vol. 3, no. 10, pp. 1182-1186, 1964.
27. W. E. Lamb, "Theory of an Optical Maser," *Physical Review,* vol. 134, pp. A1429-A1450, 1964.
28. J. M. DiDomenico, "Small-Signal Analysis of Internal (Coupling-Type) Modulation of Lasers," *Journal of Applied Physics,* vol. 35, pp. 2870-2876,1964.
29. L. E. Hargrove, R. L. Fork, and M. A. Pollack, "Locking of He-Ne Laser Modes Induced by Synchronous Intracavity Modulation," *Applied Physics Letters,* vol. 5, pp. 4-5, 1964.
30. P. W. Smith, M. A. Duguay, and E. P. Ippen, "Mode-locking of lasers,"*Progress in Quantum Electronics,* vol. 3, pp. 107-229, 1974.
31. H. Haus and Y. Silberberg, "Laser mode locking with addition of nonlinear index," *IEEE Journal of Quantum Electronics,* vol. 22, pp. 325-331, 1986.
32. N. G. Usechak, G. P. Agrawal, and J. D. Zuegel, "FM mode-locked fibre lasers operating in the autosoliton regime," *IEEE Journal of QuantumElectronics,* vol. 41, pp. 753-761, 2005.
33. H. W. Mocker and R. J. Collins, "Mode Competition and Self-locking Effects in a Q-switched Ruby Laser," *Applied Physics Letters*, vol. 7, pp. 270-273,1965.
34. C. Shank, E. Ippen, and A. Dienes, "Passive mode locking of the CW dye laser," IEEE Journal of Quantum Electronics, vol. 8, pp. 525-525, 1972.
35. L. F. Mollenauer and R. H. Stolen, "The soliton laser," *Optics Letters,* vol. 9, pp. 13-15, 1984.

36. H. Byun, D. Pudo, J. Chen, E. P. Ippen, and F. X. Kartner, "High-repetitionrate, 491 MHz, femtosecond fibre laser with low timing jitter," *Optics letters,* vol. 33, pp. 2221-2223,2008.

37. J. R. Buckley, F. W. Wise, F. Ilday, and T. Sosnowski, "Femtosecond fibre lasers with pulse energies above 10 nJ," *Optics Letters,* vol. 30, pp. 1888-1890,2005.

38. A. Chong, W. H. Renninger, and F. W. Wise, "Route to the minimum pulse duration in normal-dispersion fibre lasers," *Optics Letters,* vol. 33, pp. 2638-2640, 2008.

39. T. L. Paoli, "Saturable absorption effects in the self-pulsing (AlGa)As junction laser," *Applied Physics Letters,* vol. 34, pp. 652-655, 1979.

40. A. B. Grudinin and S. Gray, "Passive harmonic mode locking in soliton fibre lasers," *Journal of Optical Society of America B,* vol. 14, pp. 144-154, 1997.

41. U. Keller, K. J. Weingarten, F. X. Kartner, D. Kopf, B. Braun, I. D. Jung, R. Fluck, C. Honninger, N. Matuschek, and J. Aus der Au, "Semiconductor saturable absorber mirrors (SESAM's) for femtosecond to nanosecond pulse generation in solid-state lasers," IEEE Journal of Selected Topics in Quantum Electronics, vol. 2, pp. 435-453, 1996.

42. E. R. Thoen, E. M. Koontz, M. Joschko, P. Langlois, T. R. Schibli, F. X. Kartner, E. P. Ippen, and L. A. Kolodziejski, "Two-photon absorption in semiconductor saturable absorber mirrors," *Applied Physics Letters,* vol. 74,1999.

43. L. A. Gomes, L. Orsila, T. Jouhti, and O. G. Okhotnikov, "Picosecond SESAM-based ytterbium mode-locked fibre lasers," *IEEE Journal of Selected Topics in Quantum Electronics,* vol. 10, pp. 129-136, 2004.

44. B. Proctor, E. Westwig, and F. Wise, "Characterization of a Kerr-lens modelocked Ti: sapphire laser with positive group-velocity dispersion," *Optics Letters,* vol. 18, pp. 1654-1656, 1993.

45. V. P. Yanovsky, F. W. Wise, A. Cassanho, and H. P. Jenssen, "Kerr-lens mode-locked diode-pumped CnLiSGAF laser," *Optics Letters,* vol. 20, pp.1304-1306, 1995.

46. H. A. Haus, E. P. Ippen, and K. Tamura, "Additive-pulse mode locking in fibre lasers," *IEEE Journal of Quantum Electronics,* vol. 30, pp. 200-208, 1994.

47. M. Salhi, A. Haboucha, H. Leblond, and F. Sanchez, "Theoretical study of figure-eight all-fibre laser," *Physical Review A,* vol. 77, pp. 033828-9, 2008.
48. K. Andrey, L. Herve, and S. Francois, "Theoretical analysis of the operating regime of a passively-mode-locked fibre laser through nonlinear polarization rotation," *Physical Review A,* vol. 72, pp. 063811-7, 2005.
49. I. Fatih and F. W. Wise, "Multiple stable points of a soliton fibre laser with nonlinear polarization evolution," in *Nonlinear Guided Waves and Their Applications,* 2001, p. MC80.
50. V. J. Matsas, D. J. Richardson, T. P. Newson, and D. N. Payne, "Characterization of a self-starting, passively mode-locked fibre ring laser that exploits nonlinear polarization evolution," *Optics Letters,* vol. 18, pp. 358-360,1993.
51. Thesis on "Carbon-Nanotube-Based Devices for Passively Mode-Locked Fibre Laser Application" by Liu Huanhuan (2014) Nanyang Technological University.
52. Thesis on "Passively Mode-Locked Fibre Lasers" by Tian Xiaolong (2010) Nanyang Technological University.
53. S.P. Singh and N. Singh, "nonlinear effects in optical fibres: origin management and applications" *PIER 73*, 249-275, 2007.
54. R. R. Alfano, P. L. Baldeck, and P. P. Ho, "Cross-phase modulation and induced focusing due to optical nonlinearities in optical fibres and bulk materials" *J. Opt. Soc. Am. B*, Vol.6, No.4, April 1989.
55. Jayashree A. Dharmadhikari, Rucha A. Deshpande, Arpita Nath, Krithika Dota, Deepak Mathur, Aditya K. Dharmadhikari, "Effect of group velocity dispersion on supercontinuum generation and filamentation in transparent solids" *Appl. Phys. B*, 117, 471-479 (2014).
56. K. K. Chow, Y. Takushima, C. Lin, C. Shu and A. Bjarklev, "Flat super-continuum generation based on normal dispersion nonlinear photonic crystal fibre", *Electron. Lett*. vol. 42, pp.17, (2006).
57. G.P. Agrawal, *Nonlinear Fibre Optics*. 2000. 481.
58. http://optical-waveguides-modeling.net/tutorial-optical-fibre.jsp
59. http://nptel.ac.in/courses/117101054/downloads/lect23.pdf
60. http://nptel.ac.in/courses/117101002/downloads/handouts/lec35.pdf

61. F. M. Mitschke and L. F. Mollenauer, "Discovery of the soliton self-frequency shift," Opt. Lett. 11, 659-661 (1986)
62. J. P. Gordon, "Theory of the soliton self-frequency shift," Opt. Lett. 11, 662-664 (1986)
63. Alessio Gambetta, Roberta Ramponi, and Marco Marangoni, "Mid-infrared optical combs from a compact amplified Er-doped fibre oscillator," Opt. Lett. 33, 2671-2673 (2008)
64. http://nptel.ac.in/courses/117101002/downloads/Lec38.pdf
65. *Nature Photon,* 9, 557 (2012).
66. C. V. Raman, "A new radiation," Indian J. Phys. 2, 387 (1928).
67. E. J. Woodbury and W. K. Ng, Proc. IRE **50**, 2347 (1962).
68. R. H. Stolen, E. P. Ippen, *and* A. R. Tynes, "Raman Oscillation in Glass Optical Waveguide," Appl. Phys. Lett. 20, 62 (1972).
69. Fujio Shimizu, "Frequency Broadening in Liquids by a Short Light Pulse." Phys. Rev. Lett. 19, 1097 (1967).
70. R. R. Alfano, and Ed., "The Supercontinuum Laser Source, 2nd ed. (Springer, 2006).
71. Chinlon Lin and R. H. Stolen, "New nanosecond continuum for excited-state spectroscopy," Appl. Phys. Lett. 28, 216 (1976).
72. P. Baldeck and R. Alfano, "Intensity effects on the stimulated four photon spectra generated by picosecond pulses in optical fibres," J. Lightwave Technol. 5, 1712 (1987).
73. Barry Gross and Jamal T. Manassah, "Supercontinuum in the anomalous group-velocity dispersion region," J. Opt. Soc. Am. B 9, 1813-1818 (1992).
74. P. Beaud, W. Hodel, B. Zysset and H. Weber, "Ultrashort pulse propagation, pulse breakup, and fundamental soliton formation in a single-mode optical fibre," in IEEE Journal of Quantum Electronics, vol. 23, no. 11, pp. 1938-1946, (1987).
75. M. N. Islam, G. Sucha, I. Bar-Joseph, M. Wegener, J. P. Gordon, and D. S. Chemla, "Broad bandwidths from frequency-shifting solitons in fibres," Opt. Lett. 14, 370-372 (1989).
76. I. Ilev, H. Kumagai, K. Toyoda, and I. Koprinkov, "Highly efficient wideband continuum generation in a single-mode optical fibre by powerful broadband laser pumping," Appl. Opt. 35, 2548-2553 (1996).

77. T. Morioka, K. Uchiyama, S. Kawanishi, S. Suzuki and M. Saruwatari, "Multiwavelength picosecond pulse source with low jitter and high optical frequency stability based on 200 nm supercontinuum filtering," in Electronics Letters, vol. 31, no. 13, pp. 1064-1066, 22 June 1995.
78. Ö. Boyraz, J. Kim, M. N. Islam, F. Coppinger, and B. Jalali, "10 Gb/s Multiple Wavelength, Coherent Short Pulse Source Based on Spectral Carving of Supercontinuum Generated in Fibres," J. Lightwave Technol. 18, 2167- (2000).
79. Stéphane Coen, Alvin Hing Lun Chau, Rainer Leonhard, John D. Harvey, Jonathan C. Knight, William J. Wadsworth, and Philip St. J. Russell, "Supercontinuum generation by stimulated Raman scattering and parametric four-wave mixing in photonic crystal fibres," J. Opt. Soc. Am. B 19, 753-764 (2002).
80. Jinendra K. Ranka, Robert S. Windeler, and Andrew J. Stentz, "Visible continuum generation in air–silica microstructure optical fibres with anomalous dispersion at 800 nm," Opt. Lett. 25, 25-27 (2000).
81. T. A. Birks, W. J. Wadsworth, and P. St. J. Russell, "Supercontinuum generation in tapered fibres," Opt. Lett. 25, 1415-1417 (2000).
82. G.E. Town, T. Funaba, T. Ryan and K. Lyytikaine, “Optical supercontinuum generation from nanosecond pump pulses in an irregularly microstructured air-silica optical fibre,” Appl, Phys. B 77, 235 (2003).
83. John M. Dudley and Goëry Genty, “Supercontinuum light,” 66, Physics Today (2013).
84. P. Avouris, M. Freitag, and V. Perebeinos, "Carbon-nanotube photonics and optoelectronics", Nat. Photonics, 2(6), pp. 341-350, 2008.
85. 10. S. Kivistö, T. Hakulinen, A. Kaskela, B. Aitchison, D. P. Brown, A. G. Nasibulin, E.I. Kauppinen, A. Härkönen, and O.G. Okhotnikov, "Carbon nanotube films for ultrafast broadband technology", Opt. Express, 17(4), pp. 2358-2363, 2009.
86. Y. C. Chen, N. R. Raravikar, L. S. Schadler, P. M. Ajayan, Y. P. Zhao, T. M. Lu, G. C. Wang, and X. C. Zhang, "Ultrafast optical switching properties of single-wall carbon nanotube polymer composites at 1.55 μm", Appl. Phys. Lett., 81(6), pp. 975-977, 2002.

87. 8. S. Y. Set, H. Yaguchi, Y. Tanaka, and M. Jablonski, "Ultrafast fibre pulsed lasers incorporating carbon nanotubes", IEEE J. Sel. Topics Quantum Electron., 10(1), pp. 137-146, 2004.

88. X. H. Li, Y. G. Wang, Y. S. Wang, X. H. Hu, W. Zhao, X. L. Liu, J. Yu, C. X. Gao, W. Zhang, and Z. Yang, "Wavelength-Switchable and Wavelength-Tunable All-Normal-Dispersion Mode-Locked Yb-Doped Fibre Laser Based on Single-Walled Carbon Nanotube Wall Paper Absorber", IEEE Photon. J, 4(1), pp. 234-241, 2012.

89. Y. W. Song, S.Y. Set, S. Yamashita, C.S. Goh, and T. Kotake, "1300-nm pulsed fibre lasers mode-locked by purified carbon nanotubes", IEEE Photon. Technol. Lett., 17(8), pp. 1623-1625, 2005.

90. S. Yamashita, Y. Inoue, K. Hsu, T. Kotake, H. Yaguchi, D. Tanaka, M. Jablonski, and S. Y. Set, "5-GHz Pulsed Fibre Fabry–Pérot Laser Mode-Locked Using Carbon Nanotubes", IEEE Photon. Technol. Lett., 17(4), pp. 750-752, 2005.

91. M. A. Solodyankin, E. D. Obraztsova, A. S. Lobach, A. I. Chernov, A. V. Tausenev, V. I. Konov, and E. M. Dianov, "Mode-locked 1.93μm thulium fibre laser with a carbon nanotube absorber", Opt. Lett., 33(12), pp. 1336-1338, 2008.

92. Y. Senoo, N. Nishizawa, Y. Sakakibara, K. Sumimura, E. Itoga, H. Kataura, and K. Itoh, "Polarization-maintaining, high-energy, wavelength-tunable, Er-doped ultrashort pulse fibre laser using carbon-nanotube polyimide film", Opt. Express, 17(22), pp. 20233-20241, 2009.

93. M. E. Fermann, and I. Hartl, "Ultrafast fibre laser technology", IEEE J. Sel. Topics Quantum Electron., 15(1), pp. 191-206, 2009.

94. Jaroslaw Sotor, Grzegorz Sobon, Iwona Pasternak, Aleksandra Krajewska, Wlodek Strupinski, and Krzysztof M. Abramski, "Simultaneous mode-locking at 1565 nm and 1944 nm in fibre laser based on common graphene saturable absorber," Opt. Express 21,18994-19002 (2013).

95. Sivasankara Rao Yemineni, H.H. Liu and K. K. Chow, “Carbon-Nanotube-based Passively Mode-Locked Erbium-Doped Fibre Laser for Broadband Supercontinuum Generation”, in Int. Conf. on Information, Communication and Signal Processing (ICICS), Singapore, 2015.

96. H.H. Liu, K.K. Chow, S. Yamashita, S.Y. Set," Carbon-nanotube based passively Q-switched fibre laser for high energy pulse generation", Optics & Laser Technology, 45, pp. 713-716, 2013.

97. S. Y. Set, H. Yaguchi, Y. Tanaka, and M. Jablonski, "Ultrafast fibre pulsed lasers incorporating carbon nanotubes", IEEE J. Sel. Topics Quantum Electron., 10, pp. 137-146, 2004.

98. L. Nelson, D. Jones, K. Tamura, H. Haus, and E. Ippen, "Ultrashort-pulse fibre ring lasers", Appl. Phys. B: Lasers Opt., 65(2), pp. 277-294, 1997.

99. T. A. Birks, P. J. Roberts, P. St. J. Russell, D. M. Atkin, and T. J. Shepherd. Full 2-D photonic bandgaps in silica/air structures. Electron. Lett.,31(22):1941{1943, (1995).

100. J. C. Knight, T. A. Birks, P. St. J. Russell, and D. M. Atkin. All silica single-mode optical fibre with photonic crystal cladding. Opt. Lett.,21(19):1547-1549, (1996).

101. P. Russell. Photonic crystal fibres. Science, 299(5605):358-362, (2003).

102. Benabid, F., J. C. Knight, G. Antonopoulos, and P. St. J. Russell, "Stimulated Raman scattering in hydrogen-filled hollow-core photonic crystal fibre," Science 298, 399–402. (2002).

103. Knight, J. C., "Photonic crystal fibres," Nature (London) 424, 847–851. (2003).

104. Ouzounov, D. G., F. R. Ahmad, D. Müller, N. Venkataraman, M. T. Gallagher, M. G. Thomas, J. Silcox, K. W. Koch, and A.L. Gaeta, "Generation of megawatt optical solitons in hollow-core photonic band-gap fibres," Science 301, 1702–1704. (2003).

105. Mogilevtsev, D., T. A. Birks, and P. St. J. Russell, "Group-velocity dispersion in photonic crystal fibres," Opt.Lett. 23, 1662–1664. (1998).

106. Broderick, N. G. R., T. M. Monro, P. J. Bennett, and D. J. Richardson, "Nonlinearity in holey optical fibres: Measurement and future opportunities," Opt. Lett. 24, 1395–1397. (1999).

107. Kim P. Hansen & René E. Kristiansen, "Supercontinuum Generation in Photonic Crystal Fibres," NKT Photonics.

108. Ranka, J. K., R. S. Windeler, and A. J. Stentz, "Visible continuum generation in air-silica microstructure optical fibres with anomalous dispersion at 800 nm," Opt. Lett. 25, 25–27. (2000).

109. L. Provino, J. M. Dudley, H. Maillotte, N. Grossard, R. S. Windeler, and B. J. Eggleton, ‘‘Compact broadband continuum source based on microchip laser pumped microstructured fibre,’’ Electron. Lett. 37, 558–560 (2001).

110. R. Holzwarth, J. Reichert, Th. Udem, T. W. Ha¨nsch, J. C. Knight, W. J. Wadsworth, and P. St. J. Russell, ‘‘An optical frequency synthesiser for precision spectroscopy,’’ Phys. Rev. Lett. 85, 2264–2267 (2000).

111. W. J. Wadsworth, J. C. Knight, A. Ortigosa-Blanch, J. Arriaga, E. Silvestre, and P. St. J. Russell, ‘‘Soliton effects in photonic crystal fibres at 850 nm,’’ Electron. Lett. 36, 53–55 (2000).

112. Y. Kwon, K. Park, S. Hong, and Y. Jeong, "Numerical study on the supercontinuum generation in an active highly-nonlinear photonic crystal fiber with flattened all-normal dispersion," IEEE J. Quant. Electron., vol. 53, no. 5, 6100308, 2017.

113. Limin Xiao, Wei Jin, and M. S. Demokan, "Fusion splicing small-core photonic crystal fibres and single-mode fibres by repeated arc discharges," Opt. Lett. 32, 115-117 (2007).

114. T. Okuno, M. Onishi, T. Kashiwada, S. Ishikawa and M. Nishimura, "Silica-based functional fibres with enhanced nonlinearity and their applications," in IEEE Journal of Selected Topics in Quantum Electronics, vol. 5, no. 5, pp. 1385-1391, Sept.-Oct. (1999).

115. J. W. Nicholson, M. F. Yan, P. Wisk, J. Fleming, F. DiMarcello, E. Monberg, A. Yablon, C. Jørgensen, and T. Veng, "All-fibre, octave-spanning supercontinuum," Opt. Lett. 28, 643-645 (2003).

116. S N M Rifin, M Z Zulkifli, S N M Hassan, Y Munajat and H Ahmad, “Broadband supercontinuum generation with femtosecond pulse width in erbium-doped fibre laser (EDFL)”, Laser Phys. 26, 115102, (2016).

117. Weiqing Sylvestre, Meisong Liao, Lingzhen Yang, Xin Yan, Takenobu Suzuki, and Yasutake Ohishi, "All-fibre broadband supercontinuum source with high efficiency in a step-index high nonlinear silica fibre," Appl. Opt. 51, 1071-1075 (2012).

118. J.W. Nicholson, A.K. Abeeluck, C. Headley, M.F. Yan and C.G. Jørgensen, “Pulsed and continuous-wave supercontinuum generation in highly nonlinear, dispersion-shifted fibres,” 77, Appl Phys B (2003).

119. Atalla E. El-Taher, Juan D. Ania-Castañón, Vassilis Karalekas, and Paul Harper, "High efficiency supercontinuum generation using ultra-long Raman fibre cavities," Opt. Express 17, 17909-17915 (2009).
120. Takashi Hori, Jun Takayanagi, Norihiko Nishizawa, and Toshio Goto, "Flatly broadened, wideband and low noise supercontinuum generation in highly nonlinear hybrid fibre," Opt. Express 12, 317-324 (2004).
121. Sucbei Moon and Dug Y. Kim, "Generation of octave-spanning supercontinuum with 1550-nm amplified diode-laser pulses and a dispersion-shifted fibre," Opt. Express 14, 270-278 (2006).
122. Weiqing Gao, Meisong Liao, Xin Yan, Takenobu Suzuki, and Yasutake Ohishi, "All-fibre quasi-continuous wave supercontinuum generation in single-mode high-nonlinear fibre pumped by sub microsecond pulse with low peak power," Appl. Opt. 51, 2346-2350 (2012).
123. Thibaut Sylvestre, Armand Vedadi, Hervé Maillotte, Frédérique Vanholsbeeck, and Stéphane Coen, "Supercontinuum generation using continuous-wave Multiwavelength pumping and dispersion management," Opt. Lett. 31, 2036-2038 (2006).
124. Anne Boucona, Andrei Fotiadibc, Patrice Mégretb, Hervé Maillottea and Thibaut Sylvestrea, “Low-threshold all-fibre 1000 nm supercontinuum source based on highly non-linear fibre,” Opt. Commun. 281, 4095–8, (2008).
125. A. K. Abeeluck and C. Headley, “Supercontinuum growth in a highly nonlinear fibre with a low-coherence semiconductor laser diode, “Appl. Phys. Lett. 85, 4863 (2004).
126. J P Lauterio-Cruz, O Pottiez, Y E Bracamontes-Rodríguez, J C Hernández-García, E García-Sánchez, M Bello-Jimenez and E A Kuzin, “Comparative study of supercontinuum generation using standard and high-nonlinearity fibres pumped by noise-like pulses”, Laser Phys. 27, 065107 (2017).
127. F Wang, Z X Jia, C F Yao, S B Wang, M L Hu, C F Wu, Y Ohishi, W P Qin and G S Qin, “Supercontinuum generation from 437 to 2850 nm in a tapered fluorotellurite microstructured fibre,” Laser Physics Letters, 13, (2016).
128. Fang Wang, Kangkang Wang, Chuanfei Yao, Zhixu Jia, Shunbin Wang, Changfeng Wu, Guanshi Qin, Yasutake Ohishi, and Weiping Qin, "Tapered fluorotellurite

microstructured fibres for broadband supercontinuum generation," Opt. Lett. 41, 634-637 (2016).

129. J. Picot-Clemente, C. Strutynski, F. Amrani, F. Désévédavy, J-C Jules, G. Gadret, D. Deng, T. Cheng, K. Nagasaka, Y. Ohishi, B. Kibler, F. Smektala, “Enhanced supercontinuum generation in tapered tellurite suspended core fibre,” Optics Communications, 354, (2015).
130. Nan Li, Fang Wang, Chuanfei Yao, Zhixu Jia, Lei Zhang, Yan Feng, Minglie Hu, Guanshi Qin, Yasutake Ohishi, and Weiping Qin, “Coherent supercontinuum generation from 1.4 to 4 μm in a tapered fluorotellurite microstructured fibre pumped by a 1980 nm femtosecond fibre laser,” Appl. Phys. Lett. 110, 061102 (2017).
131. H H Chen, Z L Chen, X F Zhou and J Hou, “Ultraviolet-extended flat supercontinuum generation in cascaded photonic crystal fibre tapers,” Laser Physics Letters, 10, (2013).
132. Z. Chen, A. J. Taylor and A. Efimov, "Coherent mid-infrared broadband generation in non-uniform ZBLAN fibre taper," 2009 Conference on Lasers and Electro-Optics and 2009 Conference on Quantum electronics and Laser Science Conference, Baltimore, MD, 2009, pp. 1-2.
133. X. Luo et al., "Over Octave-Spanning Supercontinuum Generation in Tapered Seven-Core Photonic Crystal Fibre," in IEEE Photonics Journal, vol. 7, no. 5, pp. 1-9, (2015).
134. Huihui Li, Lixiao Wei, Xiao Zhang, Jinrong Tian and Yanrong Song, "Supercontinuum generation in tapered fibres," 2009 Asia Communications and Photonics conference and Exhibition (ACP), Shanghai, 2009, pp. 1-6.
135. K. Liu, J. Liu, H. Shi, F. Tan, and P. Wang, “High power mid-infrared supercontinuum generation in a single mode ZBLAN fibre with up to 21.8 W average output power,” Opt. Express 22(20), 24384–24391 (2014).
136. Humbach, Oliver & Fabian, H & Grzesik, U & Haken, U & Heitmann, W. Analysis of OH absorption bands in synthetic silica. Journal of Non-Crystalline Solids - J NON-CRYST SOLIDS. 203, 19-26 (1996).
137. Sivasankara Rao Yemineni, Wenn Jing Lai, Alphones Arokiaswami, Ping Shum, "Mid-IR supercontinuum generation in a single-mode ZBLAN fibre pumped by a carbon-nanotube-based passively mode-locked erbium-doped femtosecond fibre laser ", Proc.

SPIE 10516, Nonlinear Frequency Generation and Conversion: Materials and Devices XVII, 105160N (15 February 2018).

138. Md Imran Hasan, Nail Akhmediev, and Wonkeun Chang, "Mid-infrared supercontinuum generation in supercritical xenon-filled hollow-core negative curvature fibres," Opt. Lett. 41, 5122-5125 (2016).
139. L.A. Vazquez-Zuniga, X. Feng, Y. Kwon, H. Kim, J. Shi, W. Loh and Y. Jeong, "W-type highly erbium-doped active soft glass fibre with high nonlinearity," Electron. Lett., vol. 52, no. 12, pp. 1047-1048, 2016.
140. M.Poulain, M. Poulain, J. Lucas and P. Brun, 'Verres fluores au tetrafluorure de zirconium proprietes optiques d'un verre dope au Nd3+," Mater.Res. Bull.10, 243–246, (1975).
141. A. M. Heidt, J. H. V. Price, C. Baskiotis, J. S. Feehan, Z. Li, S. U. Alam, and D. J. Richardson, "Mid-infrared ZBLAN fibre supercontinuum source using picosecond diode-pumping at 2 μm," Opt. Express 21(20), 24281–24287 (2013).
142. Jacek Swiderski, "High-power mid-infrared supercontinuum sources: Current status and future perspectives," Prog. Quantum Electron. 38, 189-235 (2014).
143. K. Ohsawa, T. Shibata, K. Nakamura and S. Yoshida, "Fluorozicronate glasses for infrared transmitting optical fibres, in: Proceedings ofthe7thEuropeanConferenceonOpticalCommunication(ECOC), Copenhagen, Denmark, pp.1.1-1–1.1-4, (1981).
144. Rare-Earth-Doped Fibre Lasers and Amplifiers, in: M.J.F. Digonnet (Ed.), second edition, Marcel Dekker, New York, (2009).
145. M.Saad, in: Eric Udd, Henry H. Du, Anbo Wang(Eds.), Proceedings of SPIE, Fibre Optic Sensors and Applications VI, vol.7316, p.73160N-1–16, (2009).
146. Jiaqi Luo, Biao Sun, Jiayun Liu, Zhiyu Yan, Nanxi Li, Eng Leong Tan, Qijie Wang, and Xia Yu, "Mid-IR supercontinuum pumped by femtosecond pulses from thulium doped all-fibre amplifier," Opt. Express 24, 13939-13945 (2016).
147. Espen Lippert, Helge Fonnum, Gunnar Arisholm, and Knut Stenersen, "A 22-watt mid-infrared optical parametric oscillator with V-shaped 3-mirror ring resonator," Opt. Express 18, 26475-26483 (2010).

148. Martin Gebhardt, Christian Gaida, Pankaj Kadwani, Alex Sincore, Nils Gehlich, Cheonha Jeon, Lawrence Shah, and Martin Richardson, "High peak-power mid-infrared ZnGeP2 optical parametric oscillator pumped by a Tm: fibre master oscillator power amplifier system," Opt. Lett. 39, 1212-1215 (2014).
149. Patrick Rauter, Stefan Menzel, Anish K. Goyal, Christine A. Wang, Antonio Sanchez, George Turner, and Federico Capasso, "High-power arrays of quantum cascade laser master-oscillator power-amplifiers," Opt. Express 21, 4518-4530 (2013).